Universidade Católica Portuguesa
Faculdade de Engenharia

Reverse Engineering and Rapid Prototyping in Intervertebral Disc

Tissue Engineering

Sebastião Nicolau Dentinho van Uden

Dissertação para obtenção do Grau de Mestre em
Engenharia Biomédica: Especialização em Engenharia
Biomolecular, de Tecidos e de Órgãos

Orientador: Prof. Doutor Rui L. Reis
Co-Orientador: Doutor J. Miguel Oliveira

Júri

Prof. Doutor Manuel Barata Marques (Presidente)
Profª. Doutora Cecília Calado
Doutor Frederico Alves Ferreira
Doutor Joaquim Miguel Oliveira (Co-Orientador)

Junho de 2014

Resumo

A degeneração do disco intervertebral é considerada a maior causa de dor lombar, que por sua vez tem um impacto socioeconómico mundial na ordem dos 70 mil milhões de euros por ano. A Engenharia de Tecidos é uma área de investigação que está a crescer exponencialmente e que tem o potencial de desenvolver novos tratamentos, livres de rejeição imunológica, uma vez que são utilizadas células do próprio paciente. No entanto, é possível aumentar esse potencial de compatibilidade com o paciente combinando Engenharia Reversa com Prototipagem Rápida. Com isto visa-se o desenvolvimento de uma estrutura biodegradável e compatível tanto imunologicamente com estruturalmente, que vai sendo progressivamente substituída por novo tecido até se alcançar uma regeneração definitiva do disco intervertebral.

A prova-de-conceito preliminar desta estratégia terapêutica é reportada neste estudo através da utilização tanto de células, como a própria estrutura e morfologia, do disco intervertebral de coelho. A estrutura do anel fibroso foi replicada por Engenharia Reversa e Prototipagem Rápida em policaprolactona, enquanto que para servir como substituto do núcleo pulposo foram encapsuladas células num hidrogel de goma gelana metacrilada. A citotoxicidade, comportamento mecânico, morfologia superficial e porosidade da réplica do anel fibroso foram analisadas. Verificou-se que a porosidade é similar ao disco nativo e que o nível de biocompatibilidade está acima de 80%. As imagens de miscroscopia mostraram que as várias camadas da estrutura apresentam uma boa ligação após a solidificação do polímero. A adesão, proliferação e viabilidade celular na goma gelana metacrilada foram analisadas até 21 dias de cultura. Observou-se uma maior actividade metabólica nas células do núcleo pulposo do que na linha celular de fibroblastos, ambas encapsuladas em goma gelana metacrilada. Como trabalho futuro, pretende-se utilizar esta estratégia para tratar casos de degeneração do disco de uma forma efetiva em que o resultado final, após absorção da estrutura, é um disco intervertebral nativo biomecanicamente funcional.

Palavras-chave: Disco Intervertebral; Engenharia de Tecidos; Engenharia Reversa; Prototipagem Rápida; Tratamento Personalisado.

Abstract

Intervertebral disc (IVD) degeneration disease (IDD) is considered the main cause for low back pain (LBP), which has a world socioeconomic burden of 70 billion euros a year. Tissue Engineering (TE) is an exponentially growing area due to its potential of finding patient-specific treatments in terms of immunological compatibility by using the patient's own cells. Though, it is possible to increase TE patient-specificity by combining other technologies such as Reverse Engineering (RE) and Rapid Prototyping (RP). In this sense, it is possible to prepare a biodegradable scaffold that is both immunological and structurally compatible. This strategy has the potential to significantly increase implant integration and decrease immunological rejection, allowing the scaffold to be progressively replaced with newly synthesised tissue to ultimately regenerate the IVD into a fully functional anatomical motion segment.

Herein is reported a preliminary proof-of-concept for that strategy using rabbit IVD's cells as well as morphology and structure. In this sense, the annulus fibrosus (AF) structure was replicated by RE and RP into a polycaprolactone scaffold, and the cells were encapsulated in methacrylated gellan gum (GG-MA) hydrogel as a nucleus pulposus (NP) substitute. The AF scaffold's cytotoxicity, mechanical behaviour, porosity and superficial morphology were also analysed. It was observed a significant level of biocompatibility from the AF replica and a similar porosity in relation with the native IVD. Cell adhesion, proliferation and viability were assessed until 21 days of culture in GG-MA. The metabolic activity was higher in the NP cells than in the fibroblast cell line, both cultured in GG-MA. In the future, this novel strategy is envisaged to treat IDD, and remove LBP, by fully regenerating the intervertebral disc.

Keywords: Intervertebral Disc; Tissue Engineering; Reverse Engineering; Rapid Prototyping; Patient-specific.

Acknowledgments

I would like to express my special thanks of gratitude to the 3B's Research Group and Prof. Doutor Rui L. Reis, who not only gave me the possibility of working in this stimulating group with state-of-the-art equipment, but also for allowing me to work under his supervision. It is truly a golden opportunity to have as supervisor the President of the Tissue Engineering and Regenerative Medicine International Society, which was recently appointed Commander of the Ordem Militar de Sant'Iago de Espada by the President of the Portuguese Republic, and won the Clemson's prize among many other distinctions with no less credit. However, if there is a person that really gave me direct supervision during this project was Doutor J. Miguel Oliveira. He is my role model on how I want to be as a researcher, with collaborations, projects and prizes exponentially increasing, which will definitely make him one of the best Tissue Engineering researchers in the world. I never saw such a dedication and tireless working efficiency. I am extremely grateful to Doutora Joana Silva-Correia, who although having had a baby while I was doing my thesis managed to teach me encapsulation and culturing techniques needed for me to accomplish this work as well as proofreading my work with great detailed attention. I look at her on how to express my data in a transparent and flawless manner, with extreme ethics. I thank Doutor Vitor Correlo for helping me work with the Istron Mechanical Testing System and the Twin-screw Extruder. I would like to thank Profª. Doutora Cecília Leão for being so nice to help me find a thesis in Universidade do Minho, and in granting me the possibility to make my first contact with this thesis.

I would like to acknowledge Profª. Doutora Cecília Calado for all the support during my studies in Faculdade de Engenharia da Universidade Católica. And also together with Prof. Doutor Manuel Barata Marques for having prepared and created this really interesting and dynamic graduation, which now I am able to see how important were all those courses that at the beginning I could not understand their relevance. If I went back to the end of the highschool, I would chose this exact graduation in this Faculty again. On an entirely different subject, I appreciate all the patience and time spent while I was continually bothering both with academic association problems in my duty as vice-president of the academic association. To Prof. Pedro Simões I acknowledge my first contact with Tissue Engineering and Immunology. These were the only two courses that Prof. Pedro taught me, however I found his classes so interesting that when I was searching for a thesis my main choices were only between these two courses/fields.

I thank all people working in 3B's Research Group that helped me in my work, and most of all for the after/off work time that we spent. I met a lot of foreign people in 3B's that

shared their life stories and views, which come from completely different backgrounds and from all parts of the world.

I would like to acknowledge in a special way Daniela Pacheco for sharing with me her love for science research. I thank her for helping me to maintain focus in finishing the thesis at times that seemed this thesis would never end, which were several. When I started at 3B's I was supposed to study the state-of-the-art regarding the subject of this thesis, however, sometimes I did not want to sit on my desk reading papers, but instead to start working in the lab, she kindly showed me around and helped me gain practical experience in the lab. She proofread my work in situations that I was exhausted and could not read another sentence. Daniela made possible to come work afterhours, on weekends and holydays when I needed and she could just go enjoy her day off instead, always with the attitude "if there is work to be done, (let's) do it!". To her I express my full gratitude.

I thank my colleagues Daniel Nunes, Elisete Duarte, Patrícia Bacelar, Patrícia Silva, and Pedro Júdice for the teamwork and sense of community. As the only MSc students in our year, we were only six, but we had a far greater determination not only to achieve good grades but most of all for learning. There were times that we surrounded the Professor, which was giving the class, with questions and more questions and we only let go when we got the answer and made sure that everyone of us understood. Therefore, I am grateful for this small community feeling that made me learn the courses I had with full long-lasting understanding of the given subjects, which in the end truly helped me in the thesis.

I would like to thank Materialise NV© for allowing me to use a trial version of their software, without which it would have been impossible to make this work.

Last but definitely not least, I would like to thank my mother and my sister Catarina for all the tasty homemade food that always felt like I was eating at home. However, if this thesis was possible to happen in every sense, from getting to start it until enabling to finish it, was my father. He was the one that gave me the chance to go to Vienna, to the World TERMIS, in 2012 to find Prof. Rui Reis to ask him for this thesis. He gave me the best toy an Engineer can have, a 3D printer, which was the most important equipment I needed for this thesis, without it I could not have prepared the scaffolds. I thank my father for contributing indirectly in my decision to study/follow the "Bio" world that alongside with my innate attraction towards Engineering made me chose to study Biomedical Engineering. However, the last push to study Biomedical Engineering was given by Profª. Doutora Isabel Spencer-Martins that in 2005 opened my eyes for the potentialities of this field for the future, and that I would regret not being part of it. If I never studied Biomedical Engineering this thesis would not have been made, for that reason I am truly thankful.

Table of Contents

List of Figures

I. General Introduction: Advanced Regenerative Strategies for Intervertebral Disc Degeneration Treatment

II. Patient-Specific Tissue Engineered Total Disc Replacement

List of Tables

I. General Introduction: Advanced Regenerative Strategies for Intervertebral Disc Degeneration Treatment

II. Patient-Specific Tissue Engineered Total Disc Replacement

List of Acronyms

µCT - Micro-Computed Tomography

2D - Two-dimensional

3D - Three-dimensional

AF - Annulus Fibrosus

AFCs - Annulus Fibrosus Cells

ATB - Antibiotic Solution

BMG - Bone Matrix Gelatin

C - Cervical

CAD - Computer-aided Design

CEP - Cartilaginous Endplates

CMC - Carboxymethylcellulose

CO$_2$ - Carbon Dioxide

CT - Computed Tomography

DMEM:F12 - Dulbecco's modified Eagle's medium and nutrient mixture F12

DNA - Deoxyribonucleic acid

ECM - Extracellular Matrix

FBS - Fetal Bovine serum

f - Matemathical Function

FDM - Fused Deposition Modelling

FEM - Finite Element Method

GAG - Glycosaminoglycan

GFs - Growth Factors

GG - Gellan Gum

GG-MA - Methacrylated-Gellan Gum

GMA - Glycidyl Methacrylate

h - Compressed height of the NP

h$_0$ - Uncompressed height of the IVD

HA - Hyaluronic Acid

IDD - Intervertebral Disc Degeneration Disease

IL - Interleukin

IVD - Intervertebral Disc

k - Permeability

L - Lumbar

L929 - Lung Fibroblasts Cell Line

LA - Low Acyl

LBP - Low back pain

MMPs - Matrix Metalloproteinases

MRI - Magnetic Resonance Imaging

MSCs - Mesenchymal Stem Cells

MTS - 3-(4,5-dimethylthiazol-2-yl)-5-(3-carboxymethoxyphenyl)-2-(4-sulfophenyl)-2H-tetrazolium

MW - Molecular Weight

mRNA - Messenger ribonucleic acid

NCs - Notochordal Cells

NP - Nucleus Pulposus

NPCs - Nucleus Pulposus Cells

O$_2$ - Oxygen

OD - Optical Density

PBS - Phosphate Buffered Saline

PCL - Polycaprolactone

PEEK - Polyetheretherketone

PEG - Polyethylene Glycol

PG - Proteoglycan

PGA - Polyglycolic Acid

PLA - Polylactic Acid

PLGA - Polylactic-co-glycolic Acid

PLLA - Poly (L-lactic Acid)

PPCLM - Poly(polycaprolactone triol malate)

PVA - Polyvinyl Alcohol

PVP - Polyvinyl Pyrrolidine

RE - Reverse Engineering

RM - Regenerative Medicine

RNA - ribonucleic acid

RP - Rapid Prototyping

S - Sacral

SEM - Scanning Electron Microscopy

SLA - Stereolithography

SLS - Selective Laser Sintering

T - Thoracic

TCPS - Tissue Culture Polystyrene

TDR - Total Disc Replacement

TE - Tissue Engineering

TERM - Tissue Engineering and Regenerative Medicine

TGF - Transforming Growth Factor

UV - Ultra Violet

λ - Stretch Ratio

I. General Introduction: Advanced Regenerative Strategies for Treatment of the Intervertebral Disc degeneration

1. Impact of Low Back Pain and the Promise of Advanced Therapies

Low back pain (LBP) is a major issue in our society these days, mainly in terms of socioeconomic impact and quality of life. Intervertebral disc (IVD) degeneration disease (IDD) is believed to be the main cause for LBP[1,2]. Tissue engineering (TE) and regenerative medicine (RM; TERM) are an application of multidisciplinary tools by researchers, engineers, and physicians to construct biological substitutes that can mimic tissues for diagnostic and research, with the final purpose to regenerate diseased and injured tissues[3].

TERM is a field where a therapeutic strategy for IDD can be found, the doubt is not if it will work, but instead, how and when it will work. Indeed, many therapeutic strategies for IDD have been proposed within these two fields[4–6], and although all of these have the same purpose, they use different ways to get there. Some research groups use cultured cells directly implanted in the native tissue, whether it is with nucleus pulposus (NP) cells (NPCs)[7], annulus fibrosus (AF) cells (AFCs) and/or with stem cells[8–11].

The aim of the cell therapy strategies is to increase IVD's cell number levels and, therefore, the extracellular matrix (ECM) production. Another treatment option relies on biomolecules' injection[12], which is intended to reduce the anabolic processes and increase the catabolic processes to restore ECM levels. However, there are also other approaches that can be taken for severe cases of IDD, regarding biomechanical dysfunction or lack of proper ECM content in the IVD, using third generation biomaterials that can mimic the native tissue's physical and biochemical conditions[13]. These three strategies are the main ways within TERM fields to stop and revert IVD's degeneration process. They can be chosen according with the IVD's stage of degeneration and type of malfunction, but probably, as many research groups have been suggesting, the most adequate approach, at least for moderate and severe cases of IDD, where IVD's biomechanics is about to or is already compromised, would be a combination of two or all of these main regenerative strategies (*e.g.*, a combination of scaffold with cells and bioactive molecules)[14,15].

Bearing in mind that the world is in a difficult economic crisis and that getting enough funding for science research, as in other areas, is harder; a question must be asked - Is

researching an IVD's regeneration strategy economically worthwhile? To answer that question, it must be taken into account the size of the disease in terms of prevalence in society and its socioeconomic impact, which is statistically masked as LBP. So the dependence between LBP and IVD degeneration should be analysed. In fact, the IVD degeneration is thought to be the primary cause of LBP, causing compression of the spinal nerves and adjacent vertebrae[1,2]. By the age of 50, 97% of the population show signs of IVD degeneration[16], which is a time bomb for LBP. The incidence of LBP increases with age, creating a relationship between age related IVD degeneration and the frequency of LBP[17]. Having in account the increasing lifetime average in first world countries, incidence of LBP is increasing with it. Considering the fact that modern lifestyle tends to fulfil some LBP's risk factors, such as a large number of hours in a seated position, high levels of psychological distress, low levels of physical activity, obesity or job dissatisfaction, and the relation between IDD and LBP shows the problem is far from solved. Other risk factors for LBP are poor knowledge about self-state of health, previous back pain, pain below the knee, depression, fear avoidance behaviours, exposure to intense vibrations and smoking.

The most favourable way to analyse the economic importance/relevance of exploiting a regenerative strategy for IDD, is to check how much money is spent directly or indirectly (money not won on labour or which is spent in consequences due to LBP, *e.g.*, impairment and/or unemployment benefits) every year on treatments for LBP, and consider the percentage of LBP that is related to disc degeneration cases. Most LBP cases resolve rapidly (approximately 80-90% until the twelfth week with LBP symptom, acute LBP cases), but the remaining cases are the ones (from the twelfth week of LBP symptom forward is considered chronic LBP), which incur most of the treatment challenges and healthcare costs. In the United States, LBP is: the first cause of impairment in people younger than 45 years, the second cause to visit the physician, the third cause for surgical procedures and the fifth cause of admission in the hospital[18]. In the United Kingdom, LBP accounts for 13% of the certificated sickness leave, with estimated indirect costs to the country of 9 billion euros per year (in today's euro currency, X-Rates), and an annual direct cost to the National Health Service of 900 M€ (in today's euro currency, X-Rates)[19]. Resulting in 70 billion euros (in today's euro currency, X-Rates) in annual costs to alleviate and treat this pain[1] and it is rising.

This subject takes us to another question – Are there any good treatments for LBP? The current treatments for LBP are therapies addressed for LBP, and not for its cause, which means, that these treatments are focused on treating only the symptoms, and do not solve the actual problem, *e.g.*, IDD. The current treatments addressed to LBP, which largely include IDD's cases too, can be divided into pharmacological and non-pharmacological therapies[16].

The pharmacological treatment options include anti-inflammatories, muscle relaxants, antidepressants[20], analgesics and opioids, and injection therapy (drug's injection). Unfortunately, most of these treatment approaches have the danger of promoting addiction. On the other hand, the current treatments for chronic LBP are exercise, multidisciplinary therapy as in physical and psychological training, massage (classical/Swedish muscle massage)[8], acupuncture[21], behavioural therapy, back school, spinal manipulation[22], electromyographic biofeedback, lumbar supports, traction and transcutaneous electrical nerve stimulation. These are all treatments applied nowadays for patients with IDD, which are diagnosed with LBP, and contribute for $90 billion annual costs applied directly in LBP patients', money that could be spent in good and efficient treatments, which do not exist still. None of these treatments have shown already to be effective, sometimes it works, but it seems to depend on the cause of LBP, *e.g.*, if a patient suffers from stress a muscle relaxant can be enough to solve the condition.

Herein, it is intended to address the basic anatomy and biomechanics of the spine and IVD, as well as the degeneration process of the IVD. It also overviews the state of the art regarding the repair strategies, gene therapy and TERM strategies developed to repair and regenerate the degenerated IVD. Other advanced strategies that have been exploited in new TE approaches are also discussed, which employs the use of reverse engineering (RE) and rapid prototyping (RP) technologies in order to prepare a patient-specific TE-total disc replacement (TE-TDR) implant for middle to severe cases of IDD, *e.g.,* cases in which the AF is already compromised.

2. Spine: Anatomy and Function

The spine is composed of 33 vertebrae (9 are fused together in the sacrum and coccyx regions), most of them interspersed with IVDs, these being the biomechanical pivot of upper body motion. This allows the spine to be in the upper right position, bend and be submitted to torsion at the same time as it protects the spinal cord from trauma[23,24]. The spine provides strength and flexibility allowing the body to move in multiple spatial planes. The vertebrae composing the spine are numbered according to their spinal area location: 7 cervical (C1 to C7), 12 thoracic (T1 to T12), 5 lumbar (L1 to L5), 5 sacral (S1 to S5) and 4 coccygeal (fused vertebrae)[25].

Cervical area's main function is to support the head weight, which accounts for 8% of total bodyweight[26]. Thoracic area's range of motion is very limited and its main function is to protect the chest's internal organs by supporting the thoracic cage. The lumbar area is responsible for bearing the upper body's weight; for that reason, it has the biggest vertebrae in the entire spine. Vertebrae from both sacral and coccygeal areas are, each one, fused together.

The spine has a total of 24 IVDs, with approximately 4 cm in diameter and 7 to 10 mm thick (in the lumbar area), which account for one third of its height, and are the main responsible for its flexibility. It also allows a variety of movements, namely in three different planes: lateral bending, axial rotation and flexion-extension. When these motions are accompanied with heavy lifting, forces up to 17 kN can be created in the lumbar area[27]. In fact, this tissue is under high pressure when the body is in a vertical position, especially the lumbar area's discs, and even more when the body is in a seated position[28]. This indicates that the modern lifestyle, regarding its tendency for higher number of hours in which a person is seated, can be one more risk factor for chronic LBP and IVD degeneration.

The IVD is a complex structure composed of three different, although interdependent, types of tissue: (1) NP, (2) AF and (3) the cartilaginous endplates (CEP) (Figure 2.1)[1] located on both top and down IVD extremities which vertically delimit the AF and the NP. The NP is the gelatinous core of the IVD, and is contained by the strong and elastic AF.
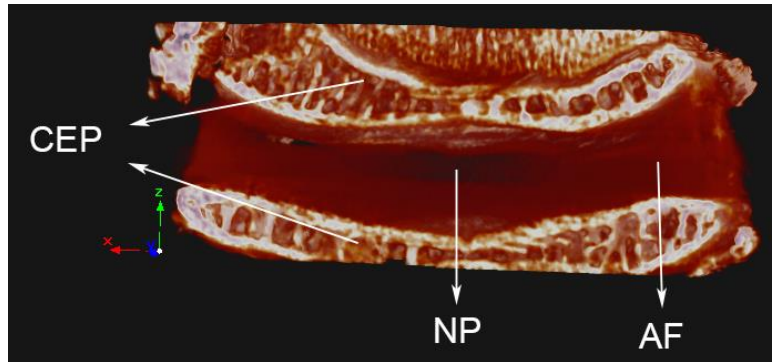
Figure 2.1. Micro-computed tomography three-dimensional reconstruction of a rabbit IVD, presenting the different components, namely: NP in the middle, AF around the NP and both top and down CEPs (Micro- computed tomography parameters: pixel size – 13.18µm, source 89kV / 112µA).

The NP's hydrogel-like consistency is due to its proteoglycan (PG) and water content, held loosely by a random network of collagen type II and elastin fibres. This structure has a high water content due to its high PG predominance in[28–31] which is about 80% and 65% (in dry weight), respectively at childhood, and drastically decreases with age[3233]. PGs are highly hydrophilic molecules, allowing them to adsorb large quantities of water, making NP's ECM to swell, giving the NP the classic hydrogel-like morphology. This morphology has viscoelastic properties, which is ideal for the NP function, and also ideal for the IVD's and spine's biomechanics.

The AF structure is responsible for contain the NP, and avoid its extrusion followed by collapse, as NP is under high pressure and its consistency does not allow weight bearing on its own. The AF surrounds the NP with 10 to 25, extremely organized and highly fibrotic, annular elastic strips called lamellas[28,31]. Although collagen type II is also present in the AF as it is in the NP, the proportion is much smaller, on the other hand the presence of collagen type I is highly predominant[30]. The collagen ratio of type I/type II increases from the NP's centre until the AF's outer periphery. Actually, the AF varies so much radially that some research groups, including ours[27] and Cassinelli *et al.*, say the IVD is composed by four structures: CEP, NP, inner AF and outer AF[17].

The outer AF is the peripheral layer of the IVD (in the transverse plane), and it is highly dense and organized[17,27]. The collagen fibres make a 60º angle with vertical axes, in the same lamella they are parallel to each other, but alternated from adjacent fibres. All together, the lamellas make a diamond mesh-like force field to contain the NP. This configuration allows the outer AF to contain large forces coming from the compression of the NP by the spine that are not contained by the inner AF[30,31,34].

The inner AF is a less organized structure than the outer AF. It is somehow a combination between the outer AF and the NP both biochemically and biologically, although more similar with the outer AF. On a healthy IVD the inner AF has a clear and smooth appearance.

CEP divides both NP and AF from the adjacent vertebrae by covering the cortical bone's surface. Vertebrae are connected to the CEPs through calcium structures, in addition the collagen fibres present in AF cross the border, tying the IVD to the vertebral bodies at its rim[29]. The CEP tissue is cartilaginous, and resembles articular cartilage in many properties. Studies have demonstrated that this tissue is the weakest of the three tissues in terms of mechanical properties[30].

The IVD's mechanism works by using the best properties of each of its three main types of tissue: CEP, stiffness; NP, uniaxial into hydrostatic pressure converter; AF, elastic resilience. This characteristics work on a force transfer cascade which begins with the spine being mechanically requested, resulting in its compression[35–38]. The uniaxial compression driven by this force is transferred through the CEPs to the NP, which reacts hydrostatically due to its fluid properties. As a result the AF ends up being pushed from within homogeneously, which reacts by containing it (Figure 2.2).
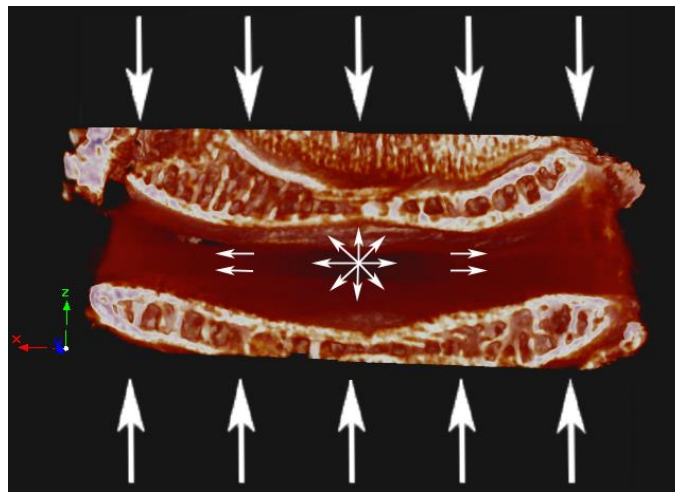
Figure 2.2. IVD's biomechanics general scheme, when the spine is mechanically requested. (Micro-computed tomography of rabbit IVD. Acquisition parameters: pixel size – 13.18μm, source 89kV / 112μA).

The assembled combination of both AF's and NP's mechanical properties make the IVD as it was composed of only one viscoelastic material ruled by two limit situations of

material mechanics: elastic solid and viscous liquid. As so, it is possible to consider, that the IVD has both elastic solid and viscous liquid properties.

3. Intervertebral Disc Degeneration (IDD)

The IVD suffers a great range of changes along the life of an individual - from the molecular phenotype expression, to cell type, to tissues' (CEPs, AF and NP) morphology. Alongside with these changes, called aging process of the IVD, can be an underlying progressing process of IDD. This disease can be triggered by an acute overloading (*e.g.,* lifting a heavy object). With aging, the needed threshold loading, to initiate the disease, progressively decreases. The degeneration of the disc converts the mild changes of aging IVD into serious conditions, *e.g.*, water loss, ECM production activity and phenotype, among several other changes at the biomolecular level. Ultimately, these changes lead to severe morphological changes, expressed in the form of pathologies.

The IVD biomechanical functioning relies on a balance between the three tissues that compose it. The same way the pressure goes along the CEPs to the NP, further to the AF, as aforementioned; the water flow follows the same pattern. In young discs, the only existent vascularisation is located inside the CEPs, which provide hydration for the whole disc[39]. The water is absorbed due to the osmotic pressure created by the biochemical components that compose most of the NP. Therefore, during loading cycles where compression forces affect the disc, the NP is strongly squeezed and the water molecules "detach" from the PGs, flowing away through the AF tissue.

As previously mentioned, the PGs are extremely hydrophilic molecules that are responsible for the 80% water composition of the NP in young IVDs[32]. A combination of spine overloading with aging leads to NP's ECM remodeling unbalance, loss of hydration, IVD height decrease, abnormal force distribution, and, ultimately, leads to the appearance of IDD morphological signs[40].

3.1. Pathophysiology

Thompson *et al.* proposed a grading scale for the anatomical changes that happen along the IDD development[41]. With the evolution of the IDD, there are a number of pathophysiologic events that can develop with it, such as: annular tears, disc prolapse, end plate damage and Schmorl's nodes, internal disc disruption, discogenic pain, disc narrowing, radial bulging, and vertebral osteophytes[42], which are addressed below.

3.1.1. Annular Tears

The annular tears (Figure 3.1) are protrusions of NP tissue into the AF. As the NP's material characteristics change and the AF tissue's elastic properties weakens, with the help of an acute overloading recurrence on the spine, the NP is extruded through the AF and therefore creating an annular tear. There are three types of annular tears: circumferential tears, peripheral tears, and radial fissures. Circumferential tears may evolve from acute overloading in older IVDs; the peripheral rim tears can be associated with trauma or with bony outgrowths, and are more frequent in the AF's anterior side; radial fissures are related with IDD and may appear on both posterior or posterolateral sides[43].

Figure 3.1. Annular tear in hernia stage.

Annular tears can be classified as contained or herniated, the last being when the NP is extruding out of the AF. From contained to herniated NP there are five levels of severity for the annular tears progression, which is the gold standard for the computed tomography (CT) classification of annular tears (Figure 3.2). Grade 0 refers to a normal health IVD; grade 1 is when the NP extrudes until the inner one-third of the AF; in grade 2 the NP leakage progressed until two-thirds of the AF; when the NP finally completes the three-thirds of extrusion through the AF, but no more than that, is on the grade 3 of annular tear classification; after the NP extruding beyond the AF outer border line the annular tear is on the fourth grade; the last stage of the annular tear progression grading scale (grade 5) is when the extrusion of the NP reaches the epidural space, that is when it may press the spinal nerve or one nerve ending, creating LBP[44].
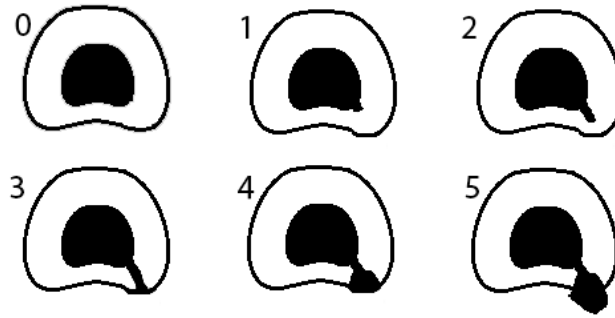
Figure 3.2. Classification of annular tears first purposed by Sach *et al.* in 1990, which has been modified by Bogduk *et al.* in 1992 and further modified by Schellhas *et al.* in 1996.

3.1.2. Disc Prolapse

When the NP is totally extruded throughout the AF there is a disc prolapse. In fact, the AF does not have any significant compressive properties, it is an elastic tissue and it acts like a rubber band when compressed, *i.e.,* when it is submitted to traction it responds increasing the reaction force the more it is stretched, however when compressed the middle part runs away towards one of the sides. Therefore, when there is no NP to convert the received force into a hydrostatic pressure, the uniaxial compressive force is not contained and comes down on the AF, which bends easily and it prolapses the disc. The difference between a disc herniation and a stage 5 annular tear is the quantity of NP content outside of place, if it is total then a disc prolapse (Figure 3.3) is about to or already did happen[45].

Figure 3.3. Scheme of a prolapsed disc, emphasized in red.

3.1.3. End Plate Damage and Schmorl's Nodes

Another typical IVD's pathology is CEP damage and the appearance of Schmorl's nodes. The CEPs are the weakest tissue of the three composing the IVD, in terms of mechanical properties[30]. In aged IVDs, when the CEPs already undergone a severe trabecular

microdamage, the tissue can suffer protrusion from the NP. The NP invades the vertebral bodies (Figure 3.4) and it ceases to be under pressure, since the force presses the AF instead, which cannot bear it and bends[42].

Figure 3.4. NP protrusions (Schmorl's nodes) into the CEPs due to trabecular microdamage driven by NP biochemical imbalance.

3.1.4. Internal Disc Disruption

Finally, the loss of water inside the NP makes its volume decrease in almost 1:1 proportional ratio, since as much as 80% of the NP is water. The decrease of NP's volume has a threshold, when this level is crossed the AF tissue seizes to be pushed by the NP. Since the NP's height is smaller than the AF, the CEPs start to compress the AF instead of the NP. The AF is not a hard tissue, thus it cannot hold compression in a functional way and internal disc disruption occurs, dividing the AF into two layers that bend to different sides, in and out[46]. Due to AF organisational morphology, which is divided in radial lamellas, tends to break apart between 2 of the 15 to 25 lamella stripes that compose the whole AF. This event creates a gap inside the AF, which significantly decreases the tissues mechanical performance, thus contributing to the progression of degeneration[47].

3.2. Biological and Molecular Changes

Biological and molecular changes underlie the morphological signs of IDD. Regarding biological changes, the cells present in degenerating IVDs suffer changes in several domains. Zhao *et al.*[48] made an extensive review on the cellular changes that happen during IDD. The

authors claim that there are cell changes in: type, density, death, proliferation, senescence, and phenotype. All these changes have an impact on molecular synthesis, which leads to an unbalanced ECM remodeling, and ultimately to loss of hydration that should be about 80% [30].

The IVD is composed of different types of cells in its different parts. The CEP as in resemblance to the hyaline cartilage is composed by chondrocytes; the outer AF is populated by elongated fibroblastic-like cells; the inner AF as more rounded chondrocyte-like cells. The cell population in CEP and AF does not change much with aging, however, it does vary greatly in the NP [48]. The CEP and the whole AF as most of the spinal structures are derived from the mesoderm germ layer, but not the NP [49]. This tissue on the other hand, has its origin on the endoderm germ layer that is also the notochordal cell's origin. These cells are largely present in young discs, but disappear by the end of the first decade of life. The notochordal cells (NCs) are gradually replaced by chondrocyte-like cells which are believed to migrate from the inner AF and/or from the CEPs [29].

There is some controversy around cell density changes. Zhao *et al.*[48] believe the cell density has its turnovers in parallel with the change of cell type in the NP. As NCs start to disappear, the cell density drops creating a positive feedback for chondrocyte-like cells migration and proliferation into the NP tissue, coming from the already mentioned tissues. These chondrocyte-like cells increase density along IDD. Bae *et al.* do not agree though, they claim that the degenerated disc's cell density is lower than that found in healthy discs [50]. But both hypotheses have strong arguments, as degeneration process progresses the CEPs start to calcify and IVD's vascular access starts to become scarce affecting the cells' nutritional route and cellular waste removal, causing increased cell death (Figure 3.5). However, with IDD progression, ingrowth of blood vessels accompanied by nerve growth occurs into the AF and even into the NP (in advanced IDD)[51]. These changes increase nutritional accessibility and waste removal rate, which can increase as well the cell density in the NP. But with nutritional availability also oxygen concentration increases inside the IVD, even more than in healthy IVDs. NPCs phenotype and activity is stimulated by hypoxia, ultimately the excessive availability to oxygen leads to normoxia, which tends to make NPCs senescent [52,53].
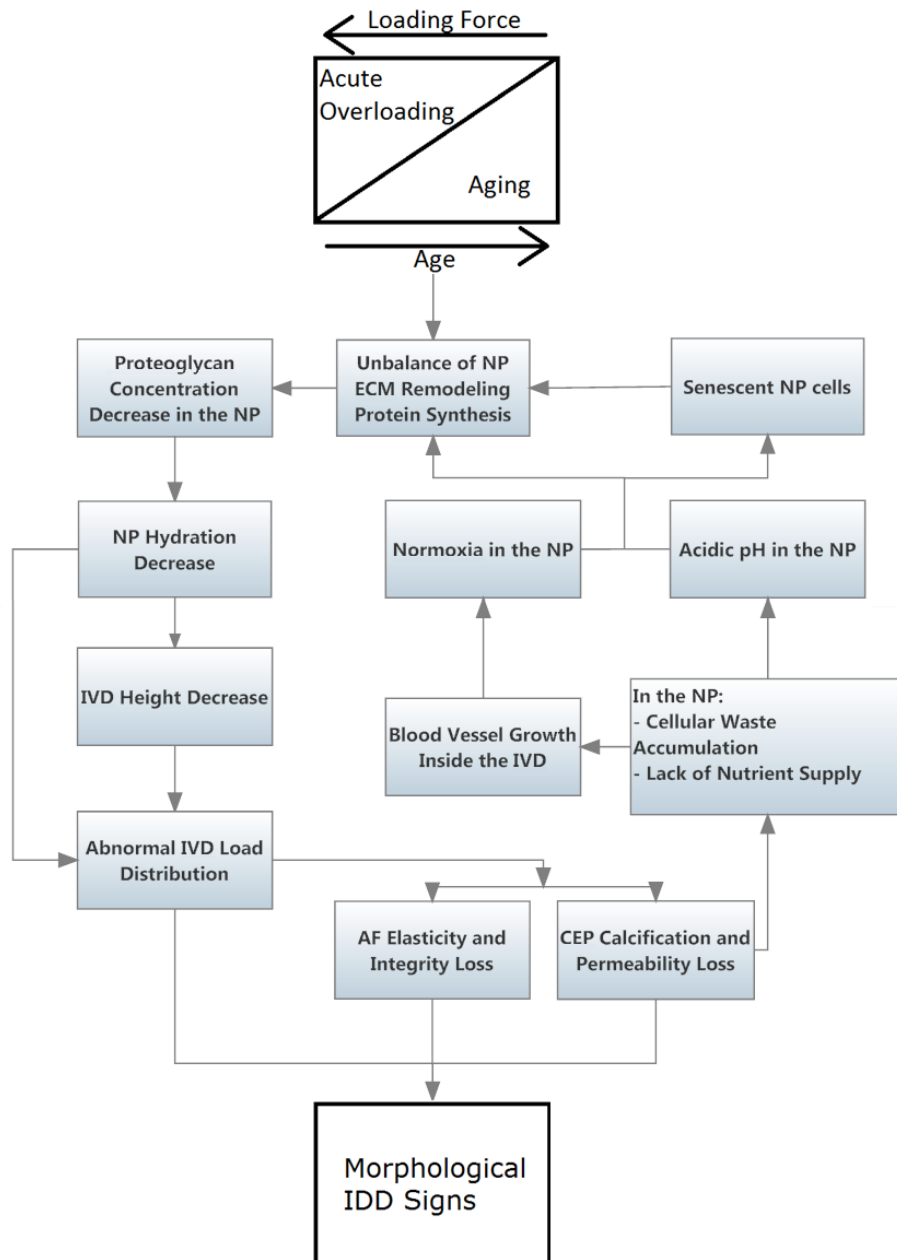
Figure 3.5. Scheme of the cascade of events associated with the morphological signs of IDD.

The cellular change, potentially most responsible for the morphological transformations observed due to IDD, is the NPC phenotype. Cell expression has direct influence in the anabolic-catabolic ECM pathway balance, as IDD progresses the catabolism increases in relation to anabolism, *i.e.,* the matrix is more degraded than it is produced. In a normal IVD, the AF is largely composed of collagen type I whereas the NP is composed of collagen type II and aggrecan, which is a type of PG. But other molecules are present in the NP, such as: collagen type I, III, V, VI, IX and XI, biglycans, decorin and fibromodulin (other types of PGs), and fibronectin[30]. In healthy IVDs there is also production of catabolic

molecules with increased expression while IDD progresses. These molecules are matrix metalloprotainases (MMPs) and aggrecanases, which break down the ECM. There are several types of MMPs expressed in the NP: type 1, 2, 3, 7, 8 and 13. In addition to that, there is also an increased cytokine production, such as: interleukin (IL)-1α, IL-1β and tumour necrosis factor-α. These molecules also promote the MMPs synthesis, having a devastating effect on the ECM[34]. Zhao *et al*. summarized a table of the biochemical changes caused by the IDD, which complements this brief description of ECM remodeling mediation[48].

The biomolecular changes throughout the IVD decrease the concentration of hydrophilic molecules in the NP. This has a strong effect on the IVD's permeability that when affected can change the IVD's biomechanics. NP's hydraulic permeability greatly depends on the magnitude of the compression force made on the disc. Heneghan *et al.*[54] defined a mathematical formula explaining this phenomenon, which is given by equation 1.

$$k(\lambda) = 2.05 \times 10^{-15}(\lambda - 0.2)^{1.13}e^{-0.01(\lambda^2 - 1)} \qquad \text{(Equation 1)}$$

Where, k, is the named permeability and, λ, is the stretch ratio, *i.e.,* the ratio between the compressed sample's height and the original height, on the apparatus used by this research group. In which, an IVD is submitted to a compression strain and the flow inlet and outlet are measured. This experiment besides giving a relation between permeability and compression, also shows that this relation does not follow a linear tendency but, instead follows an exponential tendency ($\lambda = h / h_0$, as h_0 is the uncompressed height of the IVD and is always higher than h, which is the compressed height of the NP; therefore, λ is always between 0 and 1). Until a certain level of NP compression magnitude ($\lambda \leq 0.2$), the tissue is not permeable, *i.e.,* when k = 0 or is an imaginary value. But this formula can only be applied when the NP is healthy, since when the degeneration starts the PG number decreases inside the NP and its permeability increases with it, *i.e.,* the water retention decreases and the whole IVD decreases its mechanical performance. This process is a cycle, with loss of biomechanical properties the typical loading starts to become an overloading, which also is a factor to progress the degeneration state that will in the end reduce even more the mechanical capacity, and the cycle goes on in a recessive spiral.

4. Treatment Strategies for Intervertebral Disc Repair/Regeneration

As previously stated, current treatments for LBP can cause addiction and only treat the symptoms. These treatments only work in specific situations, like in acute IVD traumas or in the beginning of the IDD's appearance. They mainly work by taking pressure out of the IVD (*e.g.*, muscle relaxants soften muscle strain over the IVD) thereby allowing the natural regeneration mechanism to solve the issue by itself. However, most of these treatments merely neutralize or reduce the patient's pain, while the IDD is still progressing[40].

In more severe cases of IDD, the natural regeneration system cannot cope anymore, either by itself or with strain releasing help (such as current treatments for LBP, *e.g.*, massage). In that case, only three strategies have the potential to remove pain completely, which are repair[55], gene therapy[56] and TERM strategies[57]. The first intends to solve IDD with artificial implants, whereas the second and third aim at the total regeneration of a patient's IVD, removing all previous signs of degeneration.

Even though gene therapy is still far away from clinical application, it promises great results in the future, not only in IVD regeneration, but also in several different kinds of diseases *e.g.*, cystic fibrosis[58]. The question of which one of these strategies is the best, cannot be answered yet, mainly due to the fact that there is still no clinically-approved IVD regeneration strategy available, despite promising potential in the currently researched treatment options[59]. Now, patients can only choose repair strategies as an alternative to current treatments in order to treat IDD.

In this section, it will be discussed the several repair approaches. Starting with the discectomy procedure, with its objective to remove the LBP generated by extruded NP material that compresses the peripheral spinal nerve or the spinal cord. This section gives a resume of some repair device strategies that not only remove LBP, but prevent it from coming back due to re-herniation after discectomy. Furthermore, the spinal fusion procedure is briefly explained, and how it treats IDD by removing the source of pain, preventing any possibility of it coming back. Well, at least in that intervertebral space, since herein it is also discussed how this procedure can stimulate adjacent IVDs to degenerate due to biomechanical imbalance through the spine after spinal fusion.

Moreover, TERM strategies to treat IDD in the NP are described and what pathways some research groups are taking to achieve that goal. This can be made whether by finding potential ways of differentiating stem cells into NPCs or by culturing isolated NPCs with growth factors (GFs) or serum-free chemically defined medium to make them metabolically

active. Then, which materials have been giving more interesting results to carry NPCs in the degenerated NP. Furthermore, it will be discussed which strategies are being followed nowadays to regenerate the AF, since without a good support, whether native or scaffold, for the NP, this will herniate on the first loading cycle. But to find the right material to mimic the complex mechanical properties of the AF is not an easy task, since it is a very efficiently organized tissue. And the synthesis of this ECM organization must, as well, be stimulated and timed with the scaffold rate of degradation.

4.1. Repair Strategy

4.1.1. Discectomy/Arthrodesis

Surgical methods for degenerative lumbar conditions include discectomy, arthrodesis or a combination of both. Discectomy is the surgical removal of NP fragments following herniation that compresses the spinal nerve. This compression distribution on the affected nerve causes pain, sensory changes, or weakness[60,61]. Discectomy is successful in relieving the radicular pain caused by the herniated disc. However, this procedure alone is unable to restore the nucleus to its original load sharing capacity, which controversially affects long-term benefits and re-herniation rates. Moreover, discectomy may accelerate the progression of disc degeneration by damaging the AF, which in turn will lead to a decrease in NP pressure, decreasing the disc height, impairing the disc's ability to rehydrate, and increasing the AF stresses and strains[61]. Besides the anatomical problems, the removal of the degenerated or damaged disc tissue typically provokes negative biomechanical changes[1,60]. Furthermore, it is unknown whether the effect of discectomy depends on the degenerative state of the disc[61].

Due to the disadvantages and limited success of discectomy procedures in general, arthrodesis was developed as an alternative method within clinical treatments. Arthrodesis, also known as spinal fusion, has been practiced since the beginning of the 20th century. Spinal fusion involves the use of bone tissue, traditionally derived from autografts, allografts, as well as the application of demineralized bone matrix, ceramics, and more recently bone morphogenetic proteins to bridge two or more vertebrae[62]. This procedure aims at stabilizing the moving segment, and slowing the progression of disc degeneration and relative pathological motion between vertebrae. Arthrodesis is based on the hypothesis that the mechanical and environmental changes will relieve the pain[63,64]. Even though spinal fusion is

a common procedure, its efficacy in treating discogenic LBP has been resulted in conflicting results[65]. Long-term consequences such as adjacent segment disease have increased concerns for the use of spinal fusion[1]. Furthermore, several changes have been observed such as dehydration, disc space narrowing, osteophyte formation, and progressive deformity at levels adjacent to a fused spinal segment[66].

4.1.2. Replacement

In an effort to improve results of fusion and to decrease the incidence of adjacent IVD degeneration, TDR techniques have been introduced and studied extensively.

Artificial disc replacement (nucleus and annulus) technology was first considered in the early 1950's to produce an implant that could mimic, to some extent, the function of the normal IVD (maintain the mobility of the intervertebral motion segment and restoring natural disc function)[62,67]. Moreover, implants for disc replacement should be biocompatible, durable, and easily implantable[68]. There are generally two types of disc arthroplasty devices, which are nucleus replacement or TDR devices, with the latter being more frequently used[1].

Nucleus substitutes are aimed at restoring disc height and returning annular fibres to their natural length. Adding to the appeal is the minimally invasive nature of this treatment method[69]. However, despite minimal invasion, a passage through the annulus for the prosthesis has to be created. Nevertheless, this approach allows the rehabilitation of the normal load distribution among the nucleus, the annulus and the facet joints, as well as promoting the healing of the annulus and thwart degeneration by themselves.

In general, the substitute should provide resistance to pressure with position change recreating the disc "bellows" effect[60]. A wide range of materials has been tried in order to replace the nucleus of the IVD, including: polymethylmethacrylate, polyvinyl alcohol (PVA)/polyvinyl pyrrolidine (PVP) copolymer, polycarbonate urethane, albumin, silicon, and stainless steel[62]. The most well-known device is the prosthetic disc nucleus, which is comprised of two sections: the first is made up of a non-degradable hydrogel pellet (polyacrylamide) and the second, which surrounds the hydrogel, is a polymer mesh or jacket composed of polyethylene[70]. However, in advanced stages of degeneration, these devices cannot be applied and TDR becomes again the most favourable approach.

TDR aims at restoring the physiological kinematics of the IVD, such as resisting wear and relieving pain, while avoiding instability and protecting the adjacent discs and facet

joints from undue degeneration[62]. Three artificial disc options have been proposed for TDR: metallic, non-metallic, or a combination of both materials[27]. SB-Charité®, a metal-polyethylene-metal construct was the first total disc arthroplasty, which is still in use today following only minor changes to the original design. Pro-disc® is another prosthesis that has been widely used[71].

Each artificial disc is composed of two or three components, which include two endplates and an articulating mechanism with either a metal-on-metal or metal-on-polymer surface. In order to keep the disc in place and provide stability within the host vertebral body, devices feature different designs - teeth-like compounds fixed into the vertebral bone; a porous coated surface onto the endplates, which promotes the growth of fibrous tissue around the device; or implant securing with screws into the recipient vertebral body[27,72]. Even though theoretically appealing, there are several challenges with current TDR strategies and also there is insufficient data to assess the performance of IVD arthroplasty adequately. Despite being in use for at least the last 20 years, there are some concerns regarding the safety and efficacy of these methods[73]. Consequently, patients may require revision surgery, which may be very dangerous due to the adjacent great vessels and the nerve plexus. Another solution, posterior fusion, requires the removal of the disc prosthesis followed by spinal fusion to immobilize the affected tissue, which again is very risky and dangerous[1,73].

Regarding the obvious downfalls of spinal fusion, the development of dynamic, or semi rigid-, constructs for lumbar spine instrumentation has emerged as an alternative option. This method is based on a load-sharing device, allowing for fusion without excessive rigidity, which, if disregarded, may lead to adjacent segment complications[74]. Some dynamic constructs have also been used without fusion[75]. Several authors have reported that posterior dynamic instrumentation, compared to rigid instrumentation, increases the amount of load transmitted through the anterior column and the interbody bone graft, which will avoid stress-shielding phenomena. Consequently, this may favour osteogenesis and enhance interbody fusion in accordance with Wolff's Law, which states that bone will adapt to the load it is placed under through piezoelectric phenomena[74].

Systems for spinal fusion can be described as pedicle screw–based constructs that are semi-rigid, or allow constrained motion in compression or flexion and extension. Pedicle screw-based systems are classically divided into semi-rigid rod systems and tension band-based posterior systems used in non-fusion technology[74]. The rigidity of these constructs depends on the material and design of the rods, which are connecting the pedicle screws. Although, solid stainless steel and titanium are commonly used in spinal fusion constructs[76], the semi-rigid constructs often include polyetheretherketone (PEEK) rods[77], nitinol rods[78],

especially cut rods (*e.g.*, Accuflex), articulated rods, and polyethylene terephthalate cords (Dynesys)[75,79].

Unlike the aforementioned prostheses that are fixed to the vertebrae by the use of pedicle screws, there are "floating devices", which are interspinous implants. These implants have the advantage of reducing the risk of implant loosening during motion[80].

During the last decade, spinal cage implantation has gained a lot of attention. This approach enhances spinal fusion and stability in cervical spine surgery, ensuring, at the same time, an adequate increase in the height and helping to correct cervical kyphosis, *i.e.,* a curvature in the cervical area of the spine[81]. PEEK cages have recently been used in cervical surgery, since they provide both strength and stiffness in the intervertebral space. A major advantage of these implants is their radio transparency and magnetic resonance imaging (MRI) compatibility, which are traditionally used in the visualization of the spinal cord and the root. Since the polymer is radiolucent, visualization in the aforementioned methods can be performed without the generation of implant artefacts in the resulting images[81].

Finally, intradiscal electrothermal therapy is a percutaneous technique reported by Saal *et al.*, and it is another option for the treatment of discogenic LBP[82]. A navigable electrothermal catheter is inserted inside the posterior annulus, which delivers heat. The proposed mechanism of action of this technique is collagen modulation, cauterization of granulation tissue, deactivation of inflammatory agents and possibly annular denervation. The heat induces the retraction of the annular collagen (collagen fibrils shrink at temperatures greater than 60ºC), therefore coagulating inflammatory tissue and nerve endings in the periphery of the disc's posterior side[82]. This heating method has been shown to produce temperatures sufficient to cause nerve fibre death as well as collagen denaturation[83]. Moreover, there are no biomechanical modifications and destabilizations after applying this procedure.

4.2. Gene Therapy

A potential therapeutic strategy next to the classic LBP management treatments and repair strategies is the gene therapy. This possibility was first thought as a way of treating chronic diseases, targeting the problem on its core by modifying, adding or disabling a gene or a cocktail of genes. Several problems occurred, when it was first tested; unfortunately the

idea gained a bad reputation and gone into a research standby for a decade[84]. Recently, the number of groups researching gene therapy started rising again, being nowadays a possibility of stopping and reverting degeneration of the IVD.

The first question when applying this strategy for IVD regeneration is – what should change on a molecular level, to stop and revert IVD's degeneration? As it has been explained above, the malfunction in the NP's ECM production and maintenance is one of the main reasons for the IVD to fail biomechanically. So, the strategy must be focused on balancing the catabolic-anabolic equilibrium into the ECM production side. For that, two things can be done, alone or together, increase the ECM anabolism and decrease the catabolic pathway. This can be done by transfecting the right genes into the NPC population, genes that codify potential therapeutic GFs and cytokines such as: transforming GF (TGF)-β1, TGF-β3, insulin like GF-1, osteogenic protein-1, IL-1, bone morphogenic protein-2, latent membrane protein-1, SOX9, among others[85]. Transfecting a combination of these genes would increase ECM production, but the reverse strategy can also show equally positive results, by silencing targeted catabolic proteins using RNA interference, such as proteolytic enzymes (*e.g.*, MMPs and disintegrin and metalloproteinase with thrombospondin motifs). This RNA suppresses the overall production of the targeted gene by using a small interfering RNA, which binds specifically to the gene's mRNA sequence, leading to a suppressed translation or increased mRNA's degradation[86,87].

After choosing the proper cocktail of genes to be delivered, another question may be posed - how does the gene reach its final destination? With few exceptions naked DNA alone is not a feasible way to deliver it to target the cells' nucleus; a vector is needed that can be viral or non-viral. Non-viral vectors are systems, which do not have viral origin, such as liposomes[88], DNA-ligand complexes[89], gene gun[90] and microbubble enhanced ultrasound[91]. However, the non-viral vectors give the host a transient gene expression that is not suitable for the treatment of chronic diseases. A longer lasting strategy must be applied, for that, viral vectors are the most favourable since they use viral's natural way of infecting the host and integrating DNA into the target cells' genome, *e.g.*, metabolism senescent cells like the ones present inside the IVD in order to enhance their activity. Viral vectors, on the other hand, bring the risk of alarming the immune system that is a huge issue in high-vascularised tissues, which is not the case as the IVD is the most avascular tissue in the body. Viral vectors utilized for gene therapy applications include adenovirus[92], adeno-associated virus[93], herpes simplex virus[94], lentivirus and retrovirus[95].

In addition to the selection of the appropriate gene and vector, another important consideration with gene therapy applications is the delivery strategy. There are two main

strategies for gene delivery as proposed by Nishida et al[96], *in vivo* and *ex vivo* (Figure 4.1). The first strategy takes fewer steps than the second, it involves the direct transfer of the vector-gene complex into the target tissue within the living host. The *ex vivo* strategy involves a more complex approach. First the cells are isolated from the host; after the culture is transfected with the desired DNA material; the cells, which were successfully genetically modified, are then implanted into the desired tissue. This strategy seems to be much safer, since while cells remain *in vitro* they can be assessed before implantation in order to control what goes inside the patient's organism; so those cells that had a bad reaction to the transfection can be removed, and only the desired cells are implanted[97]. Also, the *in vitro* culture required in *ex vivo* strategies may change cells characteristics in a way that they cannot survive in the harsh environment observed in a degenerated NP (low oxygen, low pH, poor nutrition)[98]. Mimicking the IVD's conditions is needed in order to reproduce *in vitro*, as much as possible, the IVD's cell environment, and probably the only possible strategy is to proceed with the culture in a bioreactor. On the other hand, the *in vivo* strategy has its disadvantages as well, using this approach the viral vectors are injected with an unknown concentration in comparison with the cells present in the target tissue. This relation between the number of viral particles and target cells is called multiplicity of infection, which in high values is extremely cytotoxic[52].
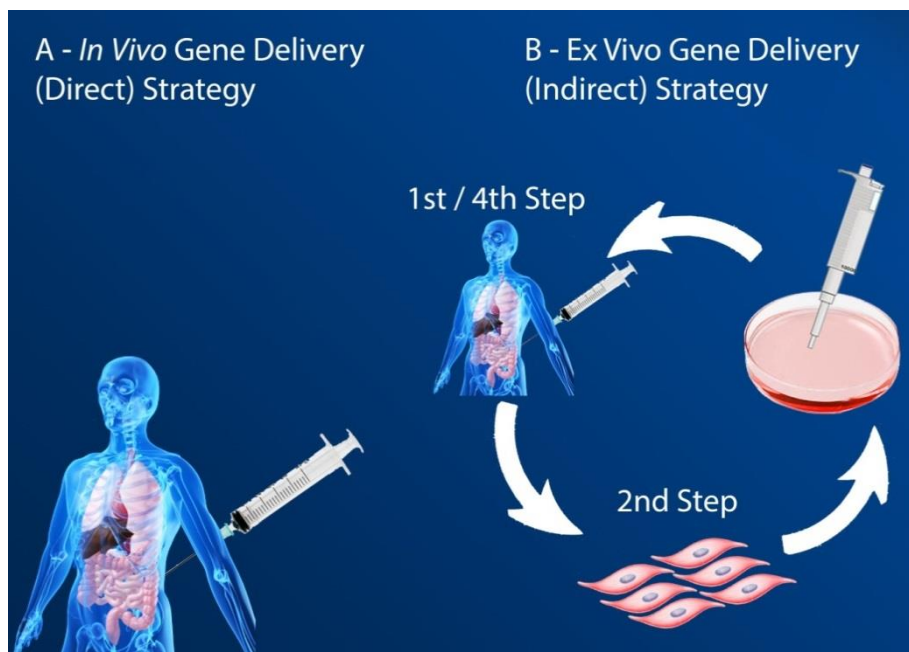
Figure 4.1. Gene delivery strategy available, A. *in vivo* – which implants the vector-gene complex within the living host – and B. *ex vivo* – which involves isolation of the host target cells (1st and 2nd steps), transfection (3rd step) and implantation (4th step).

The literature is controversial about which delivery strategy is the most proper strategy, further research is needed to unveil this topic, however, it seems relatively easy to conclude that the *in vivo* strategy, although more dangerous, seems more efficient.

The IDD can be a severely debilitating disease, but it can never be fatal. For that reason only, a treatment, such as gene therapy can be seen as an extremist strategy, since, although the disease will not kill, the cure can, as well as stimulate IDD to an even more debilitating condition (*e.g.*, paralysis)[99]. In fact, gene therapy can achieve great result without being too invasive, but only if everything goes according to plan, otherwise (*e.g.*, high multiplicity of infection, injection made in a vascular vessel or in a nerve ending) there is a real risk of killing the patient. Anyway, there are no better treatments, only appropriate treatments, and with more research, gene therapy can have a place as an IDD therapy.

4.3. Tissue Engineering and Regenerative Medicine Strategies Applied to the Regeneration of Intervertebral Disc

Since Langer and Vacanti first defined TE as "an interdisciplinary field of research that applies the principles of engineering and life sciences towards the development of biological substitutes that restore, maintain, or improve tissue function"[100] the research field went into an exponential growth. Its close companion field, RM, is going good as well since it was recently declared by The Economist as "the best market in the world right now"[101]. TERM are definitely two potential areas to find treatment strategies that can cure diseases that until now did not have an effective cure[3]. While RM targets diseases in which the main problem is in the cellular population, the TE addresses diseases in an advanced state of degeneration in which, or for any other reason (*e.g.*, tissue surgically removed for treating cancer), the tissue's mechanical stability has been compromised.

In the case of the IDD disease, TE (Figure 4.2) aims to restore disc height and biomechanical stability by repairing the tissue at first[102]. Through time the scaffold degrades and becomes bioactive, sprouting back the body's natural regeneration process that without a physical support provided by the biomaterial would not be possible. This grants a favourable environment for cells to produce not just ECM, but the right type of matrix. Cells need to be in contact with each other in order to produce the right ECM for it to be the aimed tissue. On

the other hand, for that tissue to be grown the cells must be at the density that its cell type is used to, not only that, but also the rate of nutrient supply and cellular waste removal should be similar to the native tissue. The situation is similar regarding oxygen supply and carbon dioxide removal[103]. These parameters are very important, especially for the IVD, since this is the most avascular tissue in the human body. The same presence of nerve endings in the IVD is also extremely limited, which explains the lack of symptoms until a severe state of IDD[104]. Therefore, NPCs are not used to be close to a blood vessel that provides higher concentration nutrients and oxygen. All of this influences the cell's type and what they express, as explained before, having a direct impact in the functional stability of the tissue.
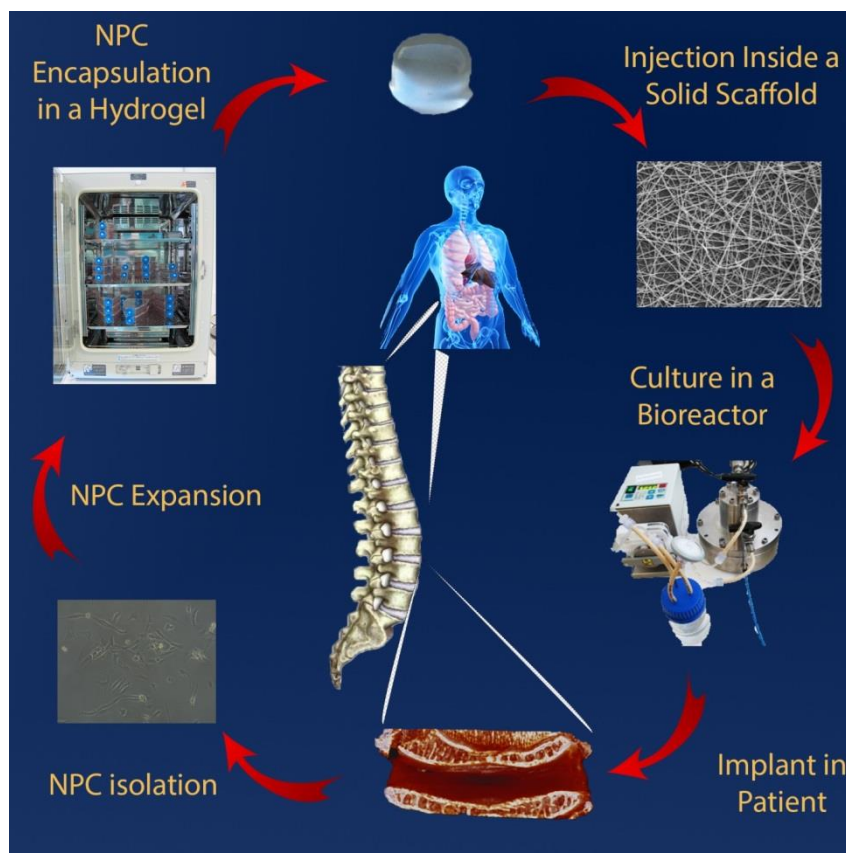
Figure 4.2. Scheme of a Tissue Engineering strategy applied to the intervertebral disc.

4.3.1. Nucleus Pulposus

The genesis of IDD is related to the loss of ECM in the NP's (Figure 2.2). The main reason for the appearing of this disease, besides it may arise due to an acute overloading of

the spine or ageing, is in the loss of water within the NP matrix. Since 80% of its content is water, a decrease in its content lead to a decrease in NP height and consequently it loses its biomechanical functionality[32]. When regenerating the NP this high water content must be maintained, therefore the hydrogels seem like the ideal candidate to mimic the native tissue due to their ability to retain water, some up to 98%[105].

Cell-based strategies aimed to regenerate the IVD concern strictly on renewing the synthesis of NP's ECM by cell injection in order to increase cell number, but more importantly to boost the active cell population. This because the reason why the ECM is lost is due to the native NPCs' change in behaviour, they seize to produce PGs at an even rate as the ECM remodelling proteins destroy it[50]. The NPCs living inside IVDs that are in an advanced state of degeneration are senescent and need to be replaced with strong and vigorous ECM cell producers.

4.3.1.1. Matrices: Biomaterials/Scaffolds

Regarding regeneration treatment strategies for IDD, when the subject is cell-based strategies it is implied that only the NP tissue is being regenerated. This because in IDD process the AF degenerates after the NP, in fact the AF degenerates mainly because of NP malfunction, due to its degenerated state[106]. So when choosing the right biomaterial to carry cells to the NP, several properties must be taken in account, as described in Table 4.1.

Table 4.1. Hydrogel requirements as NPCs carrier.

	Problem	Solution	References
1	AF should be left intact as much as possible during surgical procedure	Injectable material, so that only the area of the needle's section is hurt on the AF's	[107]
2	In order to achieve the first requirement, the material must be able to polymerise only when inside the NP. *	This polymerization can respond either to pH, ion interaction, temperature, or even light.	[108,109]
3	If the material is going to carry the cells to the NP it should improve the NP's properties, such as disc height and biomechanical function, in order for the cells to remain viable.	The material's mechanical properties should be as close as possible with the mechanical properties of the NP tissue.	[110]
4	Provide an environment that stimulates NPC's phenotype.	The material must be able to absorb a lot of water, at least 80%, which is the amount of water inside the NP.	[32]
5	The material besides biocompatible should be biodegradable.	The degradability rate must match the tissue's rate of regeneration.	[111]

*If the polymerised material is able to be injected or if the material does not polymerise *in vivo* it is very likely that the material will come right off through the needle hole, with cells included, on the first IVD loading.

With all those properties in mind, the type of material that stands out is the hydrogel (Figure 4.3). Hydrogels are polymeric networks with the capacity of absorbing water from 10 up to 100 times its dry weight.
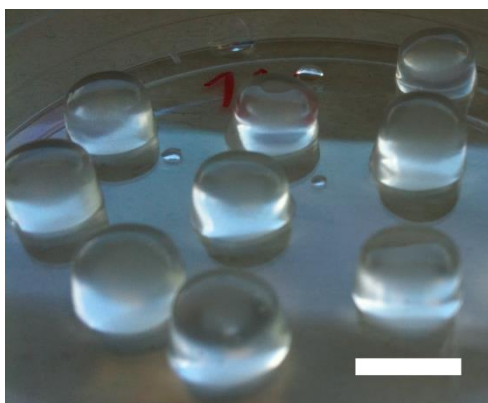
Figure 4.3. Methacrylated gellan gum discs with a diameter of 10 mm and a height of 5 mm. Scale bar: 10 mm.

Several kinds of hydrogels have been studied for cartilage regeneration, as well as specifically prepared for IVD TE strategies. Hydrogels belong to the group of polymeric materials, thus they can be divided into two types regarding their origin – natural and synthetic[112].

There is a growing interest in natural origin hydrogels, and the economic aspect is the main reason for it. As most of the naturally occurring hydrogels are extracted and not synthesised, this greatly reduces its manufacturing cost. In that sense, they also require purification processing, which sometimes involves using severely toxic solvents and reagents. Even so, in general, they are less expensive to produce than synthetic hydrogels. Other reasons for why they are getting more attractive might be their low level of cytotoxicity and their wide range of possible TE applications, such as: bioactive degradation, available to cellular remodelling, cell adherent, and biological signalling[113–115].

Although natural origin hydrogels offer a wide range of biological advantages, they generally lack the needed physical properties, as solubility and accelerated rate of degradation do not allow the tissue to regenerate in such low time. This does not suit cartilage regeneration, since they have a long regeneration time[116]. Therefore, if a natural originated hydrogel as these properties suited for cartilage then it's a very promising material. Some examples are: alginate[117], carboxymethylcellulose (CMC), chitosan, collagen, gellan gum (GG), and hyaluronic acid (HA) (Table 4.2).

Table 4.2. Natural and synthetic origin hydrogels used in intervertebral disc tissue engineering strategies – advantages and disadvantages specific for the nucleus pulposus regeneration.

Natural Origin Hydrogels	Advantages	Disadvantages	References
Alginate	Polymerization under mild conditions; Injectable *in situ*; NP's similar mechanical properties; Cell adherent.	Lack of long-term mechanical stability; Impurities make it unpredictable; Difficult to sterilize and to handle.	112,113,115,117, 118
Carboxymethylc ellulose	Biocompatible; Low-cost; Food and Drug Administration-approved; Commercially available in high-purity forms.	Lack of studies using this material.	119
Chitosan	Bioactive; Cell adherent Antibacterial activity; Non immunogenic.	Bad mechanical properties; Cytotoxic cross-linkers; Impurities make it unpredictable.	112,113,115,120
Collagen	Non immunogenic; Piezoelectric properties; Bioactive.	Bad mechanical properties; High degradation rate; Some level of toxicity (crosslinking agents).	112,113,115
Gellan Gum	Non-angiogenic; Able to polymerize until 1% (w/v); Non immunogenic; Very low manufacturing cost; Good mechanical properties and stable in long-term when methacrylated.	Weak in physiological conditions due to the exchange of divalent cations by monovalent ones.	4,59,112,113,121
Hyaluronan	Non immunogenic; Easy control over the polymer chain sizes; Bioactive; Low manufacturing cost.	Osteogenic; Cytotoxic in high concentration.	8,112,113,115
Synthetic Hydrogels	**Advantages**	**Disadvantages**	**References**
Polyethylene glycol	pH-switchable electronic properties; Photo-polymerizable; Adjustable mechanical properties; Easy control over scaffold architecture and chemical composition.	Bioinert; No cell adherence; Expensive to manufacture.	112,122–124

PVA	Catalytic activity; Increases viscosity when added to other hydrogels; Controllable crystallinity.	Bad mechanical properties; Regular chain structure; Non degradable; Expensive to manufacture.	112,120,123
PVP	Good mechanical properties; Biocompatible.	Non-degradable; Expensive to manufacture.	115,122

In contrast with natural origin hydrogels are the synthetic hydrogels. This hydrogels provide predictable and reproducible chemical and physical properties that can be tuned for different TE applications, *e.g.,* degradation rate according to the aimed tissue regeneration rate. Moreover, they are easy to blend with polymers that broaden even more the properties' possibilities of synthetic origin hydrogels[125]. Since they are made of well-known molecules, when pure, they have a low risk of immunogenicity, infection and toxicity[115,126]. Though, they lack bioactivity, and their manufacture is, in general, economically unattractive. Some examples of synthetic hydrogels for IVD TE strategies are: polyethylene glycol (PEG)[127], PVA[128] and PVP[129] (Table 4.2).

4.3.1.2. Cells

Cell therapy approach for IVD regeneration is based on injecting NP phenotype cells that are believed to produce PGs when *in situ*. Thus, the first obstacle is - what type of cells is the right one to be used? Well, if the native NPCs (Figure 4.4) are to be replaced they surely cannot be used, *i.e.,* the NPCs from the degenerated IVD cannot be used since they are senescent or they are not expressing the right phenotype.
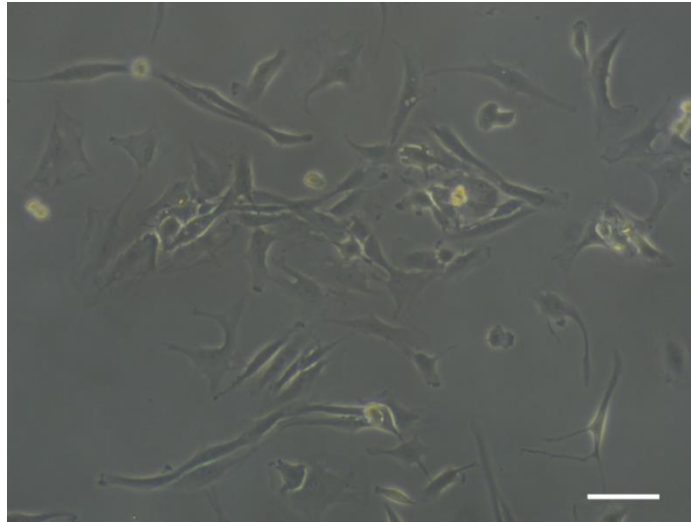
Figure 4.4. Micrographs of human NPCs after 3 days in culture. Scale bar: 50 µm.

Fortunately, it is possible for this to be a wrong statement in the near future, since Rosalin Abbott and her co-workers[12] have been working on increasing human NPCs' metabolic activity, proliferation, glycosaminoglycan (GAG) production, and stimulate non-degenerated NPC's phenotype. They believe that native NPCs from an IVD in a severe state of degeneration have, in fact, a hidden regenerative potential. The exposer of these type of cells to a notochordal conditioned media and/or GFs, namely from the TGF family, constitutes a promising strategy to enhance GAG production and be an effective treatment. They retrieved the cells from a human source and after expanding them under the aforementioned conditions they were implanted in IDD rabbit models (induced by needle-punctures).The results showed not only that cells stayed viable for up to 24 weeks but also that this strategy delayed the IDD progression.

Jennifer Maier[130] studied the effects of Foxa1 and Foxa2 genes n the notochordal sheet formation during embryogenesis, and found out that in fact they do have an indispensable role in NP tissue formation. It is believed, that the young NP tissue does not have the chondrocyte-like NPCs, but only NC cells, and the chondrocyte migrate from the inner AF tissue or from the CEPs[131]. There is the possibility that stem cell transfection with Foxa1 and Foxa2 could guide the differentiation line to NC cells, but it is a very premature statement, with the potential to be researched, though.

The prospect of using stem cells in cell-based strategies for IVD regeneration brings with it the necessary step of differentiating stem cells into fully functional NPCs. Although this is not an easy task, recent efforts (*e.g.,* induced pluripotent stem cells)[132] have been helping to reduce one part of the problem, the stem cell source. The amount of stem cells needed in the beginning

significantly depends on the method that is being followed, since the differentiation into NPCs can be done *in vitro* or *in situ*, for reasons explained below.

The *in vitro* differentiation method has the advantage of assuring that the implanted cells have the correct phenotype, although with the disadvantage of more stem cells being needed. Stem cell expansion is not trivial, and many cells are lost while differentiating into NPCs[133]. The key factor, specific for IVD regeneration treatment, is hypoxia (2% O_2), since this is the environment where NPCs live in, they can be up to 2-3mm from the closest blood vessel[52,53]. Therefore, the best way to ensure that stem cells differentiate into NPCs is by introducing them in a hypoxic environment, though a lot of cells tend to die due to the lack of oxygen therefore more stem cells are needed at start. Zhong Fang and his co-workers[133] have been working on the hypothesis of manipulating mesenchymal stem cells (MSCs) in order to make them resistant to hypoxia by adding an anti-apoptotic gene called Bcl-2. By avoiding stem cells to suffer apoptosis on the early stage of differentiation they made these pre-NP phenotype cells to be resistant to the low concentration of oxygen and thus maintaining cell number even after the later stage of differentiation. This way, the initial number of stem cells needed decreased significantly (2.2 times less). But the doubt still remains – Does this not increase the chance of cancer cells formation? Decreasing the ability of cells to resort to apoptosis is a step forward for cells to be unable to commit apoptosis, and losing the ability to die makes them virtually cancer cells. Nevertheless, this work brings great promise and if proven safe there is no reason why not to use this method, even in other strategies for IVD regeneration (*i.e.,* cell constructs).

In situ differentiation method has the advantage of using a standard approach for stem cell expansion, the process from isolated stem cells until before the injection in the NP is done the same way has it was for any other kind of tissue. Steven Leckie and his co-workers[134] developed a work following this type of cell-based method. Its purpose was to determine whether injecting human umbilical tissue-derived cells into the NP would improve the course of IDD. The authors injected cells alone (carried by a buffer), carrier alone and carrier + cells. Follow up was based on MRI, biomechanics and histology findings. The results were not close enough to the positive control (non-punctured IVDs), and failed to fully restore MRI parameters for non-degenerated IVDs. However, they were successful in slowing down the degeneration process and showed better results than the negative control (punctured IVDs). At 12 weeks the MRI results showed that cells alone and cells + carrier were significantly distinct from punctured values. Although, regarding the viscoelastic properties, the cell-free carrier and cells + carrier were significantly closer to positive control than the cells alone, though not close enough. If the biological and biochemical conditions within this tissue are not right the use of this method can stimulate the growth of blood vessels and nerve endings inside the NP, though. In the literature, there has been shown evidences, or at least suspicions, that the appearance of

blood vessels and nerve endings inside the NP might be originated by native stem cells[135]. Therefore the addition of stem cells could promote this as well as deteriorate the state of the tissue by further degenerating it, but there is still a need to further research and clarify that.

4.3.1.3. Combined therapy: Cell-laden scaffolds

Gwen Crevensten[8] used HA as a cell carrier for MSCs. Disc height was evaluated on several time-points, but with no significant results. They evaluated the cells' viability of the injected cellular population by using a cell tracker staining and observed that when using cells + carrier, the cells remained viable for up to 28 days by 100%, but no NP phenotype or biomechanical behaviour of the hydrogel, after a period of culture, was tested.

Anna Reza and Steven Nicoll[15] made a very interesting and complete study using methacrylated CMC as a carrier for NPCs. Besides analysing the matrix elaboration and functional properties NPC-laden CMC hydrogels, they also compared two different types of medium - the standard serum-containing medium formulation versus a serum-free chemically defined medium, both of them supplemented with TGF-β3. The results show why using a chemically defined medium is so important, obviously compensated by its high cost. GAG and collagen type II content was significantly greater in serum-free constructs, as well as the Young's modulus, and the equilibrium weight-swelling ratio of the same constructs approached that of the native NP tissue (22.19 vs. 19.94, respectively). These results indicate the importance of medium formulation in NP construct development demonstrated by enhanced functional matrix development by NPCs when cultured in CMC hydrogels maintained in serum-free, TGF-β3 supplement medium.

Yung-Hsin Cheng and co-workers[136] added gelatin to a thermosensitive chitosan and β-glycerol-based hydrogel to improve its mechanical strength and gelation properties. Gelatin was chosen by its low-cost, biocompatibility, biodegradability, but especially due to its gelation properties. After evaluating its feasibility to carry cells for NP regeneration, it was observed from the rheological measurements that the gelation temperature was near 33ºC, thus liquid at room temperature, and that at 37ºC its gelation time was 49 seconds. Later on, [137] the same scaffold was used in combination with ferulic acid, due to its properties, namely: anti-inflammatory, anti-diabetic, anti-carcinogenic, anti-apoptotic, anti-aging, hepatoprotective, neuroprotective, radioprotective and pulmonary protective. The aim was to perceive if this bioactive agent had similar protective and/or therapeutic effects on a degenerated IVD. The

results demonstrated that this hydrogel composite has the potential to be used as sustained-release system for hydrophobic compounds (such as ferulic acid). A down-regulation of collagen type II synthesis and substantial up-regulation collagen type I. It was observed that ferulic acid can be an interesting molecule to encapsulate in AF scaffolds, such as polycaprolactone (PCL) being this polymer hydrophobic.

Anthony Baer[118] and his colleagues studied the collagen expression and mechanical properties of NPC-laden alginate hydrogels. Interestingly the results showed a good cellular viability, but the mechanical behaviour of the cell-laden hydrogels after 21 days was not near the native NP mechanical behaviour. Putting the two different types of results together, it suggests that although IVD cells maintain their phenotype characteristics when cultured in alginate, the synthesised molecules were not able to form a mechanically functional matrix *in vitro*.

GG hydrogels (Figure 4.5) have been proposing great results as a material for cartilage regeneration[138], showing interesting features, such as its natural property of being non-angiogenic[139]. This is a crucial feature in cell-based approach upon IVD regeneration, since by keeping blood vessels away the environment inside the NP can remain hypoxic as it is in undegenerated IVDs, therefore stimulating NP phenotype even with no GF supplement.
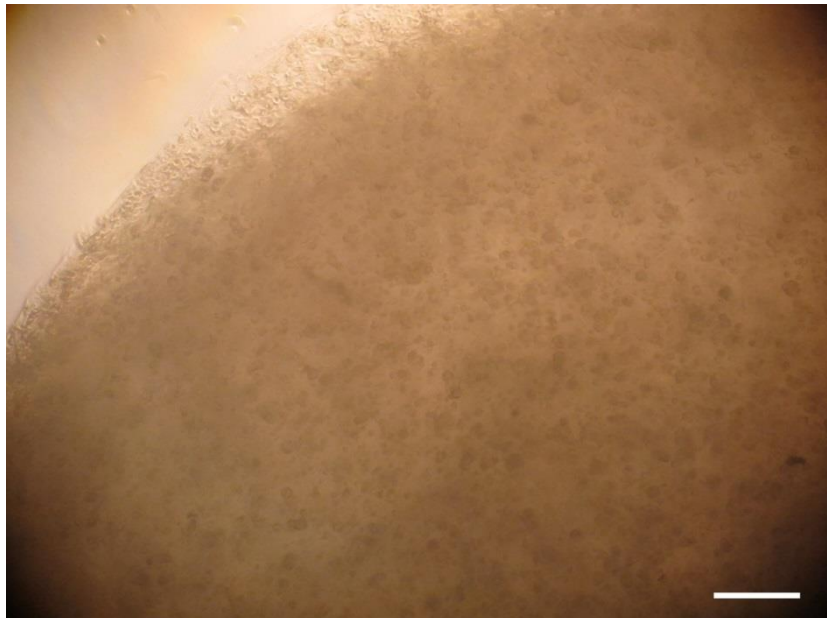
Figure 4.5. Micrograph of methacrylated gellan gum disc with a 1×10^6 rabbit NPCs encapsulated, after overnight culturing. Scale bar: 200 μm.

Silva-Correia and colleagues have been shown indicatives of GG potential for its use in cartilage regeneration[140]. A protocol for producing methacrylated-GG (GG-MA) was developed[141]. By adjusting the methacrylation reaction to 24 hours, GG-MA mechanical properties became the most suitable for NPC-based therapy. Moreover, a photo-polymerizable class of GG-MA was also developed allowing its gelification after exposure to ultra-violet (UV) light (approximately during 6 minutes). The viability tests showed that UV exposure did not significantly affected the cell number, as the cultures of photo-crosslinked GG-MA with encapsulated NPCs remained viable up to 21 days[142,143]. In 2012, the same team ran an experiment for evaluating the angiogenic potential of GG, which has shown splendid results for IVD regeneration treatment applications[59]. The same team demonstrated the methacrylated biocompatibility with both lung fibroblasts cell line (L929) cell line and human IVD cells[144]. Therefore, it shows the potential of GG-MA material to be used as an NP substitute.

4.3.2. Annulus Fibrosus

IDD has a starting point in the NP tissue, as already mentioned, but its progression is towards the adjacent tissues – AF (Figure 4.6) and CEPs. The CEPs are a critical tissue for the whole IVD's health maintenance, they are the main source of water and nutrition, and with IDD progression they tend to become calcified, therefore loosing supply permeability[145]. When this path is blocked, angiogenesis is stimulated inside the IVD that raises oxygen levels, making the NP normoxic, decreasing the NPCs capacity of PG production by slowly making them senescent[48]. This process only happens in very severe cases of IDD, though being very important for the whole IVD biological balance. When looking into the general picture, the CEPs are the third last important tissue to focus on regenerating. But maybe it is time for research surrounding IVD TE to start focusing more on the CEP regeneration in order to provide the clinics a whole spectrum of available TE therapies for IVD regeneration, from mild to severe IDD. Although this subject is not addressed here, the authors strongly believe that there is a gap in the IVD TE research that urgently needs attention.
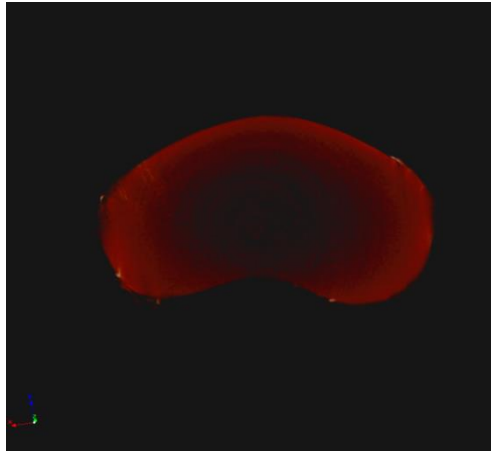
Figure 4.6. µCT top view of the AF, surrounding a dark area, which is the NP. (µCT of rabbit AF and NP. Acquisition parameters: pixel size – 13.18µm, source 89kV / 112µA).

When NP loses force-converting abilities, *i.e.,* the ability to convert uniaxial compression into hydrostatic pressure, the AF tissue seizes to be pushed aside. When this is combined with loss of NP volume due to decrease in water content or through herniated annular tears, the compression made by the spine structure on the IVD compresses the AF, instead of compressing the NP and then pushing the AF from within. When the biomechanics of the IVD are following this path of mechanical energy distribution the AF disrupts creating the internal disc disruption pathology, thus contributing to the progression of the degeneration[47]. When the AF is under this state of degeneration it is somehow hopeless to try regenerating the IVD by focusing only on the NP, since any hydrogel, with seeded cells or not, injected in the IVD, will certainly herniate through the AF after a stronger spine loading[107]. Therefore, in severe states of IDD it is as important to regenerate the AF as the NP, since any effort on regenerating the NP alone would be meaningless unless there is a functional AF to hold the NP tissue in place[146–148]. In order to do that a biphasic (NP + AF) or even a triphasic (NP + inner AF + outer AF) cell construct is needed to have the chance to succeed with the treatment. Moreover, future strategies could also address the substitution of the CEPs as well, for extreme cases of IDD.

4.3.2.1. Matrices: Biomaterials/Scaffolds

The AF varies greatly in morphology along its radius, and that is the reason why researchers claim that there are two distinct structures within the AF - the inner and the outer AF[17,27]. Actually, the biocomposite AF and NP is one whole structure with no evident borders.

The biochemistry of it simply changes gradually from the NP centre to the most peripheral layer of the outer AF. Since it is not easy to mimic the assembling complexity of the IVD's ECM molecules in order to form the macro structure, the most promising way to produce a whole IVD cell construct is by defining the borders between the different types of tissue that are to be mimicked.

There is one type of ECM component that prevail in each one of the three structures[32]. Inside the NP there is a major presence of PGs. In opposition to the NP's biochemical and morphological composition is the outer AF. This anisotropic tissue[149] is mostly made of collagen type I, therefore it is an extremely elastic type of tissue. It has a totally different type of mechanical behaviour from the NP, which is more of an isotropic viscous liquid. The inner AF, although having more collagen type II than the other two types of tissue, is like a mixture of both in terms of mechanics and biology, but having a morphological organisation closer to the outer AF, though[38].

In this sub-chapter it will be described the types of materials that are being used in research for the AF tissue regeneration strategy. Several materials have been developed and used as prime-material for preparing AF scaffolds (Figure 4.7). There are an immense amount of different composites and formulations, though they are based on the same materials, such as: polylactic acid (PLA)[150,151], polyglycolic acid (PGA)[151,152], silk[153,154], collagen[155–158] or demineralised and decellularised bone matrix (collagen base)[159], PCL[160,161], alginate, chitosan[162] and HA[150].

Figure 4.7. Photograph of a three-dimensional printed rabbit IVD replica. Scale bar: 5 mm.

Like any material to be used in a TE application, it must be biodegradable and bioresorbable as well as biocompatible while being shape-tailored. However the IVD is an anatomical structure highly subjected to complex movements and strains[163]. Therefore, the

material chosen to replace the AF, in the short-term, must have similar mechanical properties. It should have a similar Young's modulus that enables the material to sustain high forces while remaining in the elastic domain, *i.e.,* free of plastic deformation. In the long-term, it must degrade at the same timing as the implanted cells are synthesizing the tissue. This ECM remodelling is manipulated by the cells and depends on the biochemical balance existing inside the cell construct, though it is maybe also affected by a piezoelectric effect (*i.e.,* emits electrical signals when mechanically requested and vice-versa) created by the collagen, since this molecule possesses piezoelectric properties[164]. The lines of tension change dynamically with loading cycles of the spine, resulting in degradation of the AF scaffold and synthesis of new ECM. This affects piezoelectricity inside the structure; cells are attracted to where pressure is felt, since the collagen upon mechanical stimulation releases electric stimulus that attracts cells and stimulates them to produce ECM, in order for the whole tissue to be mechanically balanced. This effect is similar to what happens in almost every tissue of the human body, a very good example is bone since trabeculae and its mineralization are coincident with tension lines felt in the tissue[165]. Briefly, the way that the scaffold degrades, and how its mechanical properties vary with it, is very important for the cell construct to be successful upon implantation.

Nesti and co-workers[150] decided to use only one composite material to mimic the whole IVD structure. They say that if the IVD fails as a unit then it must be regenerated as a material composite unit. They prepared what they have called a HA nanofibrous scaffold that is made first by electrospinning of nanofibrous poly (L-lactic acid) (PLLA). The electrospun mat was then cut into $1cm^2$ sections and, after seeding the nanofibrous dense scaffold with MSCs and left overnight, a solution of HA with encapsulated cells was injected inside the PLLA cell construct. This, they say, created a pressurized pouch, cuboidal in shape, with the inner core of HA and nanofibrous elements surrounded by a sheath of dense nanofibrous scaffold.

Munirah Sha'ban and his team[151] also used polylactic acid as based material, but combined with polyglycolic acid, making a composite of polylactic-co-glycolic acid (PLGA). They also used fibrin to allow better cell adhesion to the scaffold after seeding, this way reducing cell loss in this step.

However the AF ECM is mainly made of collagen, being the principal reason why several research groups have been using it for AF scaffold preparation[155,157,158]. Scaffolds made of collagen type I or II have already shown to stimulate IVD cells to produce big PGs and long GAG chains[157,166].

4.3.2.2. Cells

The literature is consistent on this subject. Most of the research carried out for AF regeneration has used AFCs[167–169], aside from few exceptions that used MSCs[150].

The cell type native to the AF is considered fibroblast-like[170]. Fibroblast cells constitute the easiest type of primary cells to grow *in vitro*. In fact, usually they are unwanted, since sometimes they contaminate the isolated cell culture due to its higher rate of proliferation, representing the worst and most common type of autologous contamination in cell isolation procedures[171]. Therefore, there are several approaches regarding cell types seeded in AF TE scaffolds, which are still not proven worthless to research as integrated part of therapeutic strategies that aim full IVD regeneration, even for severe cases of IDD.

The most common approach seen in the literature is seeding the AF scaffold with AFCs[167–169]. These cells are easy to isolate and have the desired phenotype, since they are native to the tissue. If the study is being made *in vitro*, *i.e.,* without an *in vivo* surrounding source of native fibroblast, then the AFCs might be the most advisable option. Since acellular AF scaffold assessment would only be realistic as a model for short-term implantation, long-term results would require *in vivo* studies to observe fibroblast migration. The "keep-it-simple" approach is the acellular AF scaffold. The idea is that fibroblast cells are easy to taxis (*e.g.,* chemotaxis), and have proliferative advantage in comparison to other cell types. In this sense, the acellular approach can provide good results, since native fibroblast will migrate to the AF scaffold and proliferate, being the scaffold seeded or not.

There is a short percentage of research in AF regeneration that uses MSCs as a seeding population. The main reason is to use only one cell type in the whole IVD cell construct (since most AF regeneration research implies the regeneration of the NP as well, due to IDD line of progression), and at the same time have, as a final result, both cell types - AFCs and NPCs. Therefore, this strategy combines the advantages from both two remaining alternatives - in a way, it is a "keep-it-simple" approach but also complete. But it is not a perfect approach, since it would require using at least two different GFs, which would significantly increase the estimated cost of the future optimised approach in the clinics. Also, it compensates one type of cell "keep-it-simple" approach (*e.g.,* NPCs in hydrogel with acellular AF scaffold), since it involves two paths of differentiation would complicate the already difficult task of assessing just one path of differentiation.

4.3.2.3. Combined therapy: Cell-laden scaffolds

The great advantage of developing acellular strategies is its simplicity, rapid application and predictability. Though, as soon as the material is implanted the degradation time starts, thus it is important for cell construct's maturation, *i.e.,* ECM production to native tissue levels, to be as fast as possible. And the maturation of cell constructs *in vivo* is faster if cells are already seeded in the scaffold. Making taxis of migrating fibroblasts, from outside the cell construct, synergic, instead of fundamental for maturation. Therefore, several strategies for AF regeneration, that have been developed, use seeded cells.

Wan and co-workers[172] develop a biphasic scaffold just as an AF scaffold, *i.e.,* without focusing on NP regeneration, this way mimicking the properties of the inner and outer AF tissues. A demineralised and decellularised bone matrix gelatin (BMG) from the extracted cortical bone using as a source New Zealand white rabbit femur was prepared as the outer phase of the scaffold. After the process of demineralisation and decellularisation what remains essentially, regarding molecule composition, is a natural material with high collagen type I content, like the outer AF. To mimic the inner AF tissue, they produced a scaffold orientated in concentric sheets of poly(PCL triol malate) (PPCLM) seeded with chondrocytes in order to mimic the lamella structured cartilage-like inner AF. This strategy is interesting regarding its biomechanics, since PPCLM spiral open when NP pushes the cell-scaffold construct, but on the other hand the BMG ring does not let it unfold. Therefore, it was created a string-like effect that mimics the AF native tissue in a different biomechanical strategy. Although, the scaffolds do not mimic the lamellar structure of the native AF tissue despite contrary information, therefore the mechanical performance of the cell constructs reached not even half of the AF rabbit tissue, not being enough to withstand a tensile stress of 4 MPa. In this study, it was shown that by controlling the PPCLM polymerization time it is possible to prepare AF scaffolds with different degrading behaviours that can be tuned according with the ECM synthesis along the regeneration process. By using a PCL-based material, it was avoided the problem of increasing acidification inside the cell constructs, upon scaffold degradation, since the PCL byproducts do not acidify the environment[172].

Park and his team[173] did a study with outstanding results in terms of final silk scaffold morphology, resembling very closely with the AF tissue. After solubilizing the silk, a mixture of sodium alginate solution was added and injected it into cylindrical shaped (12 mm in diameter and 5 mm thick) silicon moulds. The moulds were subjected to a standard lyophilisation for 2 days and then water-annealed to generate the insoluble state of silk by inducing β-sheet crystallinity. The mixed alginate was removed from the scaffold by immersion in water for 24 hours and the donut-shaped silk scaffolds were achieved by simple punching. The results

showed highly dense lamellar structure with spaces between lamellas varying from 10 to 400 μm. The silk is a material very used in TE research, there is no need to point here its good biocompatibility and adhesion properties, what is in fact interesting is that this scaffold in this macro form and micro-lamellar structure has an elongation to failure very close to the human AF tissue at the first week, slightly less after 2 weeks, though. Unfortunately, regarding the Young's modulus, that in our point of view is the mechanical property that really matters, is quite far from the human AF. Their lamellar silk scaffold had a compressive Young's modulus of 0.3-0.4 MPa after 2 weeks of culture, while the human AF is around 1.23 MPa. However the work is far from effortless, since the morphological structure of the silk toroidal is a perfect scaffold, in the literal sense of the word, to guide collagen deposition. Probably, with times of culture longer than 2 weeks, the cell constructs can gain optimal mechanical properties, since silk is strong but not elastic, therefore, with further deposition of collagen the cell construct can become extremely elastic while still strong.

IVD TE research is already extensive and several obstacles are being surpassed, though there is an argument still not mentioned, the structural compatibility, not in terms of morphology but in terms of optimal fitting within the intervertebral space. Generally, NP scaffolds are gel-like so they do not enter on this subject, but AF is an elastic solid that is often mimicked by a circular shaped scaffold, not even the disc-like geometry[155]. Even if the disc-like shape is mimicked, the top and down surfaces are not prepared according to the CEPs surface, therefore what is being developed are TE-TDR implants with a high potential to suffer displacement upon spine loading when *in vivo*. A more structural patient-specific type of approach must be addressed, and that is precisely the subject discussed in the next chapter.

5. Future Advanced Strategies for Patient-specific Tissue Engineering: Reverse Engineering and Rapid Prototyping

TERM comprise different treatment strategies in which it can be applied a patient-specific type of approach. The idea is to use the know-how of patient's own cells in order to regenerate a specific tissue. This way, it stimulates the natural way of biological tissue building, in a bottom-up approach, in alternative to top-down strategy, used by repair strategies. Also, by using the patient's own cells, there is a huge decrease in the risk of implant rejection, thus being a patient-specific treatment.

The point where TERM diverges is on the use of a scaffold as a cell support, RM focus on using only cells while TE uses a scaffold combined with cells, as mentioned. In a way, RM treatments in general are patient-specific as far as they can get, but TE can still be more patient-specific that it already is, since scaffolds can be structurally produced according with the patient's needs. For example, if a bone tumour is surgically removed from a patient, and the gap that remains has a cubic geometry of 4 mm in length, then the patient needs exactly a 4 mm scaffold cube. That scaffold geometry is the most appropriate for that patient's defect, but for the next patient probably will not be. Thus, if a patient needs a TE treatment, he will need not only an immunocompatible cell source (patient's own cells) but also a structurally compatible scaffold. The authors believe that this is the challenge that TE is facing, the field needs to progress in this direction in order to produce treatments with even more patient-specificity, re-enforcing this that is the biggest advantage in the TE strategy.

In this sense, RE and rapid prototyping RP technologies can be fused together with TE in order to prepare the next generation type of cell constructs in order to fulfil the patient-specific structural needs. RE concerns the data acquisition and three-dimensional (3D) model preparation, which is followed by RP for processing the material into the desired physical form.

5.1. Reverse Engineering

RE definition first came as the process of extracting the knowledge or blueprint from anything man-made. Now with its increasing potential of use into the TE field, its definition can be extended to the process of extracting the knowledge or blueprint of any given object's structure, whether man-made or not, *e.g.*, biological. This type of engineering concerns the data

uptake of the patient's anatomical structure, more specifically the part that is in need of regeneration, this process is called two-dimensional (2D) image acquisition. Which applied to biological tissues can be made by any imaging equipment system, but it has shown to work well with MRI[174] or CT[175,176]. MRI seems more appropriate for soft tissues and the CT for hard tissues. Although, when applying RE to biological tissues a micro analyser version of these devices is advised in order to acquire the smallest details, which usually are crucial for the mechanical or physiological functioning of the whole tissue.

For conversion and processing of the acquired 2D images several types of software are needed. The acquired raw images, obtained from micro-CT (μCT), are vertical images that are a result of sequential turning either of the analysing object within the imaging device or of both emitter and receiver around the object. These images must be then converted into stack images.

Raw 2D image processing is followed by segmentation, which returns the raw 3D model of the native anatomical structure. In this step the user must select the part of interest within the 2D images. This can be done by creating a mask, and by painting with it slice-by-slice (each 2D stack image at a time) the pixels that belong to the desired anatomical structure. The mask will afterwards be the 3D model, the 2D images are kind of a guide/map for the user to paint what it is thought relevant. It is normal in acquisition to obtain over 300 images from one sample, so this step can be really time consuming. But there are ways to make it faster, in some software there are tools such as "painting with threshold" that enables masking the pixels within a specific grey-scale range. Briefly, the 2D images returned from the μCT are in a grey-scale, in which each pixel has a type of grey that corresponds to a number that is associated to a specific original density (average density of the tissue's area, which corresponds to that pixel). Therefore, if the objective is to select only the bone and not the soft tissues there is the possibility of painting with a threshold that fits in a range of whiter colours of grey-scale. When segmentation is finished a 3D model can be exported, though it usually has a great amount of information, way more than it is needed (*i.e.,* details that cannot be applied in the following steps due to technological limitations regarding RP detail resolution).

Therefore, after the 3D model (*e.g.,* STL format) is done, it needs to be processed in order to reduce its computational size for easier conversion into a 3D printable file format (it depends on the computer system capabilities). There are some software tools that can be used, such as: fix, cut, wrap and fillet, but a good tool to work with is the smoothing, which reduces the surface roughness/detail. However, this is an indispensable step, even for the best computational systems, since the 3D model must mature into a closed surface with every finite element organised in the proper way, *i.e.,* with a positive normal vector and no finite element overlapping[176].

5.2. Finite Element Method

The finite element method (FEM) is a relatively recent methodology, it was developed in the middle of the last century and started to gain interest with the evolution of computational hardware. This method requires a great deal of mathematical calculus, therefore it was only when computers gain the capabilities to handle more complex formulas that it started to be standardly used in the engineering industry. In the last two decades, it revolutionised the world of engineering, and replaced several other methods that did not require a computer, *e.g.*, finite difference method, to use almost exclusively FEM. Before that, engineers made continuum medium analysis of a specific problem by associating it to an already known and extensively studied type of problem, in order to use tables to address the values of unknown parameters. This association is very useful, but it also carries the disadvantage of adding a great deal of uncertainty to the results, *i.e.,* high error factor between real and nominal values. As a consequence of that, more (or stronger) material would have to be used in order for the given structure to be safe, resulting in higher costs than needed, among other things.

Every given geometry can be described by a mathematical model. This formula is generally a complex integral impossible to calculate (or it takes an unreasonable amount of time). FEM uses the problem solving logic called 'divide and conquer', which divides a big and complex problem into several small and simple problems easy to solve. FEM formulation provides the possibility of replacing the integral ruled under the complex domain of the structure (volume *V*) by summation of integrals ruled under sub domains of simple geometries (volume V_i). This technique is illustrated with the following example, which corresponds to the volume integral of the function *f*:

$$\int_V f \, dV = \sum_{i=1}^{n} \int_{Vi} f \, dV \tag{2}$$

In (2) it is assumed that:

$$V = \sum_{i=1}^{n} V_i \tag{3}$$

45

Each sub domain V_i matches a single finite element of simple geometry, such as a triangle, rectangle, line segment, cuboid, among others[177].

FEM is used to create a mesh after segmentation, it literally divides the surface into an assembly of triangles or rectangles (depending on the structure) with different orientations and sizes making up for the whole 3D model.

5.3. Rapid Prototyping

RP was first developed to produce realistic models of given structures, not specifically use them as parts of a mechanism but as models for those parts, in order to help easier spatial visualization. Furthermore, the field evolved into the production of objects with more complex geometries, and made of materials with capabilities of withstanding higher forces or even dynamic handling. Therefore, RP equipment started to be used for industrial production[178].

There are several types of RP technologies divided into two ways of achieving the final object, subtractive or additive manufacturing. While the first removes material until the final object is done, the second is responsible for adding layer over layer until the production is finished. The three most used technologies in 3D printing (Figure 5.2) to be used in the TE field are: (i) selective laser sintering (SLS), (ii) stereolithography (SLA), and (iii) fused deposition modelling (FDM). Other technologies for rapid prototyping are laminated object manufacturing, solid base curing, optical fabrication, photochemical machining, among others, though they will not be described here due to its low interest to be used in the AF scaffold development.

Figure 5.1. Fused Deposition Modelling, 3D printer from Makerbot™.

5.3.1. Stereolithography

SLA (Figure 5.3.1) is the additive polymerization, layer-by-layer, of a material on a moving platform by UV exposure in selective spatial points. This method requires the use of a photo-polymerizable material, which at start is in the liquid state, generally called resin. This resin is placed inside a container, which is then selectively polymerized, following the computer-aided design (CAD) of the desired final object, *i.e.,* the light beam focuses on voxels represented in the CAD model[179].

Due to the limitation for only being able to use photo-polymerizable materials, this method has the tendency to be more expensive. But, on the other hand, the outcomes of it are extremely accurate and precise, with tolerances below 0.05 mm[180,181].
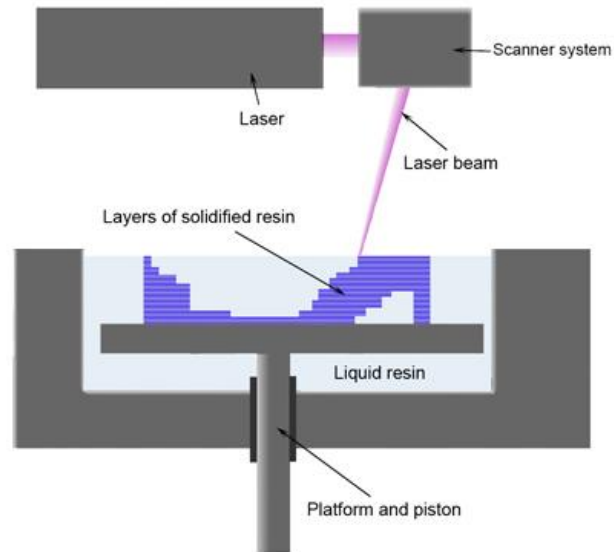
Figure 5.2. Stereolithography process explained in the form of a scheme.

5.3.2. Fused Deposition Modelling

FDM (Figure 5.3.2) uses an extruder nozzle composed by heating chamber used to fuse a material, generally a polymer or a metal. The melted material is extruded through the nozzle in areas specified by the CAD model, layer-by-layer, until the object is complete[182]. The STL file input is generally converted into a G-code file, which converts the CAD model into a group of virtual filaments that altogether make up for the 3D model. These lines are the path taken by the extruder while extruding the fused material, which after a few seconds of being at room temperature it starts to solidify.
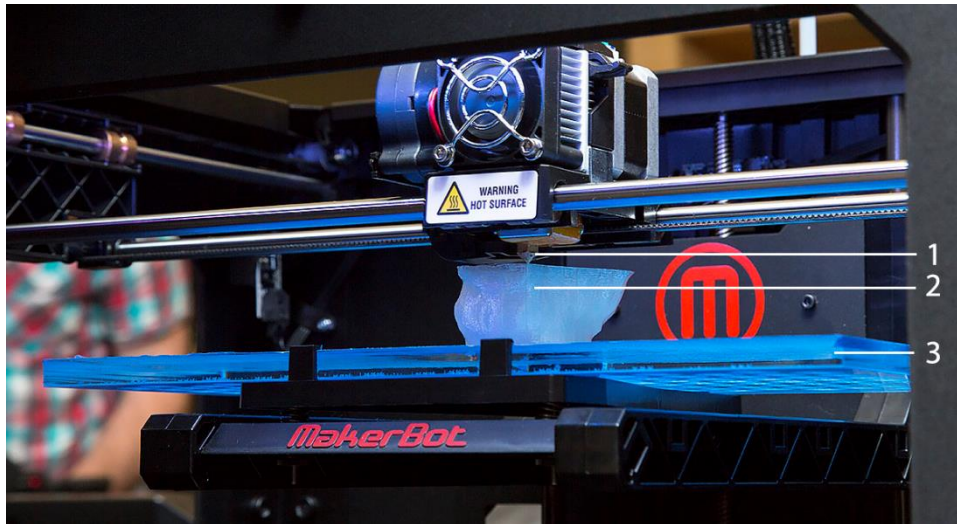
Figure 5.3. Fused Deposition Modelling process: (1) heat extruder of melted material; (2) aggregated deposited polymer filaments; (3) printing bed.

The most tempting advantage of this method is the extremely low-cost of the equipment system. Recently 3D printing based on FDM became very popular among hobbyists due to its low cost 3D printers (1,000-3,000€), and its popularity is growing with time.

Comparing with SLA this method is more appropriate to construct bigger objects due to its cheap available filament polymers: acrylonitrile butadiene styrene, PLA and PVA. Although several other materials can be used as long as the extruder's heating head is able to fuse it[183,184].

5.3.3. Selective Laser Sintering

The idea behind SLS (Figure 5.3.3) is not far from SLA, though they handle materials in different phase state. While SLA uses at start a liquid material, the second handles the material in the form of powder. This technology applies a laser in a selective way to join the granules of the powder together, *i.e.,* sintering, in order to create the 3D structure[185].
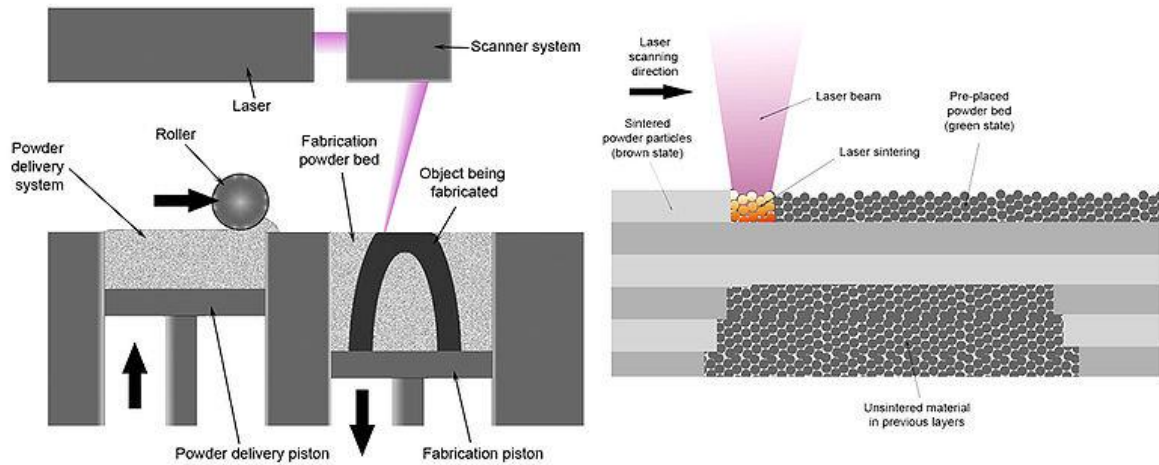
Figure 5.4. Schematic representation of Selective Laser Sintering process.

Briefly, the CAD model is first divided into a finite number of thin slices, and the data is then uploaded to the manufacturing equipment. The equipment first adds a layer of the powder material that is then exposed to a laser beam that only focuses on the respective areas of the CAD's first slice, resulting on the sintering of this layer whereas the rest of the material remains in the powder form. After, the platform moves down, and the next layer of powder material is applied, the process repeats itself by following the next slices of the CAD model until the object is finished[186,187].

In general, all structures manufactured using any of these technologies, or others, can be used for a functional purpose. It depends on the technology being applied, but it mainly depends on the material that is used. Furthermore, it is possible to analyse if a material will serve the final purpose, since it is possible to simulate the CAD model under several physical situations by introducing in the software the known values of the mechanical behaviour parameters related to the material that is after used. The result will give an estimate on if the structure made with a certain material will have the minimal requirements for a given function or not[188].

5.4. Reverse Engineering and Rapid Prototyping Technologies Applied to Tissue Engineering

The first thing that must be kept in mind, when using RE and RP in TE (Figure 5.5), is that the accuracy and resolution of the prototype in comparison with the original native tissue is limited by the less precise equipment used in the whole process – from acquisition to 3D printing. In general, the computational modelling does not interfere with the outcome resolution of the final scaffold, all it is needed is a good computer to be able to handle the amount of processes needed for the modelling. In the end, this limitation is placed between properties of the μCT and the 3D printer. Comparing the state of the art between both technologies gives a better outcome for the imaging side, which provides the conclusion that the 3D printer normally limits the resolution of the final prototype. A μCT can have a resolution down to 7μm (1072 μCT; Skyscan, Belgium) isotropic detail detection, while an SLA 3D printer has a resolution in the order of 25 μm (The Form 1 3D Printer; Formlabs, USA). All of this must be analysed before working with 3D modelling since there is no need for extensive computational processing in details smaller than the limited resolution of the whole RE and RP process (*i.e.*, <25 μm), which can be extremely time consuming.
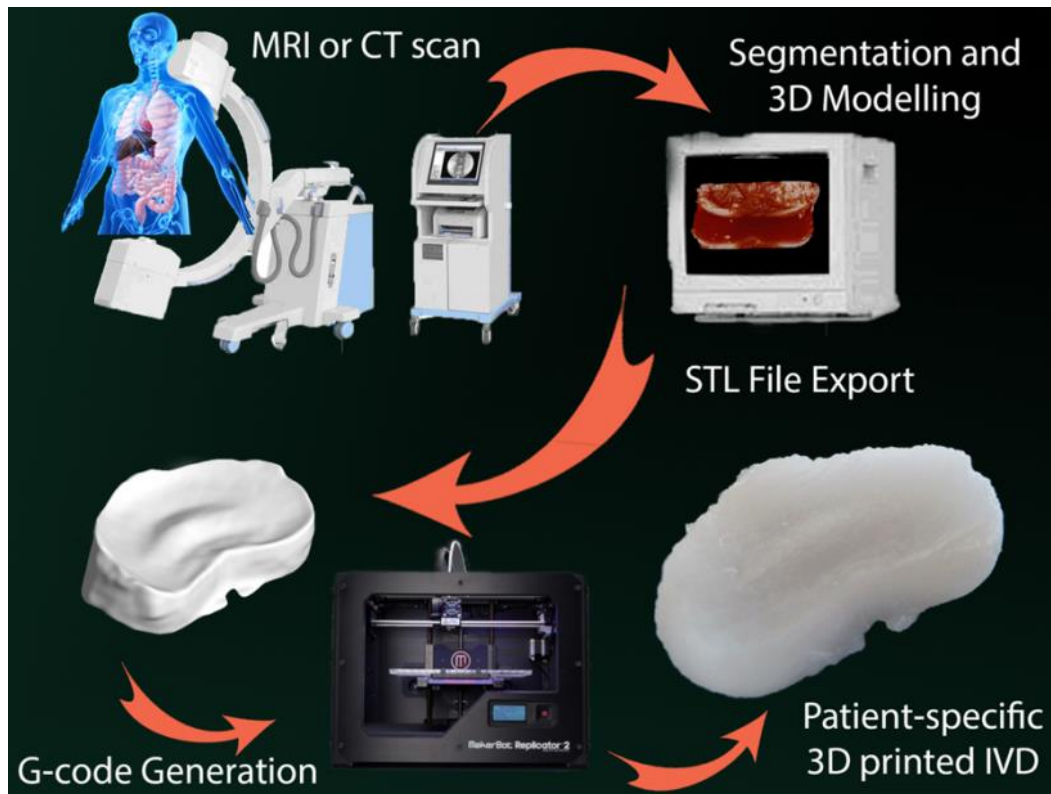
Figure 5.5. Schematic representation of Reverse Engineering and Rapid Prototyping allied to an intervertebral disc Tissue Engineering strategy (which was followed in this work).

Several strategies can be taken when using RE and RP together with TE, but can be resumed down to two strategies: solid-based scaffold preparation or solid-free-based scaffold[189]. In order to choose between strategies, one thing must be decided before – will the cell construct mature before or after implantation, *i.e.,* will it mature *in vitro* or *in situ*? This is especially important if the tissue to be replaced is subjected to mechanical stimulus or not, in other words, if the tissue has or not a biomechanical function? In a way, if a solid-based cell construct is matured *in situ* then it can be classified as a short-term repair strategy while the cell construct is maturing, and with time it has a regenerating effect, *i.e.,* in middle-term and long-term. The advantage of this approach is the low amount of time between cell isolation until implantation, but with the disadvantage of balancing the mechanical properties of the scaffold (while it degrades) versus mechanical properties of the native healthy tissue for mimicking reasons, and the degradation time versus regeneration rate (ECM production) to avoid gaps of malfunction along the treatment.

Solid-free-based cell construct is a concept developed and used by Gabor Forgacs, Anthony Atala and their co-workers[189–193]. The concept has a lifetime of around a decade, but holds great promise[189,190]. A two year company, named Organovo™, has been created based on

all the work performed by him and his team, which was considered the most innovative company in the world in its first year of life, and in 5 months had an increased share price around ~600%, though with a similar decrease afterwards but it only means that investors are watching its evolution very closely. Its concept was named Bioprinting[192], which uses high-resolution 3D printers that build structures in an additive manner, like other 3D printing technologies. But instead of delivering filaments of fused material or polymerizing specific sites of the resin material, it deposits spheroid units. Spheroids, following their definition, are units of cell pellet in a spherical shape, although it can have other shapes (*e.g.*, ellipsoids)[193]. By adding spheroids following a CAD model, the spheroids will automatically fuse together, upon cell construct maturation *in vitro*, allowing a three-dimensional support of its cells and its ECM product. Spheroids can be made of different types of cells, and several different types of spheroids can be used easily when bioprinting a cell construct. In this manner, the printing possibilities are massive with no significant degree of difficulty in comparison with its potential. Briefly, the process of making spheroids starts by releasing the cells from the culture flask and typical centrifuging. The pellet is then re-suspended in 4mL of medium and cultured in a small culture flask for one hour on a gyratory shaker. Then the solution is extracted and centrifuged at very high speed, *e.g.*, 3500 rpm. The pellet is transferred to a capillary micropipette that, then, extrudes a cell pellet filament to be further cut into small equal fragments with a diameter of 300 or 500 µm. These small pellet pieces are then left on a gyratory shaker to round up, by being cultured in suspension flasks. These spheroids have defined diameter/volume and cell number[194].

5.5. Authors' Considerations on Tissue Engineering the Intervertebral Disc Using Bioprinting Technology

Take for example the IVD structure as a possible application of this concept. Its biological formulation varies radially – from the centre to the periphery. A range of different types of spheroids could be made with different percentages of two or three types of cells (AFCs + NPCs, AFCs + MSCs, MSCs + NPCs or AFCs + MSCs + NPCs). Each type of spheroid would be introduced inside one syringe. The system would work with the same concept of regular FDM printers, with the difference of replacing the heat extruder with a precise micro-syringe pump. The ability to change the syringe in the middle of the bioprinting process would be provided, at the same time delivering precise amounts of spheroids down to one-by-one.

Each voxel, *i.e.,* 3D imaging unit (3D version of a pixel), of the 3D model would belong to one spheroid, and each layer would be bioprinted one at a time and each radial IVD filament would be printed with the same syringe/type of spheroids. This is still a preliminary idea since the cell constructs would have several maturation possibilities. However, by encapsulating also bioactive molecules that stimulate the right phenotype and with external mechanical stimulus in the right differentiation line, by using a bioreactor, with progressing pressures, it can be that the only maturation possibility would be the correct one, *i.e.,* towards a healthy native IVD. This way the native morphology of a healthy IVD would slowly appear until full maturation. Then again, this will be a rather time consuming process as well as expensive, (even) when optimized, since it would require GFs and, probably, serum-free chemically defined medium.

Bioprinting technology, despite being still under optimization, for now it seems promising to be used for regeneration of non-mechanic-subjected tissues. This way cell construct maturation can occur partially already *in vivo*. However, when the method is applied to tissues that are subjected to mechanical forces, *e.g.*, cartilage, the cell construct must almost fully mature *in vitro* before implantation, in order for it to have the capability to withstand compression present in the tissue and be able to function biomechanically (Table 5.1). This is an obstacle that solid-scaffold based TE strategies do not have, since the scaffold is mechanically functional while the tissue is maturating *in vivo*, *i.e.,* it employs a short-term repair strategy.

Table 5.1. Solid-free based TE versus solid-scaffold based TE for regeneration of mechanically subjected tissues.

Strategy	Solid-free based TE	Solid-scaffold based TE
Maturation	*In vitro*	*In vivo*
Advantages	Predictable after implantation - safer; Fast integration with surrounding tissues.	Rapid preparation and application; Simpler; Cheaper.
Disadvantages	Expensive; Complex; Slow preparation.	Less predictable; Can suffer implant displacement.

In addition, the maturation of the cell construct takes a long time if not accelerated, since the process requires production and deposition of ECM until its typical amount, on a native healthy tissue, is reached. Therefore, for tissues such as the IVD, the authors believe that bioprinting strategies still need optimization in order to be successfully used in the clinics. Moreover, solid-based cell construct's preparation looks more suitable since it enables the production of a cell constructs that can be minimally matured in a bioreactor until implantation,

and have the major part of its maturation *in vivo*. This because the cell construct has a solid part that can in the short-term after implantation serve has a repair strategy, by providing mechanical support and function for the whole tissue. At the same time, cells carried inside can produce ECM while the scaffold structure is being degraded. Therefore, a cheaper and easier alternative to bioprinting is to use SLA or FDM 3D printing in a RE solid-based TE strategy.

6. Final Remarks and Future Trends

The IVD is a complex natural shock absorber system that is arranged in an incredible fashion, taking advantage of viscous gel liquid with an elastic soft tissue. NP regeneration substitutes, namely hydrogels carrying cells look very promising, and seem ready to be tried in the clinics. But IDD settles without warning the patient until it is in a severe state, since LBP is triggered only then. Generally that is the case when the patient seeks for medical attention. Annular tears are associated with AF tissue degeneration, thus it reveals loss of full capacity to support the NP efficiently (the remaining NP volume after discectomy), as much a hydrogel (extra volume added to the remaining NP volume). Thus, strategies aiming for regeneration of both AF and NP tissues seem to have a better probability of reaching the clinics, but an ideal AF regeneration substitute is still missing.

A possible strategy, to produce an AF scaffold, is to use technologies that are only now reaching the TE field, although they have been used in industrial engineering for decades. RE combined with RP might have the potential to produce the ideal AF scaffold, though these technologies still need optimization to better analyse and reproduce the micron level, and furthermore the nano. Imaging technologies are already able to acquire data at the sub-micron level, it is a question of time until it evolves to an even higher resolution. This would provide the AF tissue's details to prepare an accurate 3D model that could then be employed in a direct laser writing RP technology system. This way the lamellar morphology of this tissue could be mimicked, which would offer a better chance for the AF tissue to regenerate, as well as the NP.

The next obstacle will probably be the implant displacement already being seen in the IVD repair field. The solution to this problem could be a biodegradable stent, surrounding the TE-TDR implant and both adjacent vertebrae that would remain in position until implant integration.

Another problem will be the lack of data imaging from how the degenerated patient's IVD was, when healthy, in order to reverse engineer it. But as long as the top and down CEPs' surface topography is recordable the only parameter lacking is the correct IVD height. And that can be calculated by statistically studying the average height of the IVD according with its other dimensions.

The future IVD TE strategies will certainly rely on stem cell differentiation. Human NPCs' isolation generally is contaminated with other types of cells from the foramen region, upon discectomy, and NPCs tend to be already senescent due to IDD. The use of these cells is interesting in TE research, but when a strategy actually goes to clinics it will need a sustainable

cell source. Therefore, the differentiation pathways towards NPC type still need to be cleared and optimized.

Moreover, the *in vitro* culture conditions for TE-TDR implant maturation are needed for this type of strategy to be successful. Thus, IVD TE lacks a tunable hypoxia (2% O_2) bioreactor for both compression and hydrostatic pressure conditions, for culturing TE-TDR implant and NP cell constructs alone, respectively.

The emerging and promising next generation of engineered NP will rely on the production of scaffolds with functional cues, aiming at driving proper IVD regeneration. In this sense, an interesting approach would be the combination of scaffolds with NPCs, or stem cells, with GFs to stimulate NPC phenotype, cell migration, differentiation and tissue remodeling, respectively. The delivery of relevant biochemical cues by drug delivery systems would allow their sequential release in a manner that mimics the temporal profile of the healing process *in vivo*. TGF-β1 has been shown to guide the differentiation of stem cells towards NPCs, whilst TGF-β3 is an important protein to maintain their phenotype. Moreover, for the regeneration to be successful in the long-term, a GF or a drug (*e.g.,* bevacizumab) release system would avoid angiogenesis on newly formed tissue[195]. Though GG based hydrogels shown to be non-angiogenic it degrades while tissue regenerates thus allowing angiogenesis to occur while tissue regeneration reaches a stable level. Therefore, a particulate system that allows the release of both proteins and drugs, in a sustained and independent fashion, would facilitate cell attachment, proliferation and differentiation of NPCs in a synergistic manner as well as disable the possibility for angiogenesis.

II. Patient-Specific Tissue Engineered Total Disc Replacement

1. Hypothesis

Intervertebral disc degeneration (IDD) is the main cause for low back pain (LBP), to which the standard available treatments address the symptoms and not the disease, possibly followed by serious side effects. A small percentage of patients become chronic, but are these cases that weigh the most in LBP's worldwide socioeconomic impact estimated at 70 billion euros per year[1]. Therefore, the cost per patient is very high meaning there is a gap in the medical market for more sophisticated treatment strategies. Therefore, effective treatments for IDD should minimize the suffering of a great number of patients as well as reduce its socioeconomic impact.

By analysing what was discussed in the *General Introduction* it can be stated that a fully regenerated intervertebral disc (IVD), in severe IDD cases, can be successfully achieved by means of using a tissue engineering (TE) strategy. In fact, TE holds the potential to have in the future the advantages of all treatment strategies: short-term repair, long-term regeneration, and LBP neutralization. Several TE strategies for the NP or total IVD regeneration have been described elsewhere in the scientific literature[4,8,15,118,137,172,173]. For nucleus pulposus (NP) regeneration alone, several hydrogels have been developed for supporting native NP cells (NPCs) (acellular scaffolds), or for carrying mesenchymal stem cells or NPCs, namely alginate[118], carboxymethylcellulose[15], hyaluronan[8], among others[1]. Gellan gum (GG) hydrogels have been suggested as a suitable platform to support NPCs functions as well as to avoid angiogenesis that helps to maintain hypoxia levels inside the NP, thus stimulating NPC's phenotype[59,105]. The methacrylation of GG allowed tuning of its mechanical properties for mimicking the NP by controlling the reaction time of the methacrylation[9,143,15,16]. However, despite the considerable progress in engineering the NP of IVD, none has led to translation to clinical implementation. One of the reasons is lack of effective strategies to regenerate damaged annulus fibrosus (AF), since the NP regeneration strategies alone cannot effectively prevent re-herniation in severe cases, and in average patients show signs of AF degeneration. Therefore a support material is needed to help holding the newly restored NP. As a component that plays a critical role in the biomechanical properties of the IVD, the structural integrity of AF is essential to confine the NP and maintain physiological intradiscal pressure upon loading[147]. The most used polymers for the production of AF scaffolds are mainly collagen[155–158], and aliphatic polyesters that includes polylactic acid [151,196], polyglycolic acid [151,152], and its copolymers. The currently available literature describes that the majority of AF scaffolds have been mainly

processed by electrospinning in the form of nanofibers, which have been showing good results[146]. Polycaprolactone (PCL) in particular, has been proposed for several biomedical applications, including TE, due to its chemical versatility[197], easy processability and tuning possibility of the mechanical properties to match a desired role[198]. Though, PCL has a bigger elastic domain than other candidate materials, *i.e.,* higher resistance to plastic deformation[147], due to its low melting-point (~60ºC).

In terms of cellular AF regeneration strategies, they mainly consist in the usage of AF cells (AFCs), which are characterized as fibroblast-like[57]. At the same time, TE strategies often face the problem of fibroblast invasion, for IVD regeneration this becomes a solution, thus making acellular AF constructs seem more appropriate.

Despite the several promising studies to fully regenerate the IVD[152,158,167,196], none until now as achieved a precise replication of a customized IVD scaffold to prepare a TE-total disc replacement (TE-TDR) implant. By observing the state-of-the-art outcomes of IDD repair strategies, which are already being applied in the clinics, it is noticeable to presume what can go wrong in implanting a TE-TDR, *i.e.,* implant displacement[170]. Therefore, patient specificity is important for achieving better implant integration (whether in a TE or in a repair approach) and thus reducing the risk of dislocation. That is precisely our main concern with this work.

Herein, it is proposed an innovative customized implant for total disc regeneration, specifically for AF substitution, by means of using reverse engineering (RE) and rapid prototyping (RP) technologies. In this sense, it was established a method using micro-computed tomography (μCT) equipment for intervertebral space stack image acquisition to three-dimensional (3D) model a customized virtual IVD replica (STL. File) for further G-Code refinement using a rabbit spine model as proof-of-concept. Injectable GG hydrogels have been shown to be a suitable platform to support and deliver cells for non-invasive injectable TE applications[138]. With this in mind, and aiming at mimicking the NP structure within the TE-TDR implant, rabbit NPCs have been encapsulated in the GG-MA hydrogels and cultured *in vitro* up to 21 days. The viability of both NPCs and lung fibroblasts cell line (L929) was investigated by Live/Dead staining assay and DNA quantification. The NPCs' proliferation profile in the methacrylated gellan gum (GG-MA) was assessed by mitochondrial activity over the 21 days of culture and compared with the same assessment for L929 cell line encapsulated as well in GG-MA.

2. Materials and Methods

2.1. Spine Segments Extraction and Discriminated Intervertebral Disc Cells Isolation

In order to fulfil this work's objectives, rabbit spine segments were extracted for the purpose of discriminated isolation of IVD cells (separated isolation of AFCs and NPCs) and μ-CT imaging analysis (a total of four rabbits were sacrificed; 4 weeks old, ~1.3 Kg; 8 weeks old, ~1.7 Kg; 9 weeks old, ~1.9 Kg; 10 weeks old: ~1.9 Kg). For each rabbit, the dorsal region was opened by 2 parallel sagittal scalpel cuts, one at each side of the vertebral column. When all the internal dorsal tissues were cut the entire spine was lifted, both top and down extremities were cut, alongside with the ribs, in order to get the vertebral column loose. Furthermore, the internal ventral tissues surrounding the spine were also cut, leaving it detached from the rest of the rabbit. The spine was separated into two segments with a scalpel incision in one of the middle-bottom thoracic IVDs (between T7 and T11 vertebrae) and placed in 50 mL conical tubes already filled with 25 mL of 10% antimycotic and antibiotic solution (ATB) in phosphate buffered saline (PBS) solution and placed at 4ºC until used.

One lower spine segment containing the lumbar IVDs was reserved for the μ-CT analysis, while the remaining spine segments were processed for IVD cells' isolation. Briefly, all muscle and ligament covering the thoracic and cervical spine segments were removed. A clean transverse scalpel cut was made in each IVD to allow access to the NP tissue. Bending the two adjacent vertebrae in opposing directions exposes the tissue. Furthermore, with the end of the scalpel blade, the NP tissue alone, *i.e.,* without pieces of AF or other adjacent tissues, was removed and placed in a Falcon tube with 25 mL of PBS. In each IVD, after the NP tissue had been removed, both parts of the AF tissue were cut off from each corresponding cartilaginous endplate (CEP) with a scalpel, washed with PBS and placed in a conical tube with 25 mL of PBS.

Both types of cells/tissue suspension were centrifuged at 340 *g* for 3 minutes, at -4ºC. The supernatant was discarded and the same PBS washing procedure was repeated 2 more times. The tissue fragments were then suspended in a solution containing the same proportions of Dulbecco's modified Eagle's medium and nutrient mixture F12 (DMEM:F12; Invitrogen, USA), with the pH adjusted to 7.4, supplemented with 10% (v/v) fetal bovine serum (FBS; Alfagene, USA), 1% (v/v) of ATB, and 0.25% (w/v) collagenase. The tubes were incubated at

37°C in a humidified atmosphere of 5% CO_2. Enzymatic digestion time-points were collected every hour, this procedure was made by filtrating the suspension using a 100 μm pore size cell strainer and further centrifuge the solution at 340 g for 3 minutes, at -4ºC. Then, instead of discarding the centrifuge supernatant this was used to wash the remaining tissue trapped in the filter in order to continue the enzymatic digestion. The pellet was re-suspended in medium and centrifuged again in the same conditions. This washing process was repeated two more times. Finally, the pellet was re-suspended in medium and seeded in T25 flasks. The AF tissue digestion retrieved more cells at the 4 hours' time-point while the NP tissue had a better outcome at the 2 hour time-point. By making several time-points while the digestion is occurring, instead of only doing one at the end of the digestion period (around 24 hours of enzymatic digestion), it avoids already freed cells to be exposed to the harsh enzymatic environment that greatly reduces the amount of sub-cultures before the cells lose significantly their native phenotype. Both cell types were expanded until the third or fourth passage before each culture assay, always having the medium replaced every second or third day.

Note: During all isolation process, cells/tissues from different rabbits were always kept separate, as well as later on through the *in vitro* assessment.

2.2. Replicating the Annulus Fibrosus: Scaffold Preparation

2.2.1. Reverse Engineering of Rabbit Intervertebral Disc

The imaging analysis and 3D modelling was performed on rabbit spine segments of the lumbar region, to access the design of the IVDs most commonly affected by IDD. After the spinal lumbar segments were extracted, the IVDs were separated from the spine segment by making scalpel straight incision alongside the CEPs and vertebrae, leaving the whole AF and NP tissues completely intact.

2.2.1.1. Micro-Computed Tomography of Rabbit Intervertebral Discs: Acquisition

The designs of fresh IVDs were acquired by μ-CT (Skyscan 1072; Skyscan, Belgium) for two-dimensional (2D) raw (images that live in the YZ plane domain) imaging acquisition.

The analysis was processed with a final magnification of 13.18 µm/pixel, and with source parameters of voltage and intensity adjusted to 89 kV and 112 µA, respectively.

2.2.1.2. Conversion and Processing of Raw 2D Images into 2D Stack Images

The NRecon software (Skyscan, Belgium) was used for processing the acquired raw 2D images. Briefly, the areas that did not contain the IVD were discarded as much as possible throughout the whole RE procedure. The grey-scale threshold was adjusted to only take into account the pixels with grey between 80 and 255 grey-scale units (every pixel below 80 was turned into 0, *i.e.,* black) to subtract any signal noise*. The images were processed for misalignment (which had a starting value of -1.5), smoothing, ring artefact reduction, beam hardening correction and finally saved as 2D stack images (images that live in the XY spatial plane domain). Before segmentation for 3D modelling and to help on that following process, the images were aligned using Dataviewer (Skyscan, Belgium).

---

* The µ-CT analysis emits a signal on one side (0º) of the acquisition chamber, which is collected on the other side (180º) of the acquisition chamber, after crossing the object being analysed. Depending on the material's (being trespassed) density, the sensor detects from none (0 or 0%) to total (1 or 100%) the amount of radiation being emitted. Thus, the amount of radiation reaching each small square that composes the sensor is converted into a number between 0 and 255 corresponding to the material's density, which is directly involved with the signal deviation. Generally the numbers are inversely proportional for the sake of intuition, since the lack of signal means that a higher density material is being analysed, which in medical imaging generally indicates bone that is white. Therefore, 0% of the signal recorded is generally represented as total white that is equal to 255 in the grey-scale while 100% signal recording is represented in black and is equal to 0 in the grey-scale. In the end each image is composed of a limited, but generally large (1024x1024 pixels), number of pixels all ranged in the grey-scale both represented by a type of grey and a number that is directly related to its original density. After 180º rotation during acquisition and several images acquired, *e.g.,* 412 images if each step takes a rotation of 0.45º, it is possible to process the images and process them into a 3D view composed of voxels that follow the same representation logic of the pixels but have an additional space parameter (cubes instead of squares).

2.2.1.3. Three Dimensional Modelling

The segmentation process of the 2D stack images was performed using Mimics software (Trial version; Materialise, Belgium) by creating only one mask, which was chosen to cover the appropriate pixels that enclosed the areas of interest in each 2D image, *i.e.,* the areas representing the AF and the NP. Therefore, the 'Threshold' tool was employed to mask the pixels of interest, which are selected according with the specified range of tissue density (represented by a specified range within the grey-scale). Then, the raw 3D mesh was exported from the mask.

In this step, the raw 3D model file previously acquired using Mimics was then uploaded to the 3-Matic software (Trial version; Materialise, Belgium). The 3D model was analysed for 'dirty' Geometry, *i.e.,* holes in the model's surface, inverted triangles, overlapping triangles and angles between elements smaller than 45° angle[199]. The holes were then closed. Triangles were reverted to an optimal position, *i.e.,* the normal vectors of each inverted triangle were converted to a positive value. Overlapping triangles were substituted by one triangle or a set of well-arranged triangles. Sets of triangles composed of angles smaller than 45^{0} were replaced by a more smother surface. Each one of the four tools herein described when applied can create defects that must be corrected with the other tools, *e.g.,* if holes are closed in a designated surface, the process can easily create other defects such as: overlapping triangles, inverted triangles, or even small angles. Therefore, this step is a positive spiral between the four corrective domains until the whole surface is corrected, according with the four surface's error checkers. Using different software could bring more or less surface's error checkers, which would contribute to a more or less faithful RE process.

After the mesh was created and corrected, it was smoothened until a desired resolution detail, in order for the afterwards exported STL file to have a reasonable size for the RP equipment to be able to 3D print it. Too much model resolution stalls the rapid prototyping process without any extra benefit, since the resolution is conditioned by the rapid prototyping equipment's resolution (100 μm). With the 3D model optimized, several different pore geometries were made on the top and down lids of the model, in order to make the interior accessible for medium to enter. These porosities were designed only on the two surfaces that are in contact with the vertebrae, in the native IVD, and even so they were restricted only to the NP area (in the middle of the surfaces following the 2D NP transaxial images). Also simplified versions of the vertebrae contact surfaces with the native IVD were also modelled to prepare the top and down moulds of the IVD as adapting pieces that will allow, in future work, for the scaffold to be pressurized while in culture, in resemblance to the native cyclic pressurized conditions known to exist in the IVD.

2.2.2. Rapid Prototyping of the Rabbit Intervertebral Disc's 3D Model

The RP was made using a desktop 3D printer (Replicator 2; Makerbot, USA), which is a fused deposition modelling (FDM) technology equipment. The AF scaffolds were printed in PCL (Flexible Filament; Makerbot, USA) at a fusion temperature of 100ºC. The parameters chosen in the 3D printing software (MakerWare; Makerbot, USA) were 1 shell, 100% infill, 100µm layer height and 200% scale of the original rabbit IVD (still half the size of a human IVD, thus more challenging due to resolution limitations). The printing speed was established for 45 mm per second of extrusion and 90 mm per second without extrusion.

2.3. Patient-Specific Annulus Fibrosus Scaffolds Assessment

2.3.1. Micro-Computed Tomography Analysis of the Replicas

The PCL scaffolds were analysed by µ-CT, following the same protocol described in the x-ray 2D slices' acquisition of the fresh rabbit IVDs (please see "*Micro-Computed Tomography of Rabbit Intervertebral Discs – Acquisition*"), with different parameter values, though. The analysis magnification was set to 19.13 µm/pixel, and the electrical voltage and current were adjusted to 37 kV and 226 µA, respectively. The resulting raw 2D images were processed also following the same protocol described above (please see "*Micro-Computed Tomography of Rabbit Intervertebral Discs – Conversion and Processing of Raw 2D Images into 2D Stack Images*") with the slight change in the grey scale threshold selected, which was set between 40 and 255.

Moreover, the CT Analyser software (Skyscan, Belgium) was used to further process and analyse the scaffolds' and native IVD's porosity and structure thickness. The processing steps comprised (a) filtering of the Gaussian blur type (3D space) with a radius of 5.0, (b) again grey-scale thresholding between 40 or 80 (scaffolds or native IVD, respectively) and 255 and (c) region-of-interest shrink-wrap mode (3D space) that stretches the model over holes with a diameter less than 4 voxels. Furthermore, the 3D analysis was made to both replicas and native IVD after each processing.

2.3.2. Scanning Electron Microscopy

The surface and porosity morphologies of the scaffold were assessed by scanning electron microscopy (SEM), without any *post*-treatment (*e.g.,* hydration, fixation) after 3D printing. Though, they were mounted onto stubs with carbon double-sided tape and further gold coated. The specimens were observed using SEM equipment (JSM-6010LV; JEOL, Japan) operating at 10 kV.

2.3.3. Mechanical Testing

The AF replica scaffolds were assessed for their mechanical properties using universal mechanical testing equipment (model 5543; Instron, USA). The surfaces of the test samples in contact with the equipment's compression plates had to be plain for a homogeneous compression of the whole scaffold. Therefore, in the segmentation process (see "*Three Dimensional Modelling*") the top and down surfaces were filled with mask until they became plain.

Moreover, in order to calculate correctly the sample's mechanical properties they had to be in a simple geometry, *e.g.,* cylinder, cuboid, and prism. Thus, the scaffolds were punched into a cylindrical shape with the largest diameter possible, which for all specimens varied between 9.8 and 10.1 mm in diameter and 6.6 and 7.0 mm in height. These measurements were made to each sample before it was loaded into the equipment, to serve as input parameters in the equipment's software.

The samples were tested in dry and hydrated states, in which the second required the extra step of immersing the samples in PBS for 5 hours before the assessment. On both states, the samples were conditioned at room temperature in a dry environment for at least 48 hours before being processed for assessment. The tests were performed under uniaxial compression and its Young's modulus was determined in the straightest linear region of the stress-strain graph, by means of using the secant method. Each condition was assessed for six replicates.

2.3.4. Scaffold's Cytotoxicity Assessment

In order to verify the possibility of using these AF scaffolds as a TE strategy, they were assessed for cytotoxicity. Therefore, AFCs and immortalized mouse L929 were independently cultured in 96-well tissue culture polystyrene (TCPS) plates at a cell density of 20×10^3 cells/well for 24 hours in chondrogenic medium solution of DMEM:F12 supplemented with 10% (v/v) FBS and 1% (v/v) ATB, at 37°C and in 5% CO_2 atmosphere. In the same time frame, both PCL scaffolds and latex (negative control) were embedded independently in 20 ml of the same type of culture medium in a quantity of 4 g and 120 cm^2 (less than 0.5 mm thick; accounting with the surface area of both sides: 2×60 cm^2) clipped in 0.5×5 cm^2 sections, respectively. Both extractions were run during 24 hours (in parallel with the cell's attachment to the TCPS), in a water-bath, at 37°C and with a shaking rate of 60 rpm.

After the 24 hour period was complete, each extraction was filtered through a 0.45 Fm membrane into a sterile conical tube. These mediums alongside with the medium without extraction (positive control) were added independently to the wells seeded with cells in the day before. All conditions were left in culture for 24 hours and 72 hours, after which the metabolic activity profile was assessed. The experiments were performed by using twelve independent measurements per condition.

2.3.4.1. MTS assay

MTS (3-(4,5-dimethylthiazol-2-yl)-5-(3-carboxymethoxyphenyl)-2-(4-sulfophenyl)-2H-tetrazolium) assay was performed to assess the metabolic activity profile previously addressed. The cultures were incubated in 350 µl of phenol red-free DMEM culture medium solution, with the already mentioned supplements, together with CellTiter 96® Aqueous One Solution Reagent (Promega, USA), containing MTS reagent, at 5:1 ratio. The samples were incubated in the dark in a humidified atmosphere at 37°C and 5% CO_2 for 3 hours. After the incubation period, 100 µL of the solution was transferred from each well in triplicate to a transparent 96-well plate. Furthermore, the optical density (OD) was determined at 490 nm, by Synergy HT multi-detection microplate reader (BioTek Instruments, USA). The resulted OD for this type of assay is proportional to the cellular activity, being what is believed to be a measurement of the cell culture's total mitochondrial activity.

2.4. Nucleus Pulposus Cell Construct Preparation

2.4.1. Methacrylated Gellan Gum Synthesis

The methacrylation of gellan gum was performed by reacting Low Acyl Gellan Gum (LA-GG; Sigma-Aldrich, Germany) with Glycidyl Methcrylate 97% (GMA; Sigma-Aldrich, Germany) at 20-fold molar excess in respect to the repeating unit of LA-GG, as previously described by Silva-Correia *et al.* (2010)[105], and based on a study performed by Li and co-workers (2003)[200]. Briefly, LA-GG was added to deionized water, at room temperature and under vigorous agitation, with required quantities in order to achieve a final concentration of 1% (w/v). The solution was then heated until 90ºC, where it was maintained constant for 30 minutes to 1 hour, aiming to dissolve the LA-GG completely. The solution was allowed to cool down to room temperature overnight. An appropriate amount of GMA was added to the solution, with the objective of achieving a 20-fold molar excess in respect to the repeating unit of GG. The pH was raised to 8.5 with 1 M sodium hydroxide (VWR, USA), and maintained constant during 24 hours, by means of using a micro syringe pump (Fusion 200; Chemyx Inc., USA). GG-MA was precipitated by adding half the solution's volume of cold acetone (VWR, USA). Moreover, the solution was dialysed against deionised water for 7 days using a cellulose membrane (MW cutoff 12 kDa; Sigma, USA), in order to remove the acetone and remaining GMA. Finally, the GG-MA was frozen at -80ºC overnight and lyophilised for 7 days to obtain it in the stable off-the-shelf state of water-free foam.

2.4.2. Preparation of Ionic Methacrylated Gellan Gum Hydrogel Discs

The lyophilised GG-MA was sterilized under an ethylene oxide gas atmosphere. The GG-MA solution was obtained by dissolving the lyophilised GG-MA in distilled water at a final concentration of 1.5% (w/v), and left overnight under vigorous agitation at room temperature. In order to achieve the polymerized disc form (6 mm in diameter and ~3.5 mm in height; 100 µL in volume) the GG-MA solution was pipetted into a multidisc polycarbonate mould plate (moulds with 6 mm in diameter and 5 mm in height), and PBS was added over to plate with enough volume to cover the mould plate. The apparatus was left this way up to 30 minutes aiming for ionic polymerization of the hydrogel.

2.4.3. In Vitro Culture Studies of Encapsulated Nucleus Pulposus Cells

2.4.3.1. In vitro cellular encapsulation

In order to encapsulate NPCs within GG-MA discs, approximately 1×10^7 cells/mL were re-suspended in 1.5% (w/v) GG-MA solution (prepared as previously described, prior to its polymerization). After homogeneous dispersion, the GG-MA cell suspension was inserted in a polycarbonate mould being further polymerized as previously described. GG-MA discs in the absence of cells were also prepared, to serve as negative control while in culture.

The GG-MA discs, with or without encapsulated NPCs, were further cultured in a chondrogenic medium solution of DMEM:F12 supplemented with 10% (v/v) FBS and 1% (v/v) ATB, at 37°C and in 5% CO_2 atmosphere for different periods of culture (depending on the type of assay performed afterwards), until up to 21 days.

2.4.3.2. Live/Dead Viability and Adhesion Assay

Cell adhesion and viability were investigated by Live/Dead assay, which consists on using two types of probes namely calcein-AM (green; Molecular Probes, Life Technologies Corporation, USA)) and propidium iodide (red; Alfagene, USA) that marks live and dead cells, respectively.

Briefly, the medium was removed and the samples were washed three times with PBS. Then, 1 mL of PBS solution containing 2 μg/mL of calcein-AM and 1 μg/mL of Propidium Iodide was added to each well and left for 1 hour at 37°C in a humidified atmosphere of CO_2. Moreover, the samples were observed under a fluorescence microscope (Axio Imager Z1m; Zeiss, Germany).

2.4.3.3. DNA quantification

Cell proliferation and viability were assessed by DNA quantification. Proliferation of NPCs cultured in GG-MA was evaluated after DNA quantification at defined culture times, namely 0 and 24 hours, 7, 14 and 21 days of culture. The DNA of each culture was quantified by using the PicoGreen Quantification Kit (Invitrogen, USA). Picogreen has fluorescence properties and binds to double-stranded DNA, therefore it allows measurement of the proportional fluorescence enhancement[201]. In each time-point each disc was transferred directly to an Eppendorf containing 1 mL of ultra-pure water (from ultra-pure water system Genpure UV/UF; TKA, Denmark) solution of 0.5% (w/v) NaOH.

The third difference in the protocol already described was the use of the vortex to help dissolve the GG-MA just before leaving the samples overnight in the -80ºC freezer. The Eppendorfs were put in a 37ºC water-bath during 1 hour, vortexed and left overnight at -80ºC in a freezer.

On the next day, the 20X Tris-EDTA buffer solution, provided in the quantification kit, was diluted upH_2O at a 1:20 ratio (therefore resulting in a 1X Tris-EDTA buffer solution). 100 μL of this solution was transferred to each well of a 96-well white opaque plate (Corning, USA). Moreover, the PicoGreen reagent (also provided in the kit) was diluted with the 1X Tris-EDTA buffer solution at a 1:200 ratio. Then, 71.3 μL of this PicoGreen solution was transferred to each well of the 96-well plate and finally 28.7 μL of each sample solution was transferred to three wells (three pipetting replicates) of the 96-well plate and it was incubated for ten minutes protected from direct light. Fluorescence was then read at 480/20 nm of excitation and 520/20 nm of emission in a Synergy HT microplate reader. A standard curve was made out of the picogreen kit's provided DNA vial (concentrations of 0, 0.25, 0.5, 1 and 2% (w/v)) for extrapolation of the samples DNA concentration, according with read absorbance for each sample. Furthermore, a solution of 50×10^5 cells/mL was centrifuged and re-suspended in ultra-pure water at the same concentration, and followed the same PicoGreen Quantification Kit procedure. Therefore, allowing a relation between cell number and DNA concentration, in order to provide the cell number present in each sample. All the experiments were replicated nine times per sample condition.

2.4.3.4. MTS Assay

The metabolic activity of the NPCs encapsulated in the GG-MA discs was evaluated by MTS assay. The protocol followed for this assessment was the same as described above (see "*Scaffold Biocompatibility*"), but instead of assessing cells attached to a 96-well plate the culture comprised the GG-MA disc constructs in 24-well plates for 1, 7, 14 and 21 days of culture.

Additionally, the viability of GG-MA discs was also evaluated for L929 cells encapsulated in GG-MA. Since GG-MA has been shown to have non-angiogenic properties, herein is assessed the metabolic activity of a fibroblast cell line in GG-MA, *i.e.,* a cell type that requires a great level of cell adhesion, in comparison with NPCs encapsulated in the same material. All the experiments were replicated nine times per sample condition.

3. Results

3.1. Reverse Engineering and Rapid Prototyping the Intervertebral Disc

3.1.1. Scaffold Preparation

The procedure of developing a customized IVD through RE and RP method would be based on CT measurements of the patients. In this sense, aiming to observe the feasibility of this strategy in the TE field, more precisely in the IVD regeneration, the μCT was used to acquire the images to model the IVD design and afterwards analyse the PCL replica to compare the 2D images of both analysis types and understand if the design is maintained after being produced (Figure 3.1).
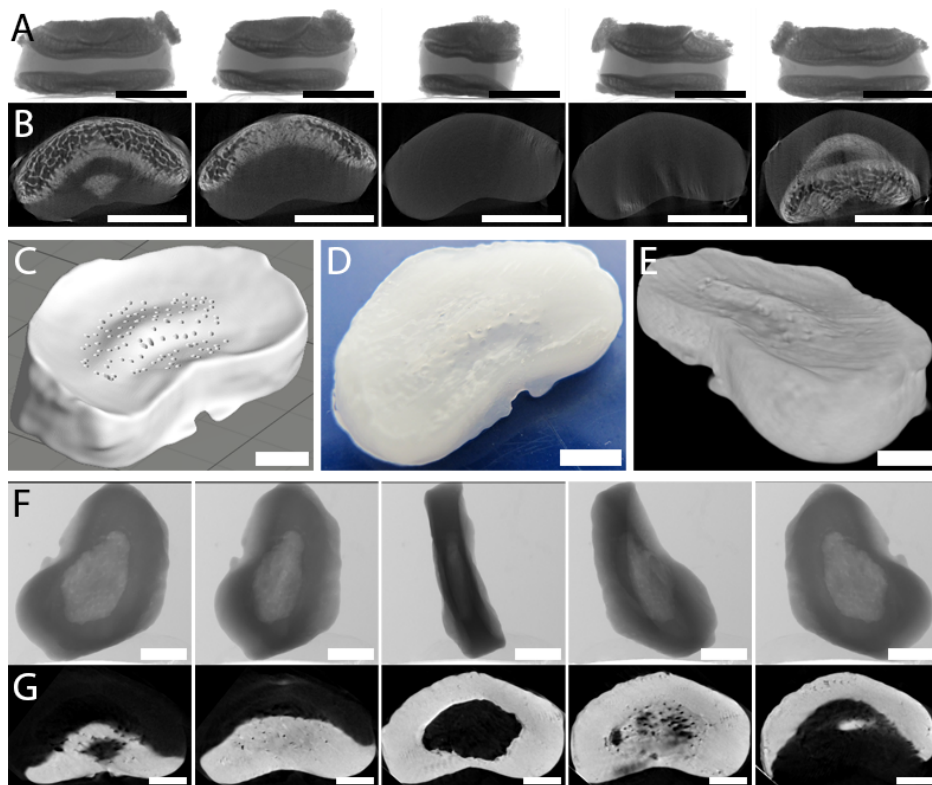
Figure 3.1. Representation of the results acquired from the main steps of intervertebral disc reverse engineering and rapid prototyping techniques: (A) raw 2D images acquired from the rabbit IVD imaging analysis (5 from a set of 412 images); (B) 2D stack images after dataset processing; (C) one of the 10 virtual representation of the IVD replica model, specifically the "small pores" model, 200% scale of the original native IVD; (D) photograph of the 3D printed geometrical model, 200% scale of the original IVD; (F) and (G) scaffold imaging acquisition and processing, respectively, 200% scale of the original IVD, analogues of (A) and (B); (E) fast rendering of the image dataset represented in (G). Scale bars correspond to 5 mm.

Thus, the raw 2D images in Figure 3.1.A (412 images in total) show both the IVD and vertebral tissues from one native rabbit intervertebral motion unit, which when processed generates the 2D stack image dataset represented by the images in Figure 3.1.B (355 images in total). The rendering of this stack image dataset generates the 3D model replica of the native IVD.

The RP customized scaffold was prepared by uploading the 3D model onto the 3D printer. The printed result is shown in Figure 3.1.D that was further analysed by the original imaging equipment used to acquire the native IVD raw images, as previously mentioned. The raw images of the scaffold are represented in Figure 3.1.F that when processed generated the dataset represented in Figure 3.1.G, which by fast rendering produced the model visualization shown in Figure 3.1.E.

While using this method of RE and RP, several models based on the original AF scaffold were produced. Several types of porosity patterns were designed (in the segmentation step), on the top and down lids of the scaffold over the NP cavity (located on the border of the IVD with the vertebrae in the original rabbit's IVDs) (Figure 3.2).
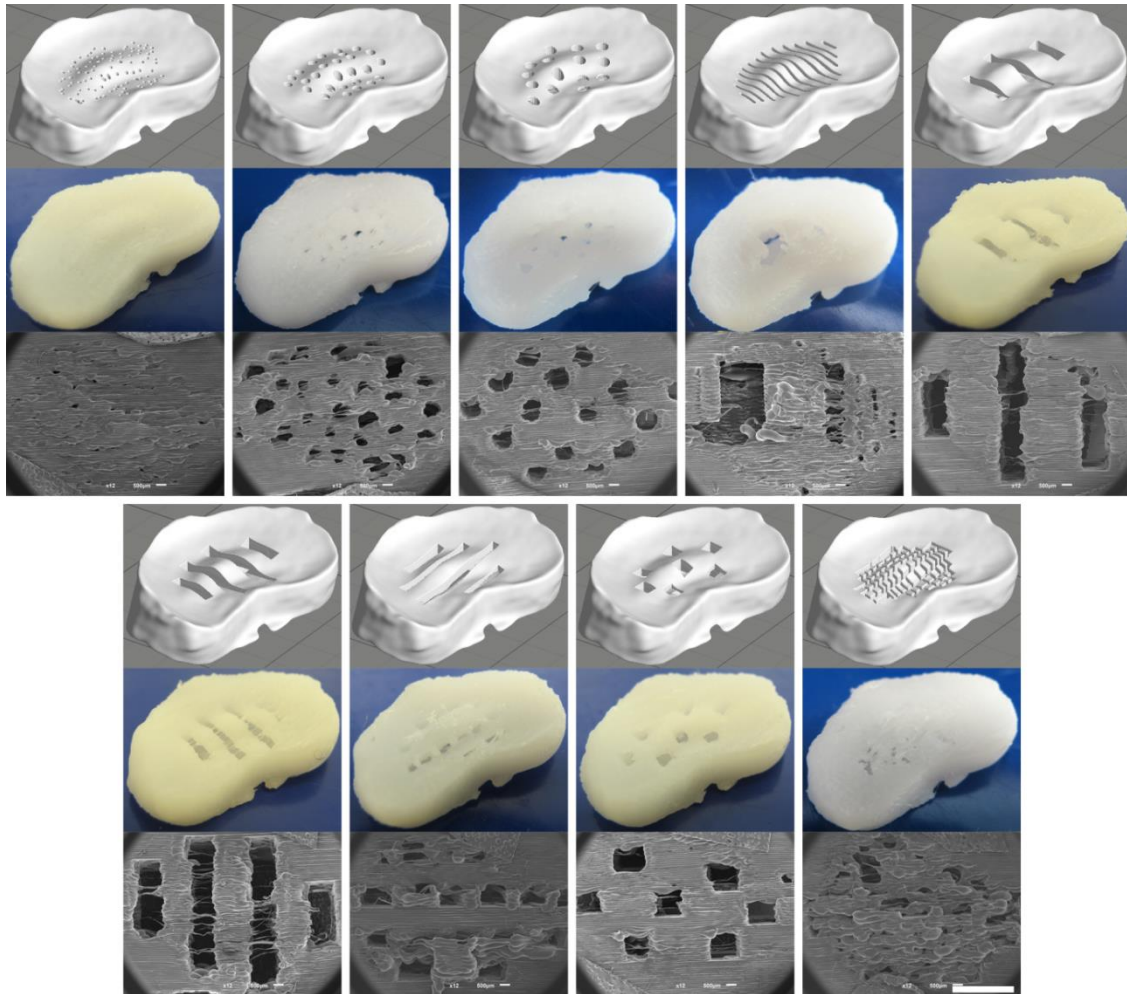
Figure 3.2. Virtual representation of IVD replica models designed with different porosities and correspondent photographs of the respective 3D printed scaffolds. Scale bar on the bottom right corresponds to 5 mm for all virtual and 3D printed models, while corresponding to 3 mm for all SEM images.

A total of 9 different models (derivatives of the original replica model, which did not have any superficial porosity) were prepared, and in order to analyse them, they were named: "*Small Pores*", "*Medium Pores*", "*Big Pores*", "*Lines*", "*4 Stripes*", "*3 Stripes*", "*4 Vertical Lines*", "*Grid*" and "*Squares*", shown in Figure 3.2 from left to right and from top to bottom, respectively.

The radial surface morphology of the scaffolds was recorded by SEM (Figure 3.3). The SEM results unveil the filament morphology deposited during the 3D printing process that otherwise is not noticeable by naked eye. It is also possible to observe the high integration between the several deposited layers, as well as the resolution between layers (100 μm).
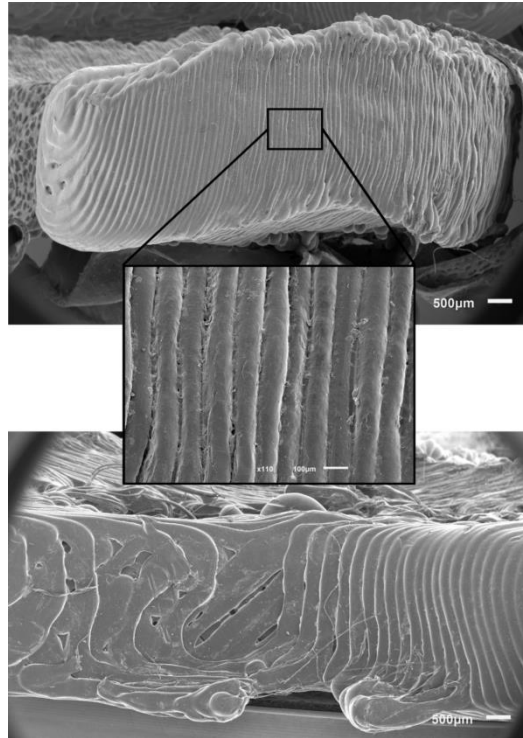
Figure 3.3. SEM images from the lateral sides of the annulus fibrosus replica: right side of the sagittal plane (on top; scale bar: 500 µm), with higher magnification (in the middle; scale bar 100 µm) and ventral side of the coronal plane, which comprise the last layers of the 3D printing process (on the bottom; scale bar 500 µm).

Additionally, in the research perspective regarding this method, thinking in future pressurized cultures, the top and down surface casts of the IVD model were also rendered, representing the models of the top and down surfaces of the vertebrae in contact with the original IVD. Also, each type of porosity designed in the IVD models was imprinted on the top and down moulds, for each model. With this apparatus composed of three pieces, shown in Figure 3.4., it is possible to culture the scaffold under anatomy-like cyclic and uniformly distributed compression (the top and down surfaces are naturally far from flat), while allowing for the culture medium to access the NP cavity through the porosity.
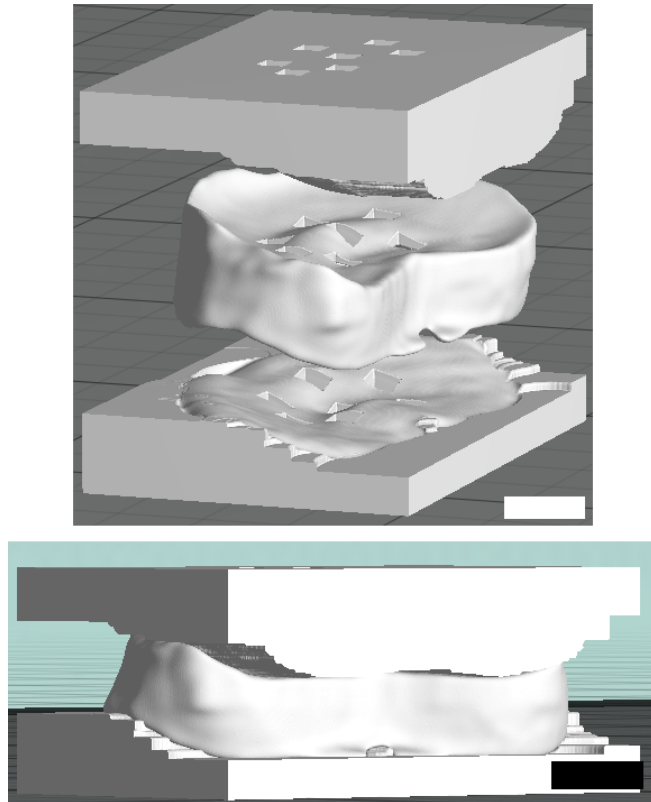
Figure 3.4. Apparatus for culturing the intervertebral disc scaffold in pressurized conditions. Scale bars: 5 mm.

3.1.2. 3D Analysis

After retrieving the aligned 2D stack images of the rabbit IVD, they were 3D analysed to serve as control results to further analyse which model has closer morphological characteristics. With this purpose in mind, the 9 different models were also 3D analysed, which results for average pore size and percentage of bulk material within the object's volume are expressed in Figure 3.5. The porosities for each scaffold were 0.027%, 0.018%, 0.042%, 0.010%, 0.030%, 0.017%, 0.016%, 7.132% and 0.021% for the "3 Stripes", "4 Stripes", "4 Vertical Lines", "Big Pores", "Grid", "Lines", "Medium Pores", "Small Pores" and "Squares" models, respectively. The native rabbit IVD, representing the positive control, had a porosity of 0.098%.

Table 3.1. Porosity of each three-dimensional printed model and rabbit intervertebral disc.

Model	Porosity (%)
Control - Rb IVD	0.098
3 Stripes	0.027
4 Stripes	0.018
4 Vertical Lines	0.042
Big Pores	0.010
Grid	0.030
Lines	0.017
Medium Pores	0.016
Small Pores	7.131
Squares	0.021
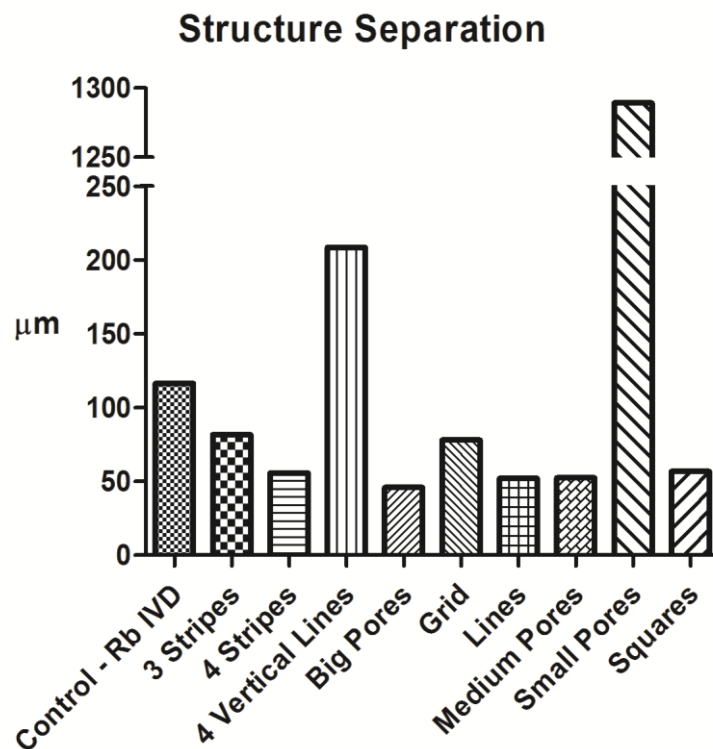
Figure 3.5. Average pore size within each three-dimensional printed model and rabbit intervertebral disc.

The analysis was set to ignore macroscopic pores over a certain size. Therefore, the designed porosities did not contribute to these results since they can be viewed by naked eye. But the pores designed in the "small pores" design were small enough to be detected in the 3D analysis, which measured in average 1289 μm.

3.1.3. Mechanical Tests

Mechanical tests were performed for each condition, being homogeneously compressed until 1 kN of uniaxial load (~105 MPa tension in the specimens' surface). The compressive load required to deform each specimen until 15% strain (deformation). Figure 3.6 shows the specimens' mechanical behaviour, of both dry and hydrated states, represented as stress-strain curves, with corresponding linear functions of the elastic domain and yield points.
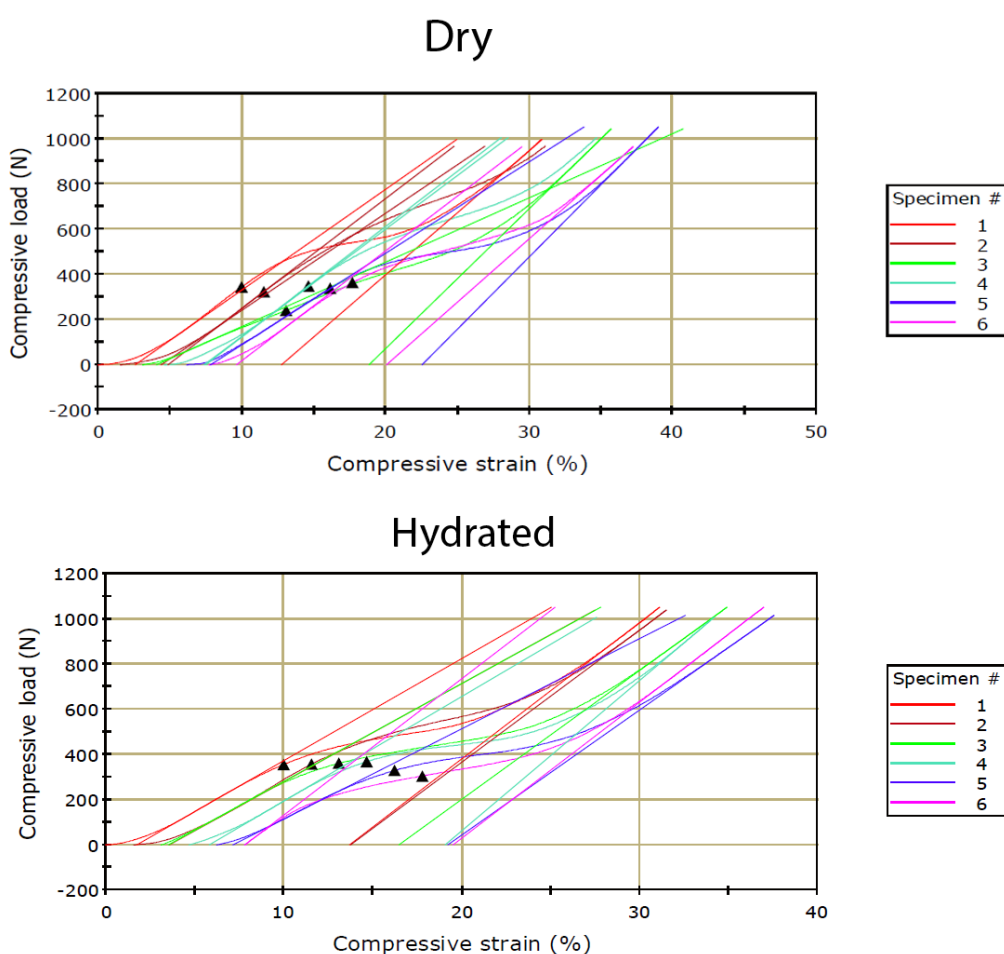
Figure 3.6. Mechanical assessment results regarding the scaffold's elastic deformation upon compressive load. The mechanical behaviour of the scaffolds in a dry state is shown at the top, while in a hydrated state the deformation is reported at the bottom. N = 6.

The average values of Young's Modulus for both specimen conditions upon compression (Figure 3.7) were 72 ± 7.8 MPa and 77 ± 5.2 MPa for dry and hydrated states, respectively.
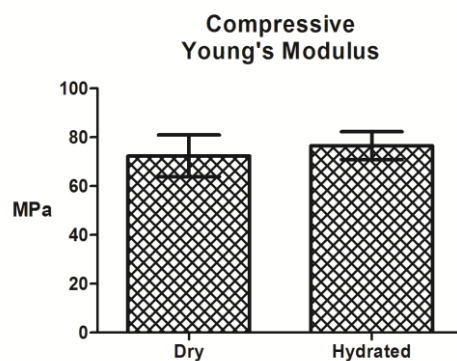
Figure 3.7. Compressive elastic deformation rate (Young's Modulus) of the scaffolds in dry and hydrated state. Results expressed as an average ± standard deviation; n = 6. T-test was performed assuming unequal variances, both conditions' compressive Young's modulus have more than 5% probability (p>0.05) of being equal next time the experiment is carried out.

Furthermore, the compressive stress values at 15% specimen strain of dry and hydrated conditions were 34.6 ± 4.1 MPa and 35.6 ± 2.23 MPa (Figure 3.8), respectively.
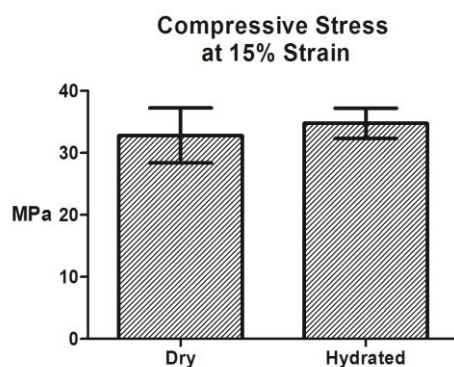
Figure 3.8. Compressive stress at 15% specimen deformation, for both dry and hydrated conditions. Results expressed as an average ± standard deviation; n = 6. T-test was performed assuming unequal variances, both conditions' stress have more than 5% probability (p>0.05) of being equal next time the experiment is carried out.

3.1.4. Cytotoxicity Screening

L929 cells and AFCs were used to assess the RP scaffolds possible cytotoxic effect. Cells were cultured in the presence of extraction medium containing leachables of the RP

scaffolds for 24 hours and 72 hours, after which the metabolic activity of both was analysed via MTS assay (Figure 3.9).
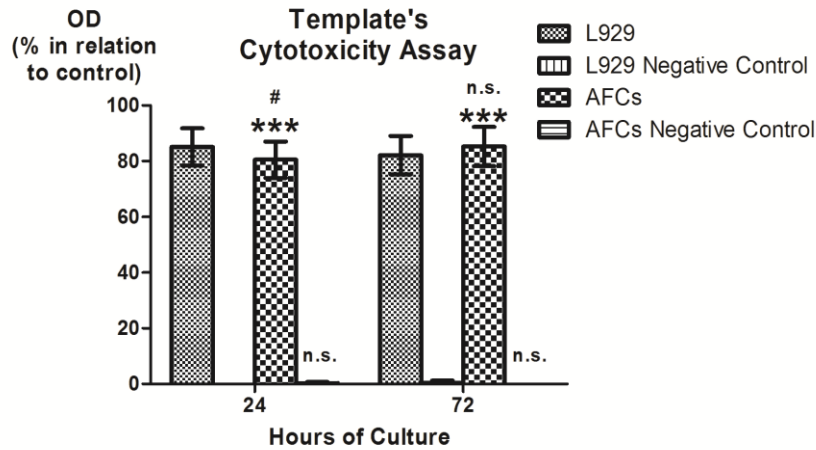
Figure 3.9. Cytotoxicity assay results for L929 cells and AFCs in culture with the scaffold extracts after 24 and 72 hours of culture. Positive control represents 100%; negative control represents 0%. Results expressed as an average ± standard deviation; n = 12. #: $p < 0.05$ vs. L929, n.s.: $p > 0.05$ vs. L929, ***: $p < 0.001$ vs. the other time-point; both L929 and AFCs cultures have less than 0.1% probability of having the similar results versus the negative control the next time the experiment is carried out.

The optical density showed that the metabolic activity of the cultures with the scaffold's extracts were over 80% (L929: 24 hours – 85%, 72 hours – 82%; AFCs: 24 hours – 81%, 72 hours – 85%) in relation to the culture with regular medium (positive control).

3.2. In vitro assessment of nucleus pulpous cells viability, adhesion and proliferation

The cellular behaviour of NPCs, regarding their properties of adhesion, proliferation and viability within GG-MA, was assessed after performing Live/Dead staining, cellular activity profile and DNA quantification, at specific time-points. For this purpose, both NPCs and L929 cells were encapsulated (separately) in GG-MA with a final cell concentration of 10 million cells per mL of hydrogel. In this sense, the viability after 1, 3, 7, 14 and 21 days in culture was analysed by Live/Dead assay (Figure 3.10).
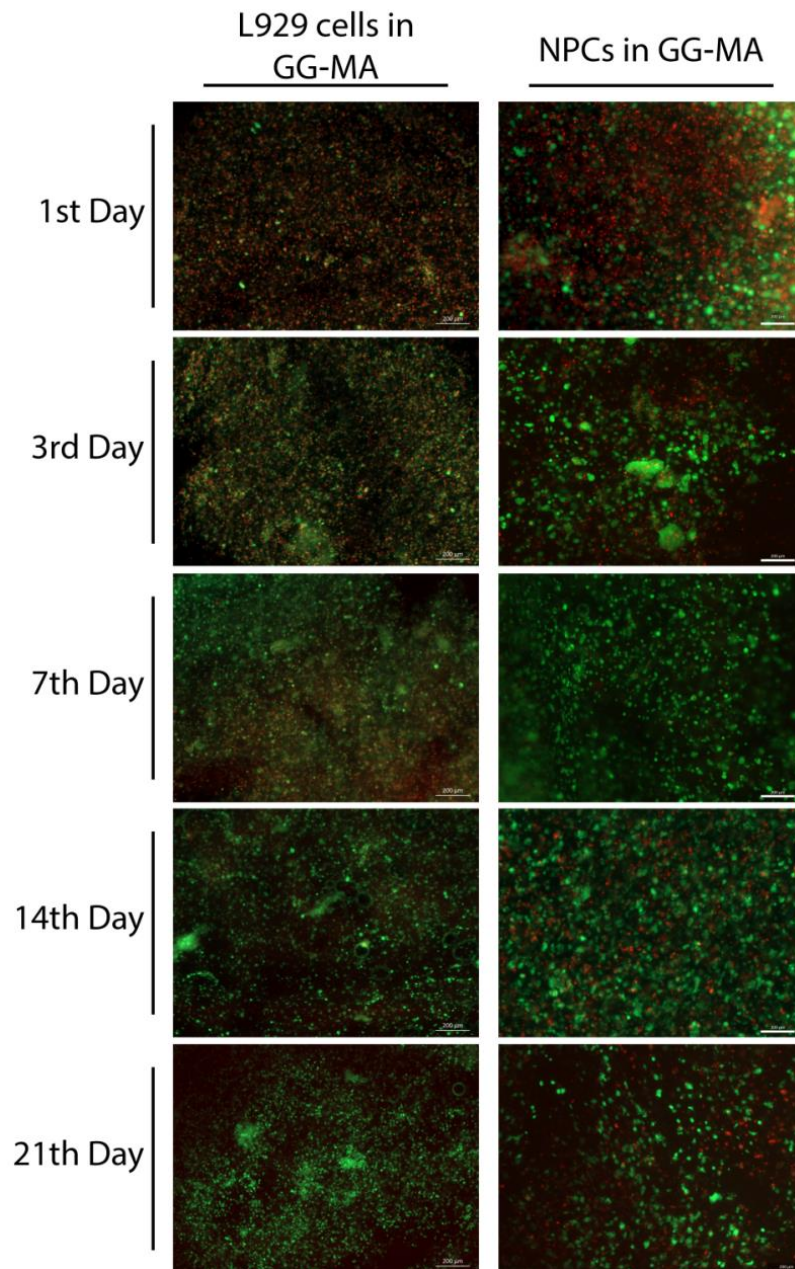
Figure 3.10. Live/Dead viability assay of L929 (on the left) cells and rabbit nucleus pulposus cells (on the right) in GG-MA discs examined under fluorescence microscopy at: 1, 3, 7, 14 and 21 days. All scale bars correspond to 200 μm.

The Live/Dead staining, marks viable cells' population as a strong green fluorescence while the dead cells are marked in red fluorescence. These results seem to show a reduction of dead cells in the first 3 days of culture (Figure 3.10; both cell types at 1 and 3 days), which is almost unnoticeable after 7 days (Figure 3.10; both cell types at 7 days), *i.e.,* the rate of cell death decreases over time. After 14 and 21 days of culture each cell type has different results.

The L929 cells do not show (Figure 3.10; L929 cells in GG-MA at 14 and 21 days), apparently, signs of dead cells, only alive cells. Concerning the NPCs culture on the other hand, it is noticeable a decrease in the number of viable cells until the final time-point of 21 days, where it is visualized an even balance between live and dead cells (Figure 3.10; NPCs in GG-MA at 14 and 21 days).

In order to corroborate the previous results, the cumulative amount of DNA existent in culture at several time-points of 0, 1, 7, 14 and 21 days of culture, was quantified (Figure 3.11).
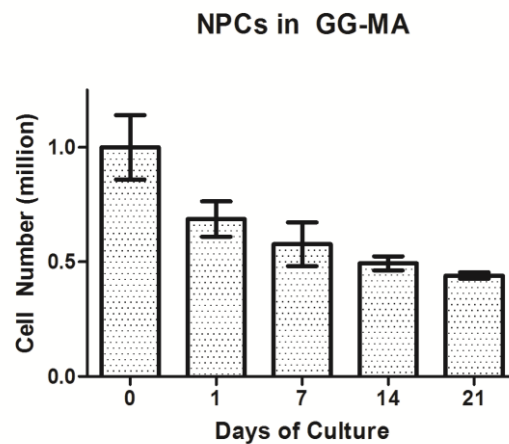
Figure 3.11. DNA content of rabbit nucleus pulposus cells seeded within GG-MA and cultured for 0, 1, 7, 14 and 21 days. Results expressed as an average ± standard deviation; n = 9. By one-way ANOVA, variances of each time-point were analysed with all others with the assuming (null hypothesis) unequal variances, p-values were: 0d vs all as well as 1d vs 14d and 21d - $P<0.001$; 7d vs 21d – $P<0.05$; 1d vs 7d, 7d vs 14d and 14d vs 21d – $P>0.05$.

Results indicated that NPCs cultured in GG-MA did not proliferate between 0 and 24 hours of culture. Furthermore, by observing the remaining three time-points, a stabilisation can be observed. Although the NPCs concentration within the GG-MA discs is always decreasing along with time, the cell number difference between time-points gets smaller and smaller, varying between 14 and 21 days by 5.1×10^4 cells, while between 0 and 24 hours there was a decrease of 2.9×10^5 cells/disc. The 21 days' time-point retrieved a cell number of 4.2×10^5 cells/disc.

The cellular proliferation of both L929 cells and NPCs was assessed via quantification of their metabolic activity at 1, 7, 14 and 21 days of culture. Figure 3.12 shows the cellular activity for both cell types encapsulated in GG-MA, with a concentration of 1 million cells per disc, and 1×10^4 cells growing in TCPS 6-well plates without GG-MA.
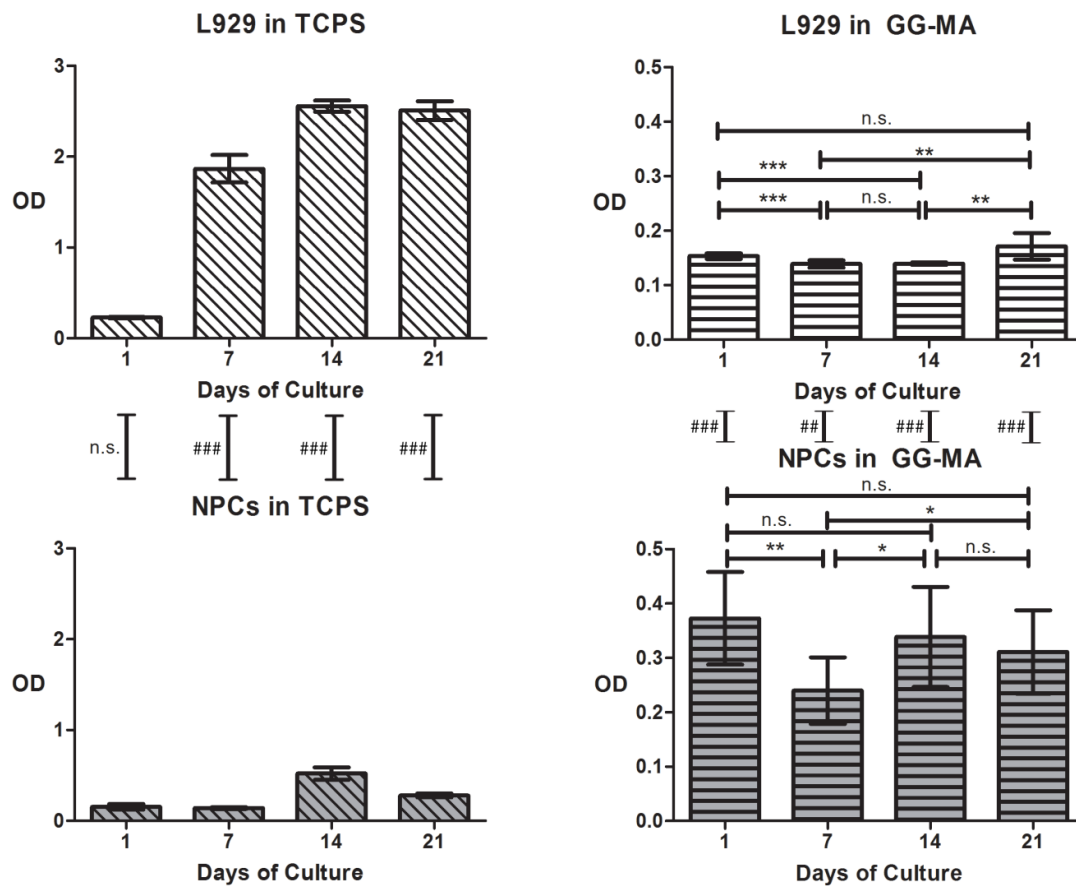
Figure 3.12. MTS assay results for 1, 7, 14, and 21 days of culture of cells encapsulated in GG-MA at a concentration of 1 x 10^7 cells/mL (on the right) and 1 x 10^4 cells seeded in TCPS 6-well plates without methacrylated gellan gum (on the left). Both culture conditions were made for L929 cells (on the top) and nucleus pulposus' cells (on the bottom). Results expressed as an average ± standard deviation, n = 9. n.s.: $p>0.05$, *: $p<0.05$, **: $p<0.01$, ***: $p<0.001$, ##: $p<0.01$, ###: $p<0.001$.

The NPCs activity in GG-MA was higher on the first day of culture when compared with the other time-points, though it decreased abruptly (~67%) after 7 days of culture. Nevertheless, by the day 14, NPCs activity increased ~143% in comparison with cellular metabolic activity at 7 days. At 21 days' time-point the metabolic activity was similar, though slightly higher, than the 7 days result.

Regarding the metabolic activity of NPCs cultured in TCPS well plate, it remained statistically the same at time-points of 1 and 7 days of culture. Though, after another 7 days of culture (14 days' time-point) the metabolic activity was ~236% higher. Moreover, by day 21 of culture the optical density decreased to ~43% in relation to the optical density observed at 14

days' time-point. Nevertheless, still the double of the first two time-points (1 and 7 days of culture).

4. Discussion

The current work aims to provide a new strategy for the setup of a TE-TDR construct. Not only that, but the final construct must, from macro- to microscopic level, faithfully and specifically replicate the native patient's IVD as it was when not degenerated. With this in mind, it was hypothesized that the combination of RE with RP together with TE would be a promising approach to achieve not only an immunocompatible cell construct, but also a structurally compatible IVD scaffold that fits precisely within the intervertebral space. Most cases of LBP caused by IDD already are in a medium to a severe state of degeneration when the patient arrive to the clinics (LBP is felt when a hernia presses adjacent nerves or when nerve endings grow inside the IVD)[202]. This means that the AF tissue is already compromised, therefore any hydrogel carrying cells with the objective of regenerating the NP cannot be held by the native AF, and herniates producing more LBP. Thus, a more complete, though not necessarily complex, TE strategy must be followed in order to treat these cases, which includes a scaffold that replaces and regenerates the AF tissue. Due to the AF's biochemical and biomechanical properties, it is expected for the scaffold to have elastic properties similar to the native natural structure and must degrade at the same rate as the new AF tissue is synthesised by the AFCs.

For this purpose, two complementary pathways were followed, one that comprises the regeneration of the AF and the other for the NP. Though, the final purpose is to combine both strategies in order to prepare a TE-TDR implant composed by a PCL scaffold, replicating the outer surface of the AF, filled with NPCs encapsulated in GG-MA hydrogels. In the future, this novel strategy is envisaged to treat IDD, and remove LBP, by fully regenerating the intervertebral disc. In another side of the same approach, this work aims as well to reinforce the feasibility of GG-MA hydrogels as a potential support for NPCs.

Several research groups are tuning up new strategies to regenerate the IVD[146–148,151–155,157,158,161,162,169,170,172,196,203–208], but most of them render to mimic the IVD shape[152], however they are not focused on patient-specificity. Not withstanding, every patient has different intervertebral geometric characteristics, and if this geometry is replicated into the implanted construct there is an increased possibility that it is successfully integrated. This geometrical patient-specificity can be achieved without extra costs (in relation to other TE strategies), just by using the patient's data already being acquired during standard diagnostic procedures. In fact, anatomical modelling can be performed by classical design-parametric features, using several types of computer aided design (CAD) software. Another possibility is the use of RE to convert the real system into a 3D virtual solid. In this sense, RE is presented as a process that is

focused on the creation of a CAD model from a physical model aiming to use the geometric model for its manufacturing. The first step of RE is focused on the data acquisition through non-invasive imaging techniques, commonly used in the hospital environment for diagnosis, namely CT or MRI technology, these models are further generated by 3D-image-based reconstruction software, such as Mimics. The 3D model is parameterized and used as a reference model for creating patient-specific anatomical models based on dimensions extracted from radiographic images.

This study describes a novel method for producing IVD scaffolds using RE and RP techniques. The underlying idea behind this method was proposed envisioning the possibility to prepare customized scaffolds for each patient individually, as previously mentioned. Herein, the RE process is in association with the RP technology of 3D printing by FDM, which does not require any solvent and offers great ease and flexibility in material handling and processing. The use of a filament modelling material also reduces its residence time in the heating compartment and allows continuous production without the need of replacing feedstock[209]. Moreover, this technique enables a very fast and low-cost method of producing scaffolds in a precise manner (resolution = 100 μm) regarding what the CAD model represents virtually.

When a patient with LBP arrives to the medical doctor's office to understand and treat his source of pain, he is advised, among other things, to be submitted to a CT or a magnetic resonance imaging (MRI) for diagnostic purposes. For the cases of IVD degeneration these images can have another purpose, and this is where the present work picks on. The stack images obtained by the imaging system are segmented into a 3D model that is the virtual replica of the patient's IVD. This 3D model, after some modelling treatment can then be uploaded to a low-cost RP FDM 3D printer that prepares a faithful replica (from 100 μm to the macroscopic level) of the patient's IVD in the desired biomaterial (any given biomaterial suitable for FDM 3D printing). By comparing the Figures 3.1.B and G it is possible to observe the pattern resemblance that in B is the shadow regions and in G are the bright regions, both representing the IVD volume, native and replica respectively. The centre image in Figure 3.1.G reveals the NP cavity that is not noticeable in the native image dataset, though the respective cavity volume was designed according with the grey-scale threshold, which left a lighter "pixel fog" over the shown cavity region. This voxels were removed to avoid unnecessary heavy processing of the model in the 3D printer software, since voxels are ~14 μm of side they are not expressed unless when in groups of at least 7 x 7 x 7 cubic voxels (343 voxels altogether) due to the 3D printer resolution limitation.

Several porosities were designed in the resulting IVD replica generating several 3D models that were afterwards 3D printed. There were some porosity patterns that could be

transposed from the virtual model to the real object, though some could not, it mainly depended of the resolution required by the pattern and the orientation of the scaffold while being prepared, since FDM technology is conditioned by gravity. The IVD replica 3D model does not include the NP volume (*i.e.,* the model is hollow), thus, if the scaffold was printed in anatomically IVD-like position, the top lid (over the NP cavity) would collapse on the bottom lid (below the NP cavity) before the PCL could solidify due to lack of support for the fused PCL being extruded. This creates the need to add support material inside the scaffold, *i.e.,* material not represented in the CAD model that is needed for the object generation, which would compromise the mechanical behaviour (and probably the biocompatibility of the final construct) of the scaffold if not removed. Therefore the scaffold was turned 90º from anterior transverse plane to inferior coronal plane, which allowed the preparation of at least 6 of the 9 porosity patterns with high matching degree. These porosities, in a future work, will be assessed for permeability to analyse which porosity better matches with the native IVD range of permeability. The non-reproduced precision details that were not transposed from the virtual model to real 3D printed object could be easily overcome if the RP system was a stereolithography (SLA) system, due to its higher resolution. However, it addresses the limitation of narrowing the range of source material available. The material needs to be photo-polymerizable that for PCL means the need to use photo-initiator, which can create a whole new set of challenges, *e.g.,* cytotoxicity. Nevertheless, it is an interesting idea to explore as well, since it enables a higher degree of resolution and does not rely directly on gravity in the solidifying site.

Herein, PCL was proposed for this procedure due to its mechanical properties, specifically its elastic domain at physiological temperature. Since the RP process will only replicate the solid part of the native IVD, *i.e.,* the AF, the substitution material should have a degree of elasticity AF-like. The PCL has been proposed for AF regeneration by several research groups[167,172,210]. This polymer possesses a very low melting point (~60ºC) that confers it a greater elastic domain than other polymers at 37ºC. This is an ideal property for an AF scaffold to have, since it must be able to sustain not only one big load, but rather several loading cycles. Therefore, it cannot sustain a loading force for the sake of plastic deformation, it must be able to be subjected to the loading and afterwards return to the original morphology, remaining ready to absorb the next loading cycle. Thus, it shall never go into plastic deformation by sustaining the pressure before reaching the Yield Point, otherwise the material will suffer from mechanical fatigue that ultimately leads to fracture.

Best *et al.* measured the compressive elastic modulus of the AF by confined compression, the resulting modulus was 0.38 MPa[211]. Umehara *et al.* demonstrated that the compressive modulus of the AF was 0.11 MPa[212]. The compressive young's modulus of the produced IVD scaffolds in dry and hydrated state was 72 MPa and 77 MPa, respectively.

Comparing to the native AF elastic modulus, it was observed a higher compressive young's modulus, however, considering that the produced scaffold presents a compact structure, it shows that in the future it would be possible to create more porous in this structure. In this study, the RP process was programmed to infill the AF volume 100%, this parameter can be lowered, which will probably decrease the Young's modulus exponentially. Moreover, as previously mentioned, the scaffold is made of PCL that presents a melting point of about 60ºC, thus if the mechanical tests were performed at physiological temperature (37ºC) instead of room temperature (~20ºC) the resulting elastic modulus would be lower.

These compressive modulus values (72 MPa and 77 MPa), for both states, can be considered very close, which shows how predictable and stable these scaffolds are, being in accordance with Lebourg *et al.* results, whom tested mechanically PCL electrospun scaffolds[213]. Although, this similarity in the mechanical behaviour between both states was already expected due to the hydrophobic nature of this material[214]. Moreover, the porosity results express that the empty volume inside the scaffolds is an average of 0.023% (not considering the NP cavity). Therefore, suggesting that the NP cavity is the key feature responsible for the difference between compressive modulus by being filled when the scaffold is hydrated.

Alongside with its good mechanical properties, the PCL degrades into non-acidic byproducts[172]. In this sense, the biocompatibility of the 3D PCL IVD scaffolds was also assessed. The mitochondrial activity, measured via MTS assay, at 24 and 72 hours produced an optical density between 81% and 85% in relation to the positive control, thus suggesting a good degree of biocompatibility. In fact, this result is not surprising since this parameter was already reported. Koepsell *et al.* prepared electrospun nanofibrous PCL scaffolds for AF TE, although it was not performed a cytotoxic assessment, the *in vitro* studies shown an increased AFCs' proliferation and activity along with culture time suggesting biocompatibility[210]. Wan *et al.* prepared an IVD construct in which the inner AF scaffold was composed of poly-(polycaprolactone triol malate). The biocompatibility evaluation using mice as a model revealed no obvious immunological reaction after 1 week[172]. Similar status results were also shown in other studies for bone[215], cartilage[216], cardiac[217], vascular[218] and skin TE[219].

As previously mentioned, the AF scaffold is hollow inside since a cavity, which replicates the NP design, is left in the 3D printing process envisioning that afterwards an injectable hydrogel containing patient's NPCs could be introduced in this cavity. Therefore, and continuing the parallelism with what happens nowadays in the clinics regarding an IVD degeneration condition, when the patient is submitted to a discectomy (procedure for a disc hernia removal) the tissue instead of being discarded is kept for NPCs isolation. These cells, after expansion or not (second surgery vs. NPCs availability), can be encapsulated within the

hydrogel and further injected in the hollow part of the PCL AF scaffold. If no cell expansion is needed, the AF scaffold can be prepared between diagnosis and surgery, and the NPCs' encapsulation in the hydrogel would be performed in the operating theatre and further injected in the AF scaffold. Then the TE-TDR construct can be implanted in the same procedure as the discectomy (which would, naturally, seize to be a discectomy). If not, then a second surgery would be needed, as it is nowadays for recurrent disc herniations that ultimately lead to a spinal fusion[220].

Ionic-polymerized low acyl GG hydrogels have been proposed by 3B's Research Group for TE strategies[121,140,144,221]. In fact, this GG based material was chosen as a carrier for NPCs for several reasons. What seems to be the one characteristic that distinguishes GG from other hydrogels is its non-angiogenic property[59]. The GG is a hydrogel with low cell adhesion characteristics, thus unwanted cell types, which generally require strong attachment to the surrounding extracellular matrix (ECM), or biomaterial, do not migrate and proliferate in the GG. Therefore, angiogenesis is avoided inside the replaced IVD, which is essential for an NP TE strategy, since avascularity stimulates NPC phenotype expression[52,53]. Moreover, the GG can be submitted to a methacrylation reaction with glycidyl methacrylate, and by controlling the time of this reaction it is possible to tailor the desired mechanical properties[121]. When methacrylation is preformed to GG, the final product is a mixture of GG and GG-MA, therefore the more time the methacrylation reaction occurs the more amount of GG-MA will be present in the final material. In fact, by allowing the GG to react with glycidyl methacrylate for 24 hours, the resulting material has a storage modulus of 89.5 ± 7.4 kPa, resulting in more favourable mechanical properties than regular GG that is 56.2 ± 1.4 kPa[144]. Briefly, the storage modulus is the ability for the material to retain mechanical energy, subjected to it, before reacting to the mechanical stimulus. In the other hand, the NP is an extremely hydrated tissue, thus the material chosen to replace must have good hydrophilic properties. GG-MA is able to polymerize with 1.5% (w/v) concentration, thus the remaining 98.5% is water. It is interesting how this material can hold more water than the NP and still have similar mechanical properties. Therefore, the GG-MA seems a promising material to be used not only for IVD regeneration but also for other TE purposes.

The *in vitro* assessment follows the results obtained in previous studies[105,144], in which the biocompatibility of GG-MA was tested with L929 cell line and human IVD cells by calcein-AM staining and cytotoxicity assay. Herein, the viability, proliferation, metabolic activity and qualitative characterization of rabbit NPCs encapsulated in GG-MA were assessed. Furthermore, L929 cells were also encapsulated within GG-MA hydrogels in order to compare the metabolic activity of NPCs with a more adherence requiring cell type. Results of DNA quantification and Live/Dead assay for the culture of NPCs in GG-MA show great cell loss after

the first day of culture. This may be due to the encapsulation process that takes some time, and while it is being followed, the cells are out of the incubator at room temperature, being exposed to harsh conditions (*e.g.,* centrifuge process, lack of medium supply, and absence of adherent surface). Therefore, this process consumes a great number of cells not directly, but due to encapsulation cell stress that can increase cell death in the first 24 hours, which was confirmed by the Live/Dead results, which after one day of culture showed a high number of dead (red) cells. These results are corroborated by DNA quantification, since it shows a decrease from 1 x 10^6 cells to 6.9 x 10^5 cells, corresponding to a decrease of cell number in approximately 30%. On the other hand, the metabolic activity was higher than any other time-point, suggesting metabolic activity triggered by encapsulation stress. However, after this short time, very few dead cells were noticed, being corroborated by the DNA quantification results. Surprisingly, the L929 cells in GG-MA culture was metabolically less active than NPCs, what was not expected since L929 are generally used as a positive control population thus retrieving higher results. As previously reported, GG-MA may be selective to different cell types, since this hydrogel has been shown to be not ideal for high adherent cell types. Thus, it is foreseen as a good platform for NP regeneration, since it does not allow the contamination by high adherence cells types, such as the IVD in relation to angiogenesis and fibroblast-like cells migrating from the AF. Therefore, these results are in accordance with what was reported by Silva-Correia *et al.* in which the non-angiogenic properties of the GG-MA are demonstrated[139].

In this work, a concentration of 1 x 10^7 cells/mL of GG-MA was used, since it is the adopted cell density described in the literature of NP regeneration strategies[8]. In this study, it was observed a decrease in cell number along with the time, thus suggesting that the initial cell seeding number is too high for these culture conditions (*i.e.,* 20% oxygen and unpressurized environment), since like in a degenerated NP the cell number decreases with normoxia conditions[48,52,53,222]. Therefore, without pressure environment and hypoxia stimulus, the seeding number of cells cannot be sustained, decreasing successively until a balanced cell concentration is achieved.

5. Concluding Remarks and Future work

The aim of this work was to develop a therapeutic TE strategy in a patient specific perspective. Thus, theoretically it is possible to apply this strategy by using the data acquired for IDD or hernia diagnosis alongside with a patient's cell source, whether NPCs harvested in discectomy surgery or stem cells.

The designed scaffold can be changed according to the native AF morphology, by replicating the lamellar structure, which can be prepared by 3D printing with equipment that possesses higher precision, such as SLA 3D printing. Probably in the next couple of years FDM 3D printers will start to have higher resolution, *i.e.,* below 100 μm, and if a 50 μm is possible, the lamellar structure can be replicated through RE and the whole scaffold may have a mechanical behaviour similar to the native AF. Moreover, with lamellar structure or with a lower infill it brings the opportunity to inject AFCs in this new porosity, allowing co-culture *in vitro* studies aiming to compare an acellular with cellular strategy (*e.g.,* AFCs seeded on the 3D printed scaffold) alongside with encapsulated NPCs in GG-MA hydrogels in the NP cavity. In the future, if technology permits the possibility of 3D printing the design of the lamellas in the scaffold, after culturing the full TE-TDR under compression stimulus it will be interesting to assess if there will be aligned growth of collagen type I filaments between the scaffolding lamellas.

This work serves as baseline data for future studies focused on culturing this cells + TE-TDR construct under a pressurised system, using the vertebral surface casts, in a hypoxia environment coupled with transforming growth factor-β3 supplement, aiming to promote and maintain the NPCs phenotype.

Moreover, different features can be coupled with the present strategy, namely the exploitation of the piezoelectric phenomena, which is an intrinsic property of collagen type I and II, known to be the protein basis of the IVD's ECM. A conductive PCL composite can be also used to stimulate electrotaxis precisely where it is needed while maintaining good mechanical properties and biocompatibility. Thus, electrical stimulus can be used to encourage AFC's to synthesise ECM in a native like alignment. The subjacent idea would be to induce the production of the first synthesized ECM in a native morphology to increase significantly the correct maturation of the cells + scaffold construct *in vivo*.

In fact, a solid approach to achieve a truly reliable IVD TE strategy would use the following steps:

- GF's cocktail optimization for MSCs differentiation into NPCs, and further encapsulation of both (GF's cocktail and MSCs) in GG-MA;

- Model and design a patient specific AF scaffold with a precise native-like lamellar structure with an electroconductive PCL composite;

- Inject a hydrogel, *e.g.,* a blend of GG-MA with silk hydrogel, containing AFCs, in the interlamellar spaces;

- Inject the GG-MA containing MSCs and GFs in the NP region of the scaffold;

- Culture this construct in a bioreactor, adapted with vertebrae casts (for homogeneous mechanical stress distribution), with 2% oxygen and under cyclic pressure until biological stabilization is achieved;

- Implantation of the construct *in vivo*.

Fortunately, there is no lack of ideas for trying to achieve a functional TE strategy to regenerate the IVD. The authors strongly believe that in the near future there will be a feasible TE strategy for the IVD in the clinics with the potential to overcome IDD.

III. Bibliography

1. Whatley, B. R. & Wen, X. Intervertebral disc (IVD): Structure, degeneration, repair and regeneration. *Mater. Sci. Eng. C* **32,** 61–77 (2012).

2. Luoma, K. *et al.* Low back pain in relation to lumbar disc degeneration. *Spine (Phila. Pa. 1976).* **25,** 487–492 (2000).

3. Berthiaume, F., Maguire, T. J. & Yarmush, M. L. Tissue engineering and regenerative medicine: history, progress, and challenges. *Annu. Rev. Chem. Biomol. Eng.* **2,** 403–430 (2011).

4. Silva-Correia, J. *et al.* Rheological and mechanical properties of acellular and cell-laden methacrylated gellan gum hydrogels. *J. Biomed. Mater. Res. A* **101,** 3438–46 (2013).

5. Abbushi, A. *et al.* Regeneration of intervertebral disc tissue by resorbable cell-free polyglycolic acid-based implants in a rabbit model of disc degeneration. *Spine (Phila. Pa. 1976).* **33,** 1527–32 (2008).

6. Bergknut, N. *et al.* The performance of a hydrogel nucleus pulposus prosthesis in an ex vivo canine model. *Biomaterials* **31,** 6782–8 (2010).

7. Vadalà, G. *et al.* In vitro interaction between muscle-derived stem cells and nucleus pulposus cells. *Spine J.* **8,** 804–9 (2008).

8. Crevensten, G. *et al.* Intervertebral disc cell therapy for regeneration: mesenchymal stem cell implantation in rat intervertebral discs. *Ann. Biomed. Eng.* **32,** 430–4 (2004).

9. Risbud, M. V *et al.* Differentiation of mesenchymal stem cells towards a nucleus pulposus-like phenotype in vitro: implications for cell-based transplantation therapy. *Spine (Phila. Pa. 1976).* **29,** 2627–32 (2004).

10. Bertram, H. *et al.* Matrix-assisted cell transfer for intervertebral disc cell therapy. *Biochem. Biophys. Res. Commun.* **331,** 1185–92 (2005).

11. Jandial, R., Aryan, H. E., Park, J., Taylor, W. T. & Snyder, E. Y. Stem cell-mediated regeneration of the intervertebral disc: cellular and molecular challenge. *Neurosurg. Focus* **24,** E21 (2008).

12. Abbott, R. D., Purmessur, D., Monsey, R. D. & Iatridis, J. C. Regenerative potential of TGFβ3 + Dex and notochordal cell conditioned media on degenerated human intervertebral disc cells. *J. Orthop. Res.* **30,** 482–8 (2012).

13. Sawamura, K. *et al.* Characterization of in vivo effects of platelet-rich plasma and biodegradable gelatin hydrogel microspheres on degenerated intervertebral discs. *Tissue Eng. Part A* **15,** 3719–27 (2009).

14. Revell, P. a *et al.* Tissue engineered intervertebral disc repair in the pig using injectable polymers. *J. Mater. Sci. Mater. Med.* **18,** 303–8 (2007).

15.   Reza, A. T. & Nicoll, S. B. Serum-free, chemically defined medium with TGF-beta(3) enhances functional properties of nucleus pulposus cell-laden carboxymethylcellulose hydrogel constructs. *Biotechnol. Bioeng.* **105,** 384–95 (2010).

16.   Diamond, S. & Borenstein, D. Chronic low back pain in a working-age adult. *Best Pract. Res. Clin. Rheumatol.* **20,** 707–20 (2006).

17.   Cassinelli, E. H., Hall, R. A. & Kang, J. D. Biochemistry of intervertebral disc degeneration and the potential for gene therapy applications. *Spine J.* **1,** 205–14 (2001).

18.   Andersson, G. B. Epidemiological features of chronic low-back pain. *Lancet* **354,** 581–5 (1999).

19.   Flowerdew, M. & Gadsby, J. A review of the treatment of chronic low back pain with acupuncture-like transcutaneous electrical nerve stimulation and transcutaneous electrical nerve stimulation. *Complement. Ther. Med.* 193–201 (1997). at <http://www.sciencedirect.com/science/article/pii/S0965229997800295>

20.   Atkinson, J. H. *et al.* A placebo-controlled randomized clinical trial of nortriptyline for chronic low back pain. *Pain* **76,** 287–96 (1998).

21.   Furlan, A. D. *et al.* Acupuncture and dry-needling for low back pain. *Cochrane database Syst. Rev.* CD001351 (2005). doi:10.1002/14651858.CD001351.pub2

22.   Assendelft, W. J. J., Morton, S. C., Yu, E. I., Suttorp, M. J. & Shekelle, P. G. Spinal manipulative therapy for low back pain. *Cochrane database Syst. Rev.* **138,** CD000447 (2004).

23.   Twomey, L. & Taylor, J. Age changes in lumbar intervertebral discs. *Acta Orthop. Scand.* **56,** 496–9 (1985).

24.   Roberts, S., Ayad, S. & Menage, P. J. Immunolocalisation of type VI collagen in the intervertebral disc. *Ann. Rheum. Dis.* **50,** 787–91 (1991).

25.   Hines, T. Anatomy of the spine: basic level. *Mayf. Clin. Spine Inst. Rep.* 1–5 (2010).

26.   Completo, A. & Fonseca, F. Fundamentos de biomecânica músculo-esquelética e ortopédica. *Publindústria* p: 23 (2011).

27.   Pereira, D. R. *et al.* Development of gellan gum-based microparticles/hydrogel matrices for application in the intervertebral disc regeneration. *Tissue Eng. Part C. Methods* **17,** 961–72 (2011).

28.   Cheung, K. M. C. & Al Ghazi, S. (i) Current understanding of low back pain and intervertebral disc degeneration: epidemiological perspectives and phenotypes for genetic studies. *Curr. Orthop.* **22,** 237–244 (2008).

29.   Roberts, S., Evans, H., Trivedi, J. & Menage, J. Histology and pathology of the human intervertebral disc. *J. Bone Joint Surg. Am.* **88 Suppl 2,** 10–4 (2006).

30.   Richardson, S. M., Mobasheri, A., Freemont, A. J. & Hoyland, J. A. Intervertebral disc biology, degeneration and novel tissue engineering and regenerative medicine therapies. *Histol. Histopathol.* **22,** 1033–41 (2007).

31.   Kalson, N. S., Richardson, S. & Hoyland, J. A. Strategies for regeneration of the intervertebral disc. *Regen. Med.* **3,** 717–29 (2008).

32.   Périé, D., Korda, D. & Iatridis, J. C. Confined compression experiments on bovine nucleus pulposus and annulus fibrosus: sensitivity of the experiment in the determination of compressive modulus and hydraulic permeability. *J. Biomech.* **38,** 2164–71 (2005).

33.   Conventry, M. B., Ghormley, R. K. & Kernohan, J. W. The Intervertebral Disc: Its Microscopic Anatomy and Pathology - Part II. Changes in the Intervertebral Disc Concomitant with Age. *J. Bone Jt. Surg.* **XXVII,** 233–247 (1945).

34.   Richardson, S. M. & Hoyland, J. A. Stem cell regeneration of degenerated intervertebral discs: current status. *Curr. Pain Headache Rep.* **12,** 83–8 (2008).

35.   Setton, L. A., Zhu, W., Weidenbaum, M., Ratcliffe, A. & Mow, V. C. Compressive properties of the cartilaginous end-plate of the baboon lumbar spine. *J. Orthop. Res.* **11,** 228–39 (1993).

36.   Miyamoto, K. *et al.* Intradiscal injections of osteogenic protein-1 restore the viscoelastic properties of degenerated intervertebral discs. *Spine J.* **6,** 692–703 (2006).

37.   Wang, Y. The Roles of Vertebra and Vertebral Endplate in Lumbar Disc Degeneration. 1–150 (2012).

38.   Iatridis, J. C., Nicoll, S. B., Michalek, A. J., Walter, B. a & Gupta, M. S. Role of biomechanics in intervertebral disc degeneration and regenerative therapies: what needs repairing in the disc and what are promising biomaterials for its repair? *Spine J.* **13,** 243–62 (2013).

39.   Woods, B. I., Sowa, G., Vo, N. & Kang, J. D. A Change in Strategy: The Use of Regenerative Medicine and Tissue Engineering to Augment the Course of Intervertebral Disc Degeneration. *Oper. Tech. Orthop.* **20,** 144–153 (2010).

40.   Silva-Correia, J., Correia, S. I., Oliveira, J. M. & Reis, R. L. Tissue engineering strategies applied in the regeneration of the human intervertebral disk. *Biotechnol. Adv.* **31,** 1514–31 (2013).

41.   Thompson, J. P., Oegema, T. R. & Bradford, D. S. Stimulation of mature canine intervertebral disc by growth factors. *Spine (Phila. Pa. 1976).* **16,** 253–60 (1991).

42.   Adams, M. A. & Roughley, P. J. What is intervertebral disc degeneration, and what causes it? *Spine (Phila. Pa. 1976).* **31,** 2151–61 (2006).

43.   Shankar, H., Scarlett, J. a & Abram, S. E. Anatomy and pathophysiology of intervertebral disc disease. *Tech. Reg. Anesth. Pain Manag.* **13,** 67–75 (2009).

44.   Raj, P. P. Intervertebral disc: anatomy-physiology-pathophysiology-treatment. *Pain Pract.* **8,** 18–44 (2008).

45.   Urban, J. & Roberts, S. Degeneration of the intervertebral disc. *Arthritis Res. Ther.* **5,** 120–130 (2003).

46.   Bogduk, N. Management of chronic low back pain. *Med. J. Aust.* **180,** 79–83 (2004).

47. Iatridis, J. C., Setton, L. a, Weidenbaum, M. & Mow, V. C. Alterations in the mechanical behavior of the human lumbar nucleus pulposus with degeneration and aging. *J. Orthop. Res.* **15,** 318–22 (1997).

48. Zhao, C.-Q., Wang, L.-M., Jiang, L.-S. & Dai, L.-Y. The cell biology of intervertebral disc aging and degeneration. *Ageing Res. Rev.* **6,** 247–261 (2007).

49. Feng, G. *et al.* Multipotential differentiation of human anulus fibrosus cells: an in vitro study. *J. Bone Joint Surg. Am.* **92,** 675–85 (2010).

50. Bae, W. C. & Masuda, K. Emerging technologies for molecular therapy for intervertebral disk degeneration. *Orthop. Clin. North Am.* **42,** 585–601, ix (2011).

51. Lee, J. M. *et al.* Interleukin-1β induces angiogenesis and innervation in human intervertebral disc degeneration. *J. Orthop. Res.* **29,** 265–9 (2011).

52. Le Maitre, C. L., Freemont, A. J. & Hoyland, J. A. A preliminary in vitro study into the use of IL-1Ra gene therapy for the inhibition of intervertebral disc degeneration. *Int. J. Exp. Pathol.* **87,** 17–28 (2006).

53. Roberts, S., Evans, E. H., Kletsas, D., Jaffray, D. C. & Eisenstein, S. M. Senescence in human intervertebral discs. *Eur. Spine J.* **15 Suppl 3,** S312–6 (2006).

54. Heneghan, P. & Riches, P. E. Determination of the strain-dependent hydraulic permeability of the compressed bovine nucleus pulposus. *J. Biomech.* **41,** 903–6 (2008).

55. Kepler, C. K. & Hilibrand, A. S. Management of adjacent segment disease after cervical spinal fusion. *Orthop. Clin. North Am.* **43,** 53–62, viii (2012).

56. Woods, B. I., Vo, N., Sowa, G. & Kang, J. D. Gene therapy for intervertebral disk degeneration. *Orthop. Clin. North Am.* **42,** 563–74, ix (2011).

57. Pereira, D. R. ., Silva-Correia, J., Oliveira, J. M. . & Reis, R. L. . Hydrogels in acellular and cellular strategies for intervertebral disc regeneration. *J. Tissue Eng. Regen. Med.* **7,** 85–98 (2013).

58. Bangel-Ruland, N. *et al.* CFTR-mRNA delivery: a novel alternative for cystic fibrosis "gene therapy."*J. Gene Med.* 1–31 (2013). doi:10.1002/jgm.2748

59. Silva-Correia, J. *et al.* Angiogenic potential of gellan-gum-based hydrogels for application in nucleus pulposus regeneration: in vivo study. *Tissue Eng. Part A* **18,** 1203–12 (2012).

60. Bao, Q. B., McCullen, G. M., Higham, P. a, Dumbleton, J. H. & Yuan, H. a. The artificial disc: theory, design and materials. *Biomaterials* **17,** 1157–67 (1996).

61. O'Connell, G. D., Malhotra, N. R., Vresilovic, E. J. & Elliott, D. M. The effect of nucleotomy and the dependence of degeneration of human intervertebral disc strain in axial compression. *Spine (Phila. Pa. 1976).* **36,** 1765–71 (2011).

62. Schizas, C., Kulik, G. & Kosmopoulos, V. Disc degeneration: current surgical options. *Eur. Cell. Mater.* **20,** 306–15 (2010).

63. Hanley, E. N. & David, S. M. Lumbar arthrodesis for the treatment of back pain. *J. Bone Joint Surg. Am.* **81,** 716–30 (1999).

64. Kishen, T. J. & Diwan, A. D. Fusion versus disk replacement for degenerative conditions of the lumbar and cervical spine: quid est testimonium? *Orthop. Clin. North Am.* **41,** 167–81 (2010).

65. Gibson, J. N., Grant, I. C. & Waddell, G. The Cochrane review of surgery for lumbar disc prolapse and degenerative lumbar spondylosis. *Spine (Phila. Pa. 1976).* **24,** 1820–32 (1999).

66. Gillet, P. The fate of the adjacent motion segments after lumbar fusion. *J. Spinal Disord. Tech.* **16,** 338–45 (2003).

67. Eyre, D., Benya, P. & Buckwalter, J. in *New Perspect. Low Back Pain* (Frymoyer, J. & Gordon, S.) 147–152 (AAOS, 1989).

68. Shah, V. B., Krishnan, A. & Hegde, S. K. New Horizons in Spinal Surgery: Spine Arthroplasty. *Apollo Med.* **2,** 89–95 (2005).

69. Fraser, R. in *The Lumbar Spine* (Herkowitz, H., Dvorak, J., Bell, G., Nordin, M. & Grob, D.) 393–398 (Lippincott Williams & Wilkins, 2004).

70. Di Martino, A., Vaccaro, A. R., Lee, J. Y., Denaro, V. & Lim, M. R. Nucleus pulposus replacement: basic science and indications for clinical use. *Spine (Phila. Pa. 1976).* **30,** S16–22 (2005).

71. Zigler, J. E. Lumbar spine arthroplasty using the ProDisc II. *Spine J.* **4,** 260S–267S (2004).

72. Rodrigues, L., Voloch, P. & Cavallari, F. in *Low Back Pain Pathog. Treat.* (Sakai, Y.) 163–188 (InTech, 2012).

73. Boelen, E. J. H. *et al.* Intrinsically radiopaque hydrogels for nucleus pulposus replacement. *Biomaterials* **26,** 6674–83 (2005).

74. Barrey, C., Perrin, G. & Champain, S. Pedicle-Screw-Based Dynamic Systems and Degenerative Lumbar Diseases: Biomechanical and Clinical Experiences of Dynamic Fusion with Isobar TTL. *ISRN Orthop.* **2013,** 1–10 (2013).

75. Kelly, M. P., Mok, J. M. & Berven, S. Dynamic constructs for spinal fusion: an evidence-based review. *Orthop. Clin. North Am.* **41,** 203–15 (2010).

76. Rutherford, E. E., Tarplett, L. J., Davies, E. M., Harley, J. M. & King, L. J. Lumbar spine fusion and stabilization: hardware, techniques, and imaging appearances. *Radiographics* **27,** 1737–49 (2007).

77. Ormond, D. R., Albert, L. & Das, K. Polyetheretherketone (PEEK) Rods in Lumbar Spine Degenerative Disease: A Case Series. *J. Spinal Disord. Tech.* 2012 (2012). doi:10.1097/BSD.0b013e318277cb9b

78.   Kim, Y.-S. *et al.* Nitinol spring rod dynamic stabilization system and Nitinol memory loops in surgical treatment for lumbar disc disorders: short-term follow up. *Neurosurg. Focus* **22,** E10 (2007).

79.   Barrey, C. Y., Ponnappan, R. K., Song, J. & Vaccaro, A. R. Biomechanical Evaluation of Pedicle Screw-Based Dynamic Stabilization Devices for the Lumbar Spine: A Systematic Review. *SAS J.* **2,** 159–170 (2008).

80.   Sengupta, D. in *The Lumbar Spine* (Herkowitz, H., Dvorak, J., Bell, G., Nordin, M. & Grob, D.) 373–383 (Lippincott Williams & Wilkins, 2004).

81.   Kahraman, S. *et al.* Is dysphonia permanent or temporary after anterior cervical approach? *Eur. Spine J.* **16,** 2092–5 (2007).

82.   Saal, J. A. & Saal, J. S. Intradiscal electrothermal treatment for chronic discogenic low back pain: prospective outcome study with a minimum 2-year follow-up. *Spine (Phila. Pa. 1976).* **27,** 966–73; discussion 973–4 (2002).

83.   Lee, M. S., Cooper, G., Lutz, G. E., Lutz, C. & Hong, H. M. Intradiscal electrothermal therapy (IDET) for treatment of chronic lumbar discogenic pain: a minimum 2-year clinical outcome study. *Pain Physician* **6,** 443–8 (2003).

84.   Yarborough, M. & Sharp, R. R. Public trust and research a decade later: what have we learned since Jesse Gelsinger's death? *Mol. Genet. Metab.* **97,** 4–5 (2009).

85.   Freimark, D. & Czermak, P. Cell-based regeneration of intervertebral disc defects: review and concepts. *Int. J. Artif. Organs* **32,** 197–203 (2009).

86.   Zhou, H. W., Lou, S. Q. & Zhang, K. Recovery of function in osteoarthritic chondrocytes induced by p16INK4a-specific siRNA in vitro. *Rheumatology (Oxford).* **43,** 555–68 (2004).

87.   Reddi, a H. Inhibition of cell death in the intervertebral disc by caspase 3 small interfering RNA. *Arthritis Rheum.* **63,** 1477–8 (2011).

88.   Ganly, S. *et al.* Liposomal surface coatings of metal stents for efficient non-viral gene delivery to the injured vasculature. *J. Control. Release* **167,** 109–19 (2013).

89.   Perales, J. C., Ferkol, T., Molas, M. & Hanson, R. W. An evaluation of receptor-mediated gene transfer using synthetic DNA-ligand complexes. *Eur. J. Biochem.* **226,** 255–66 (1994).

90.   Nguyen-Hoai, T. *et al.* HER2/neu DNA vaccination by intradermal gene delivery in a mouse tumor model: Gene gun is superior to jet injector in inducing CTL responses and protective immunity. *Oncoimmunology* **1,** 1537–1545 (2012).

91.   Liu, Y. *et al.* Effect of microbubble-enhanced ultrasound on prostate permeability: a potential therapeutic method for prostate disease. *Urology* **81,** 921.e1–7 (2013).

92.   Huang, Z. Q., Zheng, Z. M. & Yan, J. Transgenic expression of human IGF1 in intervertebral degenerative discs. *J. Int. Med. Res.* **39,** 446–55 (2011).

93.   Leckie, S. K. *et al.* Injection of AAV2-BMP2 and AAV2-TIMP1 into the nucleus pulposus slows the course of intervertebral disc degeneration in an in vivo rabbit model. *Spine J.* **12,** 7–20 (2012).

94.   Goins, W. F. *et al.* Herpes simplex virus vector-mediated gene delivery for the treatment of lower urinary tract pain. *Gene Ther.* **16,** 558–69 (2009).

95.   Suh, L. H. *et al.* Cryopreservation and lentiviral-mediated genetic modification of human primary cultured corneal endothelial cells. *Invest. Ophthalmol. Vis. Sci.* **48,** 3056–61 (2007).

96.   Nishida, K., Gilbertson, L. G., Robbins, P. D., Evans, C. H. & Kang, J. D. Potential applications of gene therapy to the treatment of intervertebral disc disorders. *Clin. Orthop. Relat. Res.* S234–41 (2000). at <http://link.springer.com/chapter/10.1007/978-1-4612-2126-5_4>

97.   Woods, B. I., Vo, N., Sowa, G. & Kang, J. D. Gene therapy for intervertebral disk degeneration. *Orthop. Clin. North Am.* **42,** 563–74, ix (2011).

98.   Shimer, A. L., Chadderdon, R. C., Gilbertson, L. G. & Kang, J. D. Gene therapy approaches for intervertebral disc degeneration. *Spine (Phila. Pa. 1976).* **29,** 2770–2778 (2004).

99.   Wallach, C. J. *et al.* Safety assessment of intradiscal gene transfer: a pilot study. *Spine J.* **6,** 107–12 (2006).

100.   Langer, R. & Vacanti, J. P. Tissue engineering. *Science* **260,** 920–6 (1993).

101.   Regenerative medicine. *Econ.* **February,** (2013).

102.   Kelm, J. M. & Fussenegger, M. Scaffold-free cell delivery for use in regenerative medicine. *Adv. Drug Deliv. Rev.* **62,** 753–64 (2010).

103.   Fuchs, E., Tumbar, T. & Guasch, G. Socializing with the neighbors: stem cells and their niche. *Cell* **116,** 769–78 (2004).

104.   Sakai, D. Stem cell regeneration of the intervertebral disk. *Orthop. Clin. North Am.* **42,** 555–62, viii–ix (2011).

105.   Silva-Correia, J. *et al.* Gellan gum-based hydrogels for intervertebral disc tissue-engineering applications. *J. Tissue Eng. Regen. Med.* **5,** e97–107 (2011).

106.   Bertagnoli, R. *et al.* Mechanical testing of a novel hydrogel nucleus replacement implant. *Spine J.* **5,** 672–681 (2005).

107.   Boyd, L. M. & Carter, A. J. Injectable biomaterials and vertebral endplate treatment for repair and regeneration of the intervertebral disc. *Eur. Spine J.* **15 Suppl 3,** S414–21 (2006).

108.   Wilke, H.-J., Heuer, F., Neidlinger-Wilke, C. & Claes, L. Is a collagen scaffold for a tissue engineered nucleus replacement capable of restoring disc height and stability in an animal model? *Eur. Spine J.* **15 Suppl 3,** S433–8 (2006).

109. Van Tomme, S. R., Storm, G. & Hennink, W. E. In situ gelling hydrogels for pharmaceutical and biomedical applications. *Int. J. Pharm.* **355,** 1–18 (2008).

110. Roughley, P. *et al.* The potential of chitosan-based gels containing intervertebral disc cells for nucleus pulposus supplementation. *Biomaterials* **27,** 388–96 (2006).

111. Alsberg, E. *et al.* Regulating bone formation via controlled scaffold degradation. *J. Dent. Res.* **82,** 903–8 (2003).

112. Varghese, S. & Elisseeff, J. in *Polym. Regen. Med.* (Werner, C.) 95 – 144 (Springer, 2006). doi:10.1007/12_072

113. Shogren, R. & Bagley, E. in *Biopolym. Util. nature's Adv. Mater.* (Iman, S., Greene, R. & Zaidi, B.) 2 – 11 (1999).

114. Malafaya, P. B., Silva, G. a & Reis, R. L. Natural-origin polymers as carriers and scaffolds for biomolecules and cell delivery in tissue engineering applications. *Adv. Drug Deliv. Rev.* **59,** 207–33 (2007).

115. Puppi, D., Chiellini, F., Piras, A. M. & Chiellini, E. Polymeric materials for bone and cartilage repair. *Prog. Polym. Sci.* **35,** 403–440 (2010).

116. Temenoff, J. S. & Mikos, a G. Review: tissue engineering for regeneration of articular cartilage. *Biomaterials* **21,** 431–40 (2000).

117. Bron, J. L., Vonk, L. a, Smit, T. H. & Koenderink, G. H. Engineering alginate for intervertebral disc repair. *J. Mech. Behav. Biomed. Mater.* **4,** 1196–205 (2011).

118. Baer, a E., Wang, J. Y., Kraus, V. B. & Setton, L. a. Collagen gene expression and mechanical properties of intervertebral disc cell-alginate cultures. *J. Orthop. Res.* **19,** 2–10 (2001).

119. Reza, A. T. & Nicoll, S. B. Characterization of novel photocrosslinked carboxymethylcellulose hydrogels for encapsulation of nucleus pulposus cells. *Acta Biomater.* **6,** 179–86 (2010).

120. Berger, J., Reist, M., Mayer, J. ., Felt, O. & Gurny, R. Structure and interactions in chitosan hydrogels formed by complexation or aggregation for biomedical applications. *Eur. J. Pharm. Biopharm.* **57,** 35–52 (2004).

121. Coutinho, D. F. *et al.* Modified Gellan Gum hydrogels with tunable physical and mechanical properties. *Biomaterials* **31,** 7494–502 (2010).

122. Spiller, K. L., Laurencin, S. J., Charlton, D., Maher, S. a & Lowman, A. M. Superporous hydrogels for cartilage repair: Evaluation of the morphological and mechanical properties. *Acta Biomater.* **4,** 17–25 (2008).

123. Schexnailder, P. & Schmidt, G. Nanocomposite polymer hydrogels. *Colloid Polym. Sci.* **287,** 1–11 (2008).

124. Zhu, J. Bioactive modification of poly(ethylene glycol) hydrogels for tissue engineering. *Biomaterials* **31,** 4639–56 (2010).

125.   Place, E. S., George, J. H., Williams, C. K. & Stevens, M. M. Synthetic polymer scaffolds for tissue engineering. *Chem. Soc. Rev.* **38,** 1139–51 (2009).

126.   Rezwan, K., Chen, Q. Z., Blaker, J. J. & Boccaccini, A. R. Biodegradable and bioactive porous polymer/inorganic composite scaffolds for bone tissue engineering. *Biomaterials* **27,** 3413–31 (2006).

127.   Thomas, J. D., Fussell, G., Sarkar, S., Lowman, A. M. & Marcolongo, M. Synthesis and recovery characteristics of branched and grafted PNIPAAm-PEG hydrogels for the development of an injectable load-bearing nucleus pulposus replacement. *Acta Biomater.* **6,** 1319–28 (2010).

128.   Wang, B. H. & Campbell, G. Formulations of polyvinyl alcohol cryogel that mimic the biomechanical properties of soft tissues in the natural lumbar intervertebral disc. *Spine (Phila. Pa. 1976).* **34,** 2745–53 (2009).

129.   Joshi, A. *et al.* Functional compressive mechanics of a PVA/PVP nucleus pulposus replacement. *Biomaterials* **27,** 176–84 (2006).

130.   Maier, J. a, Lo, Y. & Harfe, B. D. Foxa1 and Foxa2 are required for formation of the intervertebral discs. *PLoS One* **8,** e55528 (2013).

131.   Kim, K.-W. *et al.* Notochordal cells stimulate migration of cartilage end plate chondrocytes of the intervertebral disc in in vitro cell migration assays. *Spine J.* **9,** 323–9 (2009).

132.   Takahashi, K. & Yamanaka, S. Induction of pluripotent stem cells from mouse embryonic and adult fibroblast cultures by defined factors. *Cell* **126,** 663–76 (2006).

133.   Fang, Z. *et al.* Differentiation of GFP-Bcl-2-engineered mesenchymal stem cells towards a nucleus pulposus-like phenotype under hypoxia in vitro. *Biochem. Biophys. Res. Commun.* **432,** 444–50 (2013).

134.   Leckie, S. K. *et al.* Injection of human umbilical tissue-derived cells into the nucleus pulposus alters the course of intervertebral disc degeneration in vivo. *Spine J.* **13,** 263–72 (2013).

135.   Huang, Y.-C., Leung, V. Y. L., Lu, W. W. & Luk, K. D. K. The effects of microenvironment in mesenchymal stem cell-based regeneration of intervertebral disc. *Spine J.* **13,** 352–62 (2013).

136.   Cheng, Y.-H. *et al.* Thermosensitive chitosan-gelatin-glycerol phosphate hydrogels as a cell carrier for nucleus pulposus regeneration: an in vitro study. *Tissue Eng. Part A* **16,** 695–703 (2010).

137.   Cheng, Y.-H., Yang, S.-H. & Lin, F.-H. Thermosensitive chitosan-gelatin-glycerol phosphate hydrogel as a controlled release system of ferulic acid for nucleus pulposus regeneration. *Biomaterials* **32,** 6953–61 (2011).

138.   Oliveira, J. T. *et al.* Gellan gum: a new biomaterial for cartilage tissue engineering applications. *J. Biomed. Mater. Res. A* **93,** 852–63 (2010).

139. Silva-Correia, J. *et al.* Angiogenic potential of gellan-gum-based hydrogels for application in nucleus pulposus regeneration: in vivo study. *Tissue Eng. Part A* **18,** 1203–12 (2012).

140. Oliveira, J. T. *et al.* Gellan gum: a new biomaterial for cartilage tissue engineering applications. *J. Biomed. Mater. Res. A* **93,** 852–63 (2010).

141. Silva, D. *et al.* PHOTO-CROSSLINKED GELLAN GUM-BASED HYDROGELS: PREPARATION METHODS AND USES THEREOF. *WO Pat. ...* (2011). at <http://patentscope.wipo.int/search/en/WO2011119059>

142. Silva-Correia, J. *et al.* Gellan gum-based hydrogels for intervertebral disc tissue-engineering applications. *J. Tissue Eng. Regen. Med.* **5,** e97–107 (2011).

143. Silva-Correia, J., Oliveira, J., Teixeira, J., Amandi, R. & Reis, R. Photo-crosslinked gellan gum-based hydrogels: preparation methods and uses thereof. WO Patent 2011119059 A1 (2011).

144. Silva-Correia, J. *et al.* Biocompatibility evaluation of ionic- and photo-crosslinked methacrylated gellan gum hydrogels: in vitro and in vivo study. *Adv. Healthc. Mater.* **2,** 568–75 (2013).

145. Vo, N. V *et al.* Expression and regulation of metalloproteinases and their inhibitors in intervertebral disc aging and degeneration. *Spine J.* **13,** 331–41 (2013).

146. Jin, L., Shimmer, A. L. & Li, X. The challenge and advancement of annulus fibrosus tissue engineering. *Eur. Spine J.* **22,** 1090–100 (2013).

147. Hudson, K. D., Alimi, M., Grunert, P., Härtl, R. & Bonassar, L. J. Recent advances in biological therapies for disc degeneration: tissue engineering of the annulus fibrosus, nucleus pulposus and whole intervertebral discs. *Curr. Opin. Biotechnol.* (2013). doi:10.1016/j.copbio.2013.04.012

148. Sharifi, S. *et al.* An annulus fibrosus closure device based on a biodegradable shape-memory polymer network. *Biomaterials* **34,** 8105–13 (2013).

149. Sun, D. D. N. & Leong, K. W. A nonlinear hyperelastic mixture theory model for anisotropy, transport, and swelling of annulus fibrosus. *Ann. Biomed. Eng.* **32,** 92–102 (2004).

150. Nesti, L. J. *et al.* Intervertebral disc tissue engineering using a novel hyaluronic acid-nanofibrous scaffold (HANFS) amalgam. *Tissue Eng. Part A* **14,** 1527–37 (2008).

151. Sha'ban, M., Kim, S. H., Idrus, R. B. & Khang, G. Fibrin and poly(lactic-co-glycolic acid) hybrid scaffold promotes early chondrogenesis of articular chondrocytes: an in vitro study. *J. Orthop. Surg. Res.* **3,** 17 (2008).

152. Mizuno, H. *et al.* Tissue-engineered composites of anulus fibrosus and nucleus pulposus for intervertebral disc replacement. *Spine (Phila. Pa. 1976).* **29,** 1290–7; discussion 1297–8 (2004).

153.   Chang, G., Kim, H.-J., Kaplan, D., Vunjak-Novakovic, G. & Kandel, R. a. Porous silk scaffolds can be used for tissue engineering annulus fibrosus. *Eur. Spine J.* **16,** 1848–57 (2007).

154.   Park, S. *et al.* Annulus fibrosus tissue engineering using lamellar silk scaffolds. *J. Tissue Eng. Regen. Med.* **6 Suppl 3,** s24–33 (2012).

155.   Sato, M. *et al.* An atelocollagen honeycomb-shaped scaffold with a membrane seal (ACHMS-scaffold) for the culture of annulus fibrosus cells from an intervertebral disc. *J. Biomed. Mater. Res. A* **64,** 248–56 (2003).

156.   Sato, M. *et al.* Tissue engineering of the intervertebral disc with cultured annulus fibrosus cells using atelocollagen honeycomb-shaped scaffold with a membrane seal (ACHMS scaffold). *Med. Biol. Eng. Comput.* **41,** 365–71 (2003).

157.   Saad, L. & Spector, M. Effects of collagen type on the behavior of adult canine annulus fibrosus cells in collagen-glycosaminoglycan scaffolds. *J. Biomed. Mater. Res. A* **71,** 233–41 (2004).

158.   Bowles, R. D. *et al.* Image-based tissue engineering of a total intervertebral disc implant for restoration of function to the rat lumbar spine. *NMR Biomed.* **25,** 443–51 (2012).

159.   Pan, Y. *et al.* Cells scaffold complex for Intervertebral disc Anulus Fibrosus tissue engineering: in vitro culture and product analysis. *Mol. Biol. Rep.* **39,** 8581–94 (2012).

160.   Nerurkar, N. L., Elliott, D. M. & Mauck, R. L. Mechanical design criteria for intervertebral disc tissue engineering. *J. Biomech.* **43,** 1017–30 (2010).

161.   Lazebnik, M. *et al.* Biomimetic method for combining the nucleus pulposus and annulus fibrosus for intervertebral disc tissue engineering. *J. Tissue Eng. Regen. Med.* **5,** e179–87 (2011).

162.   Shao, X. & Hunter, C. J. Developing an alginate/chitosan hybrid fiber scaffold for annulus fibrosus cells. *J. Biomed. Mater. Res. A* **82,** 701–10 (2007).

163.   Pattappa, G. *et al.* Diversity of intervertebral disc cells: phenotype and function. *J. Anat.* **221,** 480–96 (2012).

164.   Denning, D., Paukshto, M. V, Habelitz, S. & Rodriguez, B. J. Piezoelectric properties of aligned collagen membranes. *J. Biomed. Mater. Res. B. Appl. Biomater.* 1–9 (2013). doi:10.1002/jbm.b.33006

165.   Marino, A. & Becker, R. O. Piezoelectric effect and growth control in bone. *Nature* **228,** 473–4 (1970).

166.   Schneider, T. O., Mueller, S. M., Shortkroff, S. & Spector, M. Expression of alpha-smooth muscle actin in canine intervertebral disc cells in situ and in collagen-glycosaminoglycan matrices in vitro. *J. Orthop. Res.* **17,** 192–9 (1999).

167.   Nerurkar, N. L., Elliott, D. M. & Mauck, R. L. Mechanics of oriented electrospun nanofibrous scaffolds for annulus fibrosus tissue engineering. *J. Orthop. Res.* **25,** 1018–28 (2007).

168. Bowles, R. D., Gebhard, H. H., Härtl, R. & Bonassar, L. J. Tissue-engineered intervertebral discs produce new matrix, maintain disc height, and restore biomechanical function to the rodent spine. *Proc. Natl. Acad. Sci. U. S. A.* **108,** 13106–11 (2011).

169. Pan, Y. *et al.* Cells scaffold complex for Intervertebral disc Anulus Fibrosus tissue engineering: in vitro culture and product analysis. *Mol. Biol. Rep.* **39,** 8581–94 (2012).

170. Guterl, C. C. *et al.* Challenges and strategies in the repair of ruptured annulus fibrosus. *Eur. Cell. Mater.* **25,** 1–21 (2013).

171. Bangel-Ruland, N. *et al.* CFTR-mRNA delivery: a novel alternative for cystic fibrosis "gene therapy."*J. Gene Med.* **42,** 585–601 (2013).

172. Wan, Y., Feng, G., Shen, F. H., Laurencin, C. T. & Li, X. Biphasic scaffold for annulus fibrosus tissue regeneration. *Biomaterials* **29,** 643–52 (2008).

173. Park, S.-H. *et al.* Intervertebral disk tissue engineering using biphasic silk composite scaffolds. *Tissue Eng. Part A* **18,** 447–58 (2012).

174. Damadian, R. V. Apparatus and method for detecting cancer in tissue. *US Pat. 3,789,832* (1974).

175. Hounsfield, G. N. Radiography. US Patent 4,115,698 (1978).

176. Raja, V. & Fernandes, K. Reverse engineering: an industrial perspective. (2008). at <http://scholar.google.com/scholar?hl=en&btnG=Search&q=intitle:Reverse+Engineering+-+An+Industrial+Perspective#0>

177. Azevedo, Á. Método dos elementos finitos. *Fac. Eng. da Univ. do Porto* (2003). at <http://www.alvaroazevedo.com/publications/books/livro_mef_aa_1ed/doc/Livro_MEF_AA.pdf>

178. Wright, P. K. 21st Century Manufacturing. 164–167 (2001).

179. Hull, C. Apparatus for production of three-dimensional objects by stereolithography. *US Pat. 4,575,330* (1986). at <http://www.google.com/patents?hl=en&lr=&vid=USPAT4575330&id=ye8zAAAAEBAJ&oi=fnd&dq=Apparatus+for+production+of+three-dimensional+objects+by+stereolithography&printsec=abstract>

180. Sabol, J. V, Grant, G. T., Liacouras, P. & Rouse, S. Digital image capture and rapid prototyping of the maxillofacial defect. *J. Prosthodont.* **20,** 310–4 (2011).

181. Ozan, O., Seker, E., Kurtulmus-Yilmaz, S. & Ersoy, A. E. Clinical application of stereolithographic surgical guide with a handpiece guidance apparatus: a case report. *J. Oral Implantol.* **38,** 603–9 (2012).

182. Crump, S. Apparatus and method for creating three-dimensional objects. *US Pat. 5,121,329* (1992). at <http://www.google.com/patents?hl=en&lr=&vid=USPAT5121329&id=VPApAAAAEBAJ&oi=fnd&dq=APPARATUS+AND+METHOD+FOR+CREATING+THREE-DIMENSIONAL+OBJECTS&printsec=abstract>

183. Shah, M. Auricular prosthesis fabrication using computer-aided design and rapid prototyping technologies. *Prosthet. Orthot. Int.* (2013). doi:10.1177/0309364613504779

184. Xuan, Y. *et al.* A specific groove design for individualized healing in a canine partial sternal defect model by a polycaprolactone/hydroxyapatite scaffold coated with bone marrow stromal cells. *J. Biomed. Mater. Res. A* 1–8 (2013). doi:10.1002/jbm.a.35012

185. Deckard, C. Method and apparatus for producing parts by selective sintering. *US Pat. 4,863,538* (1989). at <http://www.google.com/patents?hl=en&lr=&vid=USPAT4863538&id=nCMsAAAAE BAJ&oi=fnd&dq=Method+and+apparatus+for+producing+parts+by+selective+sintering &printsec=abstract>

186. Lee, M.-Y. *et al.* Laser sintered porous polycaprolacone scaffolds loaded with hyaluronic acid and gelatin-grafted thermoresponsive hydrogel for cartilage tissue engineering. *Biomed. Mater. Eng.* **23,** 533–43 (2013).

187. Liao, H., Lee, M., Tsai, W., Wang, H. & Lu, W. Osteogenesis of adipose-derived stem cells on polycaprolactone-β-tricalcium phosphate scaffold fabricated via selective laser sintering and surface coating with collagen type I. *J. Tissue Eng. Regen. Med.* (2013). doi:10.1002/term.1811

188. Doyle, H., Lohfeld, S. & McHugh, P. Predicting the Elastic Properties of Selective Laser Sintered PCL/β-TCP Bone Scaffold Materials Using Computational Modelling. *Ann. Biomed. Eng.* (2013). doi:10.1007/s10439-013-0913-4

189. Marga, F. *et al.* Toward engineering functional organ modules by additive manufacturing. *Biofabrication* **4,** 022001 (2012).

190. Mironov, V., Boland, T., Trusk, T., Forgacs, G. & Markwald, R. R. Organ printing: computer-aided jet-based 3D tissue engineering. *Trends Biotechnol.* **21,** 157–61 (2003).

191. Jakab, K., Neagu, A., Mironov, V., Markwald, R. R. & Forgacs, G. Engineering biological structures of prescribed shape using self-assembling multicellular systems. *Proc. Natl. Acad. Sci. U. S. A.* **101,** 2864–9 (2004).

192. Jakab, K., Damon, B., Neagu, A., Kachurin, A. & Forgacs, G. Three-dimensional tissue constructs built by bioprinting. *Biorheology* **43,** 509–13 (2006).

193. Mironov, V. *et al.* Organ printing: tissue spheroids as building blocks. *Biomaterials* **30,** 2164–74 (2009).

194. Jakab, K., Neagu, A., Mironov, V. & Forgacs, G. Organ printing: fiction or science. *Biorheology* **41,** 371–5 (2004).

195. Grossman, R. *et al.* Combination of anti-VEGF therapy and temozolomide in two experimental human glioma models. *J. Neurooncol.* 59–65 (2013). doi:10.1007/s11060-013-1268-2

196. Nesti, L. J. *et al.* Intervertebral disc tissue engineering using a novel hyaluronic acid-nanofibrous scaffold (HANFS) amalgam. *Tissue Eng. Part A* **14,** 1527–37 (2008).

197. Suggs, L. & Mikos, A. in *Phys. Prop. Polym. Handb.* (JE, M.) 615–624 (American Institute of Physics, 1996).

198. Htay, a. S., Teoh, S. H. & Hutmacher, D. W. Development of perforated microthin poly(ε-caprolactone) films as matrices for membrane tissue engineering. *J. Biomater. Sci. Polym. Ed.* **15,** 683–700 (2004).

199. Wang, Z., Srinivasan, K. & Hills, M. A. COMPLEX "DIRTY" GEOMETRY HANDLING WITH AN INTERIOR-TO-BOUNDARY GRID GENERATION METHOD. *Am. Inst. Aeronaut. Astronaut.* 1–11 (2001). at <http://arc.aiaa.org/doi/pdf/10.2514/6.2001-2538>

200. Li, Q., Wang, D. & Elisseeff, J. H. Heterogeneous-Phase Reaction of Glycidyl Methacrylate and Chondroitin Sulfate: Mechanism of Ring-Opening−Transesterification Competition. *Macromolecules* **36,** 2556–2562 (2003).

201. Singer, V. L., Jones, L. J., Yue, S. T. & Haugland, R. P. Characterization of PicoGreen reagent and development of a fluorescence-based solution assay for double-stranded DNA quantitation. *Anal. Biochem.* **249,** 228–38 (1997).

202. Thompson, J. P. *et al.* Preliminary evaluation of a scheme for grading the gross morphology of the human intervertebral disc. *Spine (Phila. Pa. 1976).* **15,** 411–5 (1990).

203. Gebhard, H. *et al.* Biological intervertebral disc replacement: an in vivo model and comparison of two surgical techniques to approach the rat caudal disc. *Evid. Based. Spine. Care. J.* **2,** 29–35 (2011).

204. James, A. R., Bowles, R. D., Gebhard, H. H., Bonassar, L. J. & Härtl, R. Tissue-engineered total disc replacement: final outcomes of a murine caudal disc in vivo study. *Evid. Based. Spine. Care. J.* **2,** 55–6 (2011).

205. Munirah, S., Kim, S. H., Ruszymah, B. H. & Khang, G. The use of fibrin and poly(lactic-co-glycolic acid) hybrid scaffold for articular cartilage tissue engineering: an in vivo analysis. *Eur. Cell. Mater.* **15,** 41–52 (2008).

206. Nerurkar, N. L., Mauck, R. L. & Elliott, D. M. Modeling interlamellar interactions in angle-ply biologic laminates for annulus fibrosus tissue engineering. *Biomech. Model. Mechanobiol.* **10,** 973–84 (2011).

207. Wilda, H. & Gough, J. E. In vitro studies of annulus fibrosus disc cell attachment, differentiation and matrix production on PDLLA/45S5 Bioglass composite films. *Biomaterials* **27,** 5220–9 (2006).

208. Zhuang, Y. *et al.* Construction of tissue-engineered composite intervertebral disc and preliminary morphological and biochemical evaluation. *Biochem. Biophys. Res. Commun.* **407,** 327–32 (2011).

209. Zein, I., Hutmacher, D. W., Tan, K. C. & Teoh, S. H. Fused deposition modeling of novel scaffold architectures for tissue engineering applications. *Biomaterials* **23,** 1169–85 (2002).

210. Koepsell, L., Zhang, L., Neufeld, D., Fong, H. & Deng, Y. Electrospun nanofibrous polycaprolactone scaffolds for tissue engineering of annulus fibrosus. *Macromol. Biosci.* **11,** 391–9 (2011).

211. Best, B. A. *et al.* Compressive mechanical properties of the human anulus fibrosus and their relationship to biochemical composition. *Spine (Phila. Pa. 1976).* **19,** 212–21 (1994).

212. Umehara, S. *et al.* Effects of degeneration on the elastic modulus distribution in the lumbar intervertebral disc. *Spine (Phila. Pa. 1976).* **21,** 811–9; discussion 820 (1996).

213. Lebourg, M., Rochina, J. R., Sousa, T., Mano, J. & Ribelles, J. L. G. Different hyaluronic acid morphology modulates primary articular chondrocyte behavior in hyaluronic acid-coated polycaprolactone scaffolds. *J. Biomed. Mater. Res. A* **101,** 518–27 (2013).

214. Zhu, Y., Gao, C. & Shen, J. Surface modification of polycaprolactone with poly(methacrylic acid) and gelatin covalent immobilization for promoting its cytocompatibility. *Biomaterials* **23,** 4889–95 (2002).

215. Causa, F. *et al.* Poly-epsilon-caprolactone/hydroxyapatite composites for bone regeneration: in vitro characterization and human osteoblast response. *J. Biomed. Mater. Res. A* **76,** 151–62 (2006).

216. Banu, N., Banu, Y., Sakai, M., Mashino, T. & Tsuchiya, T. Biodegradable polymers in chondrogenesis of human articular chondrocytes. *J. Artif. Organs* **8,** 184–91 (2005).

217. Park, H., Radisic, M., Lim, J. O., Chang, B. H. & Vunjak-Novakovic, G. A novel composite scaffold for cardiac tissue engineering. *In Vitro Cell. Dev. Biol. Anim.* **41,** 188–96 (2005).

218. Sarkar, S., Lee, G. Y., Wong, J. Y. & Desai, T. a. Development and characterization of a porous micro-patterned scaffold for vascular tissue engineering applications. *Biomaterials* **27,** 4775–82 (2006).

219. Chung, T.-W., Wang, Y.-Z., Huang, Y.-Y., Pan, C.-I. & Wang, S.-S. Poly (epsilon-caprolactone) grafted with nano-structured chitosan enhances growth of human dermal fibroblasts. *Artif. Organs* **30,** 35–41 (2006).

220. Bouma, G. J., Barth, M., Ledic, D. & Vilendecic, M. The high-risk discectomy patient: prevention of reherniation in patients with large anular defects using an anular closure device. *Eur. Spine J.* **22,** 1030–6 (2013).

221. Thorvaldsson, A. *et al.* Development of nanofiber-reinforced hydrogel scaffolds for nucleus pulposus regeneration by a combination of electrospinning and spraying technique. *J. Appl. Polym. Sci.* **128,** 1158–1163 (2013).

222. Feng, G., Li, L., Hong, Y., Liu, H. & Song, Y. Hypoxia promotes nucleus pulposus phenotype in 3D scaffolds in vitro and in vivo: Laboratory investigation. *... Neurosurg. Spine* 13870 (2014). doi:10.3171/2014.4.SPINE13870.